US Army Corps of Engineers

Performance Evaluation of the New Orleans and Southeast Louisiana Hurricane Protection System

Final Report of the Interagency Performance Evaluation Task Force

Volume VIII – Engineering and Operational Risk and Reliability Analysis

November 2007

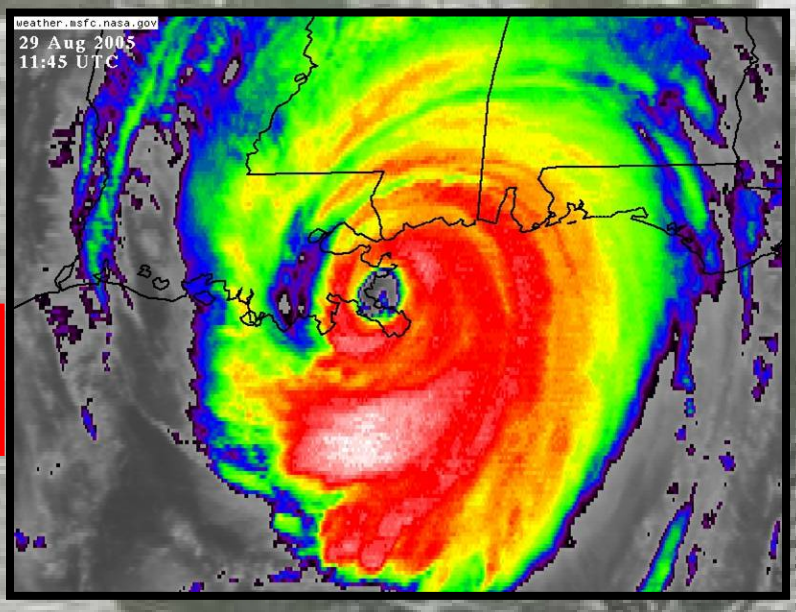

INTERIM DRAFT

Volume I – Executive Summary and Overview
Volume II – Geodetic Vertical and Water Level Datums
Volume III – The Hurricane Protection System
Volume IV – The Storm
Volume V – The Performance – Levees and Floodwalls
Volume VI – The Performance – Interior Drainage and Pumping
Volume VII – The Consequences
Volume VIII – Engineering and Operational Risk and Reliability Analysis
Volume IX – General Appendices

Volume VIII
Engineering and Operational Risk and Reliability Analysis

Contents

Executive Summary

The mission of the Interagency Performance Evaluation Task Force (IPET) risk and reliability analysis was to examine risks to life and property posed by hurricanes in New Orleans for two conditions: First, with the hurricane protection system (HPS) in place prior to Katrina (pre-Katrina), and second with the HPS reconstructed after Katrina and as existing in June 2006 (current). The risk analysis considered the expected performance of the various elements of the system and the consequences associated with that performance. The purpose of the analysis was to identify areas protected by the HPS that are vulnerable to flooding, to identify the causes of that vulnerability, and to provide estimates of the frequency of flooding within each drainage basin. The comparison of pre-Katrina and current risks was made to understand the effectiveness of the repairs and improvements.

The risk analysis results are intended to provide decision makers with information concerning the vulnerabilities of the current HPS and how potential investments could reduce those vulnerabilities. However, the analysis is not intended to identify final design elevations of proposed levees or floodwalls. The hurricane surge and wave studies on which the risk analysis is based are not of the detail required to establish design elevations. Additional detailed hydrologic and engineering studies will be required to make final decisions concerning the height of the HPS necessary for future conditions.

The risk analysis intends to answer specific questions concerning the performance of the HPS:

- What was the reliability of the pre-Katrina HPS for preventing flooding of protected areas given the range of hurricanes expected to impact New Orleans?

- What would have been the reliability of the pre-Katrina HPS for preventing flooding of protected areas for the range of hurricanes expected to impact New Orleans if the planned system had been completed, which it was not at the time of the storm?

- What was the reliability of the current post-Katrina HPS for preventing flooding of protected areas given the range of hurricanes expected to impact New Orleans? Specifically, what is the annual rate of occurrence of system failure due to the range of expected hurricane events?

- What are the annual rates of occurrence of economic consequences and loss of life resulting from failures of the HPS given the range of hurricanes expected to impact New Orleans?

- What is the uncertainty in these estimates of annual rates of occurrence?

The pre-Katrina risk analysis does not attempt to recreate the design intent or knowledge that the designers used to determine the configuration of the HPS. Instead, the risk analysis used engineering parameters, foundation conditions, and operational information gained by IPET through exploration and testing after the hurricane. Also, the changed, post-Katrina

demographics of the local areas protected by the system were not considered when estimating consequences. In some areas, many homes and much of the infrastructure were destroyed by the hurricane, and some homes and infrastructure may not be rebuilt. Therefore, the pre-Katrina populations and property values were impacted and will have to be considered in future analyses, but they were not considered here. Consequence information used in the risk analysis was provided by the Consequence Team, as reported in IPET Volume VII (USACE 2006).

A risk analysis methodology is developed and presented in this report for hurricane protection systems. The methodology is intended to inform decision and policy makers. Risk is quantified using a probabilistic framework to obtain elevation and loss-exceedance rates that are based on a spectrum of hurricanes determined using a joint probability distribution of the parameters that define hurricane intensity. The predicted surges, waves, and rainfall are used to evaluate the performance of a hurricane protection system consisting of a series of basins and sub-basins that define the interior drainage characteristics of the system. Protection against flooding is provided by levees, floodwalls, closure gates, an interior drainage system, and pumping stations. Stage-storage relationships define the characteristics of sub-basins and the population and property at risk. The risk analysis methodology and results allows decision makers to evaluate alternatives for managing risk such as providing increased hurricane protection, increasing evacuation effectiveness, changing land-use policy, enhancing hurricane protection system operations, and increasing public and governmental preparedness.

System failure refers to the failure of the HPS to provide protection from flooding in one or more protected areas, and it can also be thought of as the occurrence of flood inundation. The effectiveness of the protection system also depends upon how well the operational elements of the system perform. Elements such as road closure structures, gate operations, and pumping plants, which require human operation and proper installation during a flood fight, can dramatically impact flood levels. The lessons learned concerning the observed performance of these elements during Katrina were considered in the analysis.

Risk refers to expected losses in lives and dollars, calculated by multiplying the probability of system failure by the consequences associated with that failure. In order to compare the performance of the pre- and post-Katrina systems, frequency of inundation was used as the primary measure of effectiveness. Risk-based inundation mapping and associated stage-frequency curves are intended for estimating relative risks for the purpose of identifying areas of vulnerability. These estimates should not be compared to inundation mapping conducted under the Federal Emergency Management Agency's (FEMA's) National Flood Insurance Program (NFIP) because the methods and purpose of the respective analyses are different.

The effectiveness of the repairs and improvements made to the hurricane protection system can best be measured by comparing the predicted inundation elevation-exceedance relationships for the Pre-Katrina HPS and Current HPS. The risk analysis results show that moderate inundation reductions have been achieved for more frequent events of less than 0.01 probability per year, but that predicted inundation elevations are mostly unchanged, and there is still significant risk of inundation for less frequent storms.

Team Members

Co-Lead		
Jerry L. Foster, PE	HQUSACE	Project Manager
Bruce Muller, PE	USBR	Asst. Project Manager
Headquarters Liaison		
Donald R. Dressler, PE	HQUSACE	Project Sponsor
Anjana Chudgar	HQUSACE	Project Monitor
Members		
Bilal M. Ayyub, PhD, PE	UMD	Lead FoRTE Model Developer
Gregory B. Baecher, PhD	UMD	Geotechnical Reliability
Brian Blanton	UNC	ADCIRC/STWAVE Modeler
David Bowles, PhD	USU	Consequences
Sheree Castain, PG	USACE-NAB	Geotechnical Data Review
Jennifer Chowning	USACE-LRL	GIS Mapping
David Cole, PE	USACE-NAE	System Definition
Robert Dean, PhD	University of Florida	Wave Modeler & Coastal Engineering
David Descouteax	PE USACE-NAE	System Definition
David Divoky	Watershed Concepts	Lead Hurricane Modeling
Bruce Ellingwood, PhD	Georgia Tech	Technical Review
Alex Garneau, PE	USACE-NAE	System Definition
Brian Glock, PG	USACE-NAB	Geotechnical Data Review
Richalie Griffith	USACE-NAE	System Definitions & GIS Mapping
H. Wayne Jones	ERDC-ITL	Program Manager & System Definitions
Mark Kaminskiy	PhD UMD	Risk Methodology
Burton Kemp	MVN (Ret.)	Field Geologist
Fredrick Krimgold, PhD	Virginia Tech	Consequences
Therese McAllister, PhD, PE	NIST	Reliability & Technical Review
Marty McCann, PhD	JBA	Uncertainty Analysis
William McGill, PE	UMD	Risk Modeler
Robert C. Patev, PE	USACE-NAE	Lead Geotechnical and Reliability

David Schaaf, PE	USACE-LRL	System Definition
James Snyder, PG	USACE-NAB	Geotechnical Data Review
Terry Sullivan, PE	USACE-LRL	Field Surveys
Pat Taylor	ERDC-GSL	Field Surveys
Nancy Towne	ERDC-ITL	GIS Mapping
Thomas Rossbach, PG	USACE-NAB	Geotechnical Data Review
Gregory Walker	ERDC-ITL	Programmer
Mathew Watts	USACE-LRL	Field Surveys
Allyson Windham	ERDC-ITL	GIS Mapping
John Winkleman	USACE-NAE	ADCIRC and GIS Interpretation

Introduction

A primary contributor to the flooding of New Orleans during Hurricane Katrina was the failure of levees and floodwalls that make up the hurricane protection system (HPS), and in some parts of the system, their overtopping by storm surge. The HPS had been designed to provide protection from storm-induced surges and waves, in an attempt to control naturally occurring conditions. The HPS was designed to perform this function without imposing unacceptable risks to public safety, property, and welfare; however, some level of risk always remains. Even with the reconstruction and strengthening of the HPS in the future, some risk will remain.

The term *risk* is used in many ways to define hazards, losses, and potential outcomes. In the engineering community, *risk* is generally considered to be the potential for loss resulting from exposure to some uncertain hazard or event. Risk is usually defined for engineering purposes as follows:

$$Risk = Hazard\ probability \times Vulnerability \times Consequences\ of\ failure \quad (1)$$

in which *hazard probability* is the rate or uncertainty of occurrence of the causal event, in the present case, the annual probability of storm surges and waves of given description; *vulnerability* is the reliability with which the constructed system withstands the loads or other demands caused by the hazard; and *consequences of failure* are the costs in lives and dollars accruing in the event of a failure (Ayyub 2003; Bedford and Cooke 2001; Morgan and Henrion 1990). In the present study, risk is represented as an exceedance probability of the severity of consequences, that is, as the annual probability of experiencing consequences greater than some level.

Equation 1 defines risk but also suggests ways to manage risk, by making the system more reliable or by reducing potential consequences of failure. Reliability can be influenced by strengthening existing structures or by adding additional protection. Consequences can be influenced, for example, by developing response plans or by limiting floodplain development. In

densely populated areas, simply increasing system reliability may not reduce risks to acceptable levels, and increasing consequences through continued floodplain development can offset improvements in reliability.

Decisions concerning investments in systems designed to control natural hazards are best made by explicitly and quantitatively considering the risks that the systems pose to public safety and property. Application of risk analysis to the HPS of New Orleans is challenging because the system is a complex of levees, floodwalls, pumping stations, and other components that serve a large geographical region. Also, the capability to model hurricanes and their effects is limited. Nonetheless, both methodologies have improved greatly in recent years and have become important tools for decision making.

Hurricane models can predict winds, waves, and surges only with limited accuracy, and the reliability models used to predict levee performance when subjected to hurricane forces are similarly limited. Hence, the risk profiles of hurricane-induced flooding cannot be established with certainty. Risk analysis, therefore, must include not just a best estimate of risk but also an estimate of the uncertainty in that best estimate. By identifying the sources of uncertainty in the analysis, measures, such as gathering additional data, can be taken to reduce the uncertainty and improve the risk estimates.

The risk model was developed to meet the needs of the Interagency Performance Evaluation Task Force. The risk analysis involved several key steps, which are described individually in other chapters. The principal of these were:

1. **Defining the physical features of the system** (systems definition). This required an accurate inventory of all in place components that provide protection against storm surge and waves, including cross sections and strength parameters of components, transitions between elements, differences in the crest elevations along the perimeter of the HPS, and varying foundation conditions.

2. **Modeling hurricane occurrence and effects** (hazard analysis). Hurricane modeling involved a combination of statistical analysis of historical storm frequencies in the Gulf of Mexico and extensive numerical simulations of the surge and wave fields caused by hurricanes. The risk analysis team relied on the results of IPET Volume III for its input on hurricane recurrence frequencies and on surge and wave effects.

3. **Assessing the effectiveness of the protection system** (reliability analysis). The analysis of the capacity of the HPS to withstand predicted levels of hurricane surge and wave loads involved structural and geotechnical reliability modeling and hydraulic uncertainty analysis to yield probabilistic predictions of the capacity of the system. The effectiveness of protection also depends on human factors, for example, timely road and railroad closures, gate operations, and functioning of pumping stations. Lessons learned from Katrina and other natural disasters were used in modeling these human factors.

4. **Characterizing inundation** (hydraulic analysis). Potential flooding of drainage basins that could follow hurricane events was predicted by hydraulic analysis of possible breaches and overtopping and by consideration of the performance of the interior

drainage and pumping systems. The pumping system is an important element that controls flooding during and after a storm, but it is not designed to handle hurricane events. The risk analysis team relied on the results of IPET Volume VI for its input on pumping and interior drainage.

5. **Predicting loss of life and dollar costs of inundation (consequences).** Hurricane-induced flooding leads to the potential for loss of life and economic costs. The risk analysis led to predictions of inundation volumes and flooding levels under various scenarios. The risk analysis team relied on the results of IPET Volume VII for its input on loss of live and dollar consequences.

These five key steps were integrated together using event tree and systems simulation techniques, as described in the chapter entitled, *risk analysis methodology*, to generate overall risks.

Analysis Boundaries

An initial step in the risk and reliability analysis was to clearly define the bounds of the study and the physical descriptions of the various components of a HPS. These included defining the geographic bounds of the study region and the elements of the HPS, the resolution of information and analysis to be performed, and analysis assumptions and constraints.

Study Region and Hurricane Protection System

The analysis examines risks to New Orleans and southeast Louisiana associated with the performance of the HPS. The region considered and the major features of the HPS are shown in Figure 1.

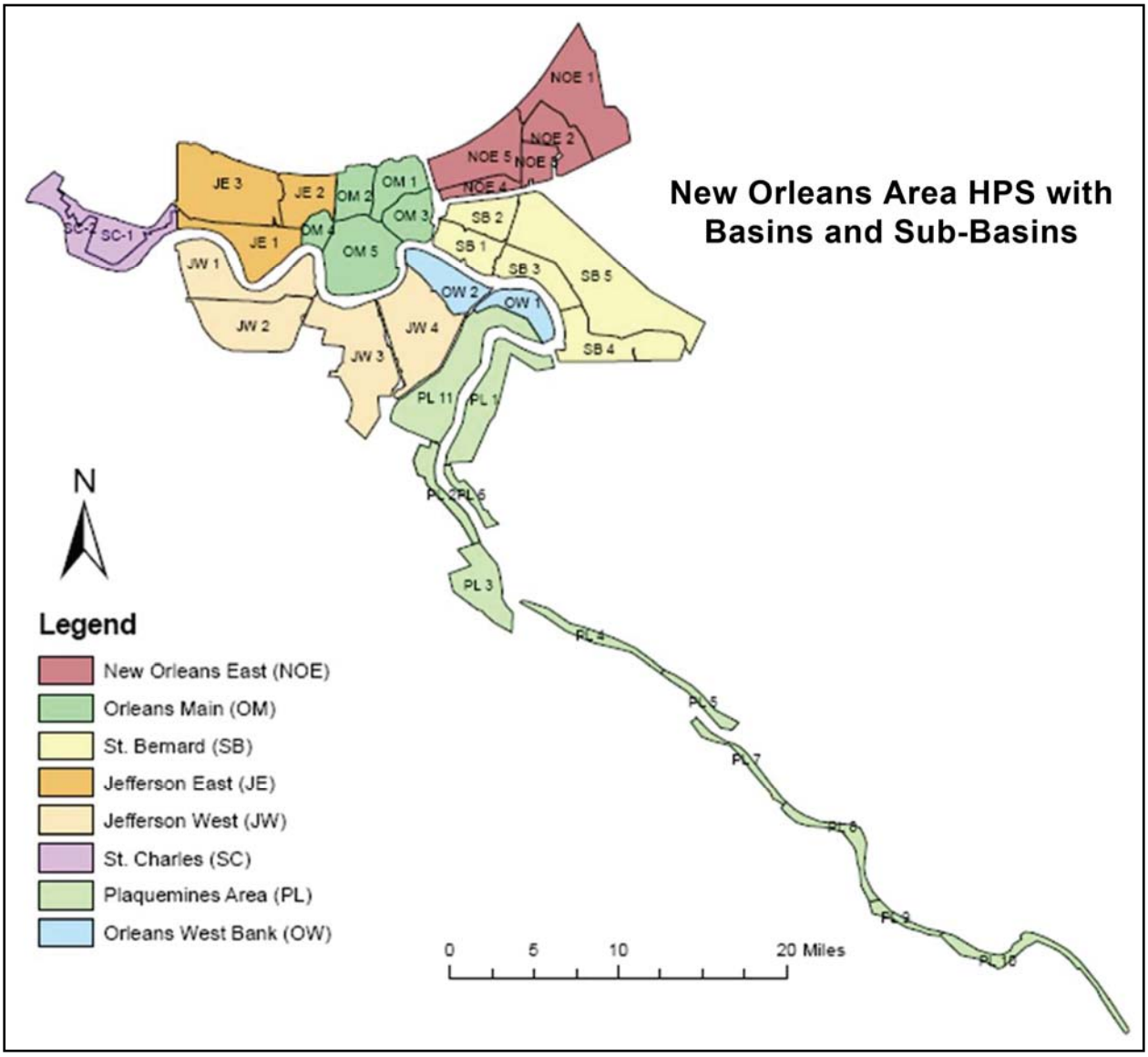

Figure 1. Map of New Orleans and the Southeast Louisiana area showing the geographic bounds of the study region considered in the risk analysis.

Physical Description of the HPS

The HPS comprises a variety of subsystems, structures, and components, which include earthen levees, floodwalls, transitions between levees and walls, gates, ramps, and pumping stations. Additional interior components of the HPS such as canals, wall closures, power supply systems, and operations personnel were indirectly considered in the analysis. The system is a combination of low-lying tracts of land that form artificial hydrologic entities enclosed by levees and floodwalls, called basins, which are independently maintained and operated by local parishes and levee boards.

Detailed physical descriptions for each basin based on current conditions are provided by the U.S. Army Corps of Engineers (USACE) (2006). Data collected during site inspections were used to define characteristics of the basins and their interdependence for use in the risk model. This was a critical and time-consuming step in the development of the risk model that has yielded a comprehensive description of the entire HPS protecting the New Orleans area. These descriptions were developed by examining available information gathered by IPET including the following:

- General Design Memoranda (GDM) and supporting design documents
- High resolution aerials photos from Pre-Katrina and Post-Katrina
- Construction documents and plans
- Inspection reports
- Katrina damage reports
- Detailed field surveys conducted by the Risk Team to verify the location and configurations of the HPS

The information gathered was incorporated into detailed geographic information system (GIS)-based maps of each basin that included locations of all features (walls, levees, pumping stations, and closure gates), geotechnical information (boring logs, geologic profiles), aerial photographs, and photos of each feature.

Analysis Assumptions and Constraints

As part of the process of developing the risk analysis model, it was necessary to identify key assumptions and analysis constraints. Constraints refer to events or situations that were not modeled or considered explicitly in the analysis. The assumptions and constraints are provided at the appropriate location in subsequent sections. The analysis limitations and constraints are summarized below:

- Modeling procedures that existed prior to Katrina were used.

- Geographic area was limited to elements of the HPS in the basins listed.

- The risk model does not produce temporal profiles, but it includes spatial profiles accumulated over the entire durations of respective storms.

- The risk model includes assumptions in the parameters used in various major aspects of the HPS characterization, hurricane simulation, reliability analysis inundation analysis, and consequence analysis.

- Hazards and consequences not considered in the risk analysis include the following: Wind damage to buildings; Barge Impact; Fire; Civil unrest; Indirect economic consequences; Effect of a release of hazardous materials; and Environmental consequences.

- The performance of the evacuation plan for New Orleans was not explicitly modeled in the risk analysis. Evacuation effectiveness is, however, considered in the consequence analysis.

Risk Analysis Methodology

Probabilistic risk analysis used to develop the overall risk analysis methodology of the HPS as presented in Figure 2. Subsequent sections describe individual parts of the methodology.

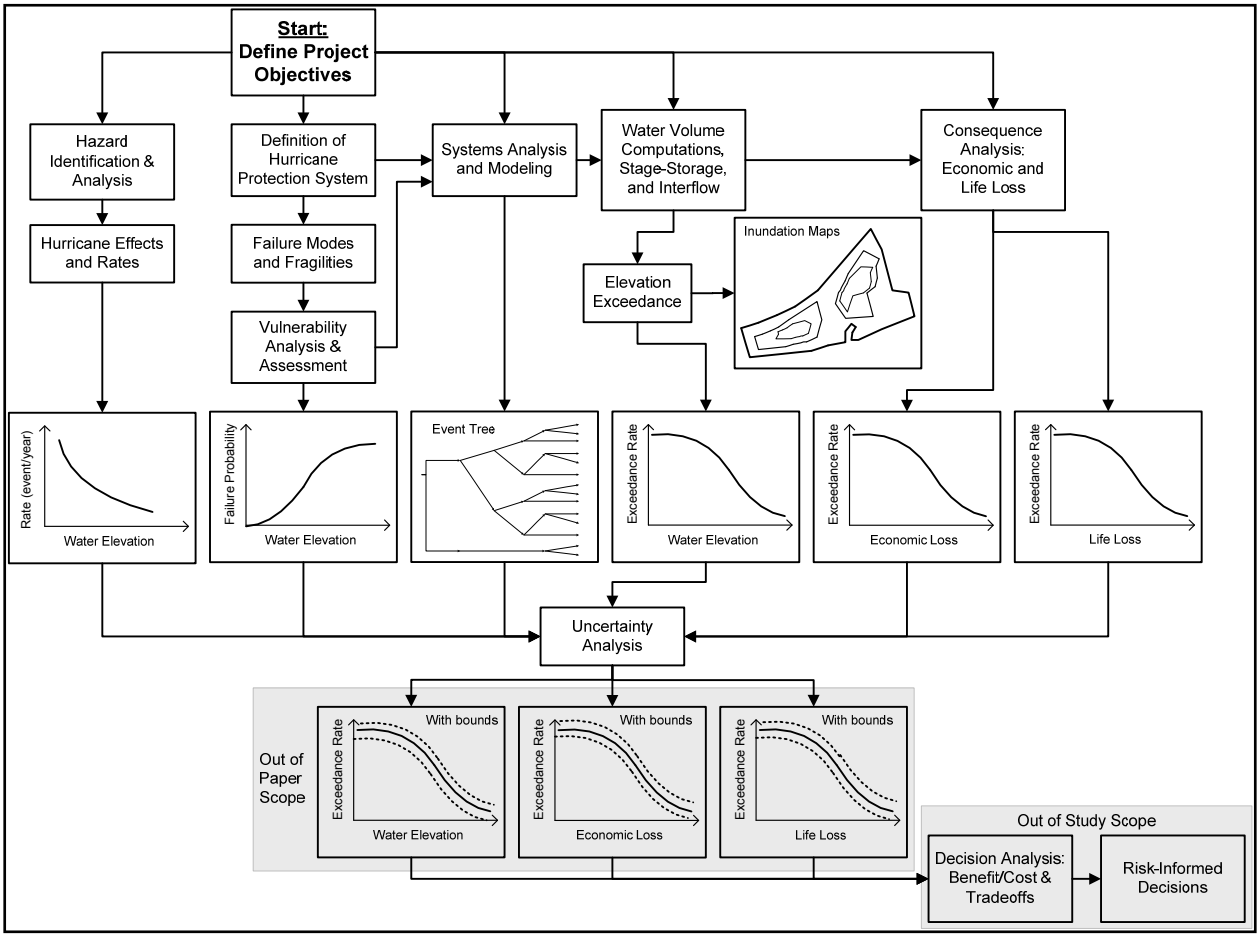

Figure 2. Overall risk analysis methodology.

Contributing Factors and Their Interrelationships

The development of the risk analysis model was facilitated by the preparation of an influence diagram. The process of creating an influence diagram helped establish a basic understanding of the elements of the HPS and their relationship to the overall system performance during a hurricane event and the analysis of consequences and risks. The influence diagram for the HPS and the analysis of consequences are shown in Figure 3. There are four parts to the influence

diagram: Value nodes (rounded-corner box), chance nodes (circular areas), decision nodes (square-corner boxes), and factors and dependencies in the form of arrows.

The influence diagram shown in Figure 3 was used to develop an event (or probability) tree for the HPS. Figure 4 shows an initial probability tree derived from the influence diagram in Figure 3. The top events across the tree identify the random events whose performance during and immediately after the hurricane could contribute to flooding in a protected area. The tree begins with the initiating event, a hurricane that generates a storm surge, winds, and rainfall in the region.

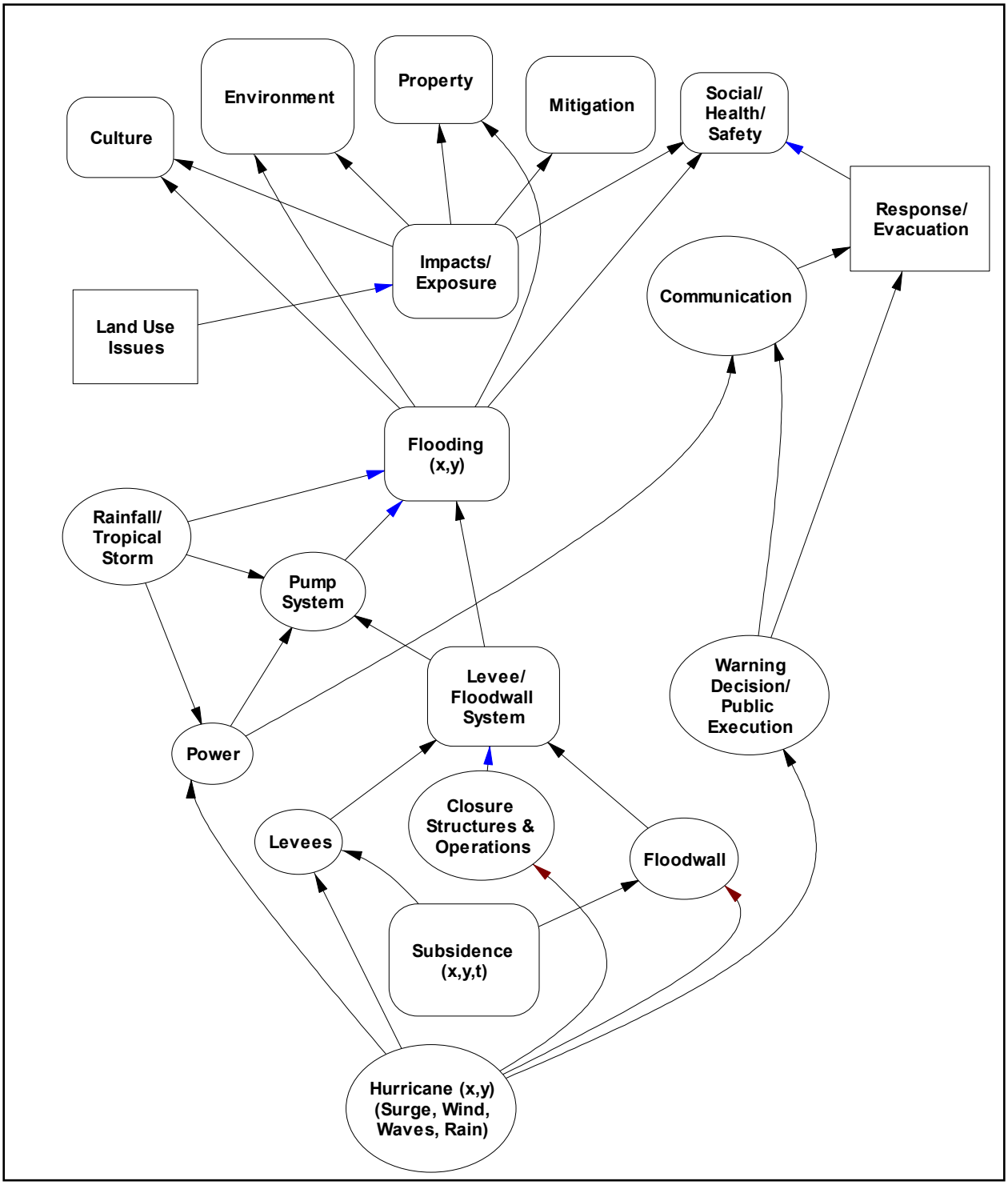

Figure 3. Influence diagrams for risk analysis.

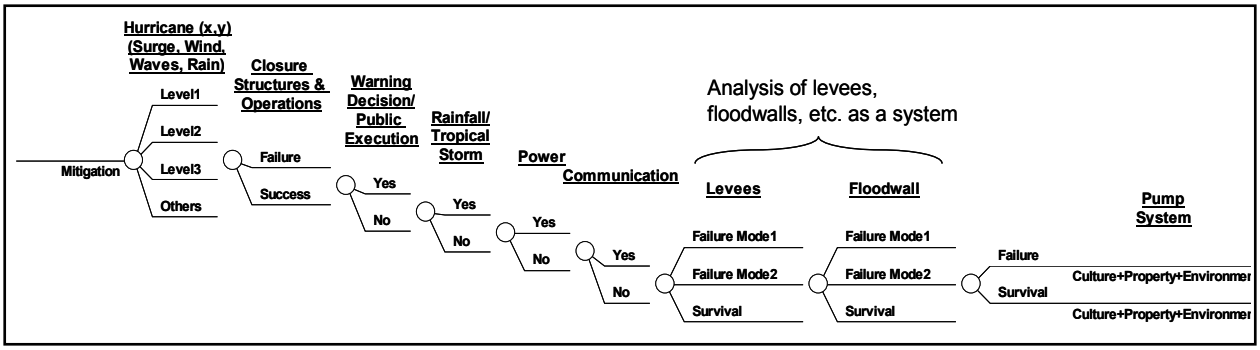

Figure 4. Probability Tree for the Hurricane Protection System

Hurricane Protection System Definition

The HPS as illustrated in Figure 1 was discretized for the reliability and risk analysis as schematically shown in Figure 5. The system consists of basins, sub-basins, and reaches. The definition of these hurricane protection basins, sub-basins, and reaches are based on the following considerations:

- Local levee board jurisdiction
- Structure type (levee or floodwall)
- Engineering parameters (cross section, elevation, materials, etc.)
- Foundation and soil strength parameters

Reaches (R) of each basin are defined of varying length as a discretization of the protection length such that each reach has about the same properties and exposure conditions and are uniquely identified using sequential numbers as illustrated for New Orleans East in Figure 5. The system was also defined by point features such as closure gates (highway and railroad) as well as transitions such as between levees and walls, pump stations, gates and ramps. Detailed maps and descriptions of each basin are provided in the IPET report (USACE 2006).

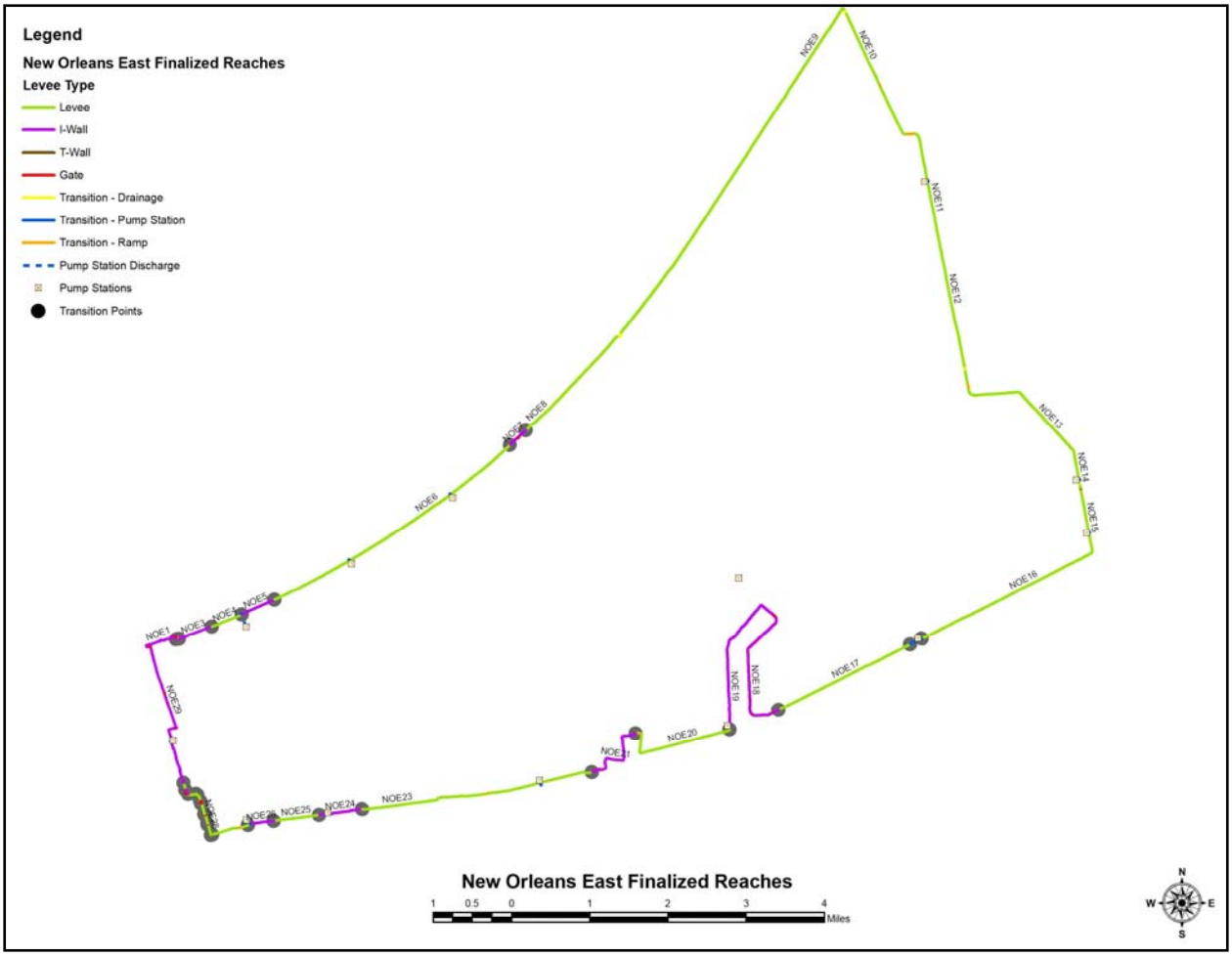

Figure 5. Schematic representation of the the New Orleans East HPS.

Probabilistic Risk Model

Risk associated with the HPS is quantified through a regional hurricane rate (λ) and the probability $P(C > c)$ with which a consequence measure (C) exceeds different levels (c). The loss-exceedance probability per event is evaluated as

$$P(C > c) = \sum_i \sum_j P(h_i) P(S_j \mid h_i) P(C > c \mid h_i, S_j) \tag{2}$$

An annual loss exceedance rate was estimated as follows:

$$\lambda(C > c) = \sum_i \sum_j \lambda P(h_i) P(S_j \mid h_i) \times P(C > c \mid h_i, S_j) \tag{3}$$

where $P(h_i)$ is the probability of hurricane events of type i, $P(S_j|h_i)$ is the probability that the system is left in state j from the occurrence of h_i, and $P(C > c \mid h_i, S_j)$ is the probability that the consequence C exceeds level c under (h_i, S_j). Summation is over all hurricane types i and all system states j in a suitable discretization. Simulation studies of hurricanes for risk analysis require the use of representative combinations of hurricane parameters and their respective probabilities. The outcome of this process is a set of hurricane simulation cases and their respective conditional rates $\lambda P(h_i)$.

Evaluation of the regional hurricane rate λ and the probability $P(h_i)$, the conditional probabilities $P(S_j \mid h_i)$, and the conditional probabilities $P(C > c \mid h_i, S_j)$ is the main objective of the hurricane model, the system model, and the consequence model, respectively. The probability $P(S_j \mid h_i)$ covers the states of the components of the HPS, such as closure structure and operations, precipitation levels, electric power availability, failure modes of levees and floodwalls, and pumping station reliability. To assess the state of the HPS given a hurricane event requires an evaluation of the reliability of individual structures, systems, and components (e.g., levees, floodwalls, pump systems) when they are exposed to the loads and effects of the hurricane (e.g., the peak surge, wave action) and the relationship of these elements to the overall function of the system to prevent flooding in protected areas.

Event Tree

The probability tree of Figure 4 was simplified to determine the rate of flooding elevations and displaying the results as inundation contours within the basins. The processes of transforming inundation to consequences is simplified by grouping communication, warning decision, and public execution into an *exposure factor* parameter applied to lives and property at risk, and grouping power and pumping availability into one event. The resulting event tree appropriately branched out is shown in Figure 6. The top events of the tree are defined in Table 1.

Table 1. Summary of the Event Tree Top Events	
Top Event	**Description**
Hurricane initiating event	The hurricane initiating event is a mapping of hydrographs of the peak flood surge with waves in the study area with a hurricane rate λ. This event was denoted $h_i(x,y)$ and has a probability of occurrence $P(h_i(x,y))$ and a rate of occurrence of $\lambda P(h_i(x,y))$.
Closure structure and operations (C)	This event models whether the hurricane protection system closures, i.e., gates, have been sealed prior to the hurricane. This event depends on a number of factors as illustrated in the influence diagram of Figure 3. The closure structures are treated in groups in terms of probability of being closed in preparation for the arrival of a hurricane. This event was used to account for variations in local practices and effectiveness relating to closures and their operations.
Precipitation inflow (Q)	This event corresponds to the rainfall that occurs during a hurricane event. The precipitation inflow per sub-basin is treated as a random variable.
Drainage, pumping, and power (P)	This event models the availability of power (normal power) for the pump systems. This event is modeled in the event tree to represent a common mode of failure for the pump systems and is included in developing a model for drainage and pumping efficiency or lack thereof including backflow through pumps. The event also models the availability of the pump system and its ability to handle a particular floodwater volume. This event is treated in aggregate with drainage effectiveness and power reliability including backflow through pumps.
Overtopping (O)	This event models the failure of the enclosure/protection system due to overtopping, given that failure has not occurred by some other (non-overtopping) failure mode. If failure (breach) does not occur, flooding due to overtopping could still result.
Breach (B)	This event models the failure of the enclosure/protection system (e.g., levees/floodwalls, closures) during the hurricane, exclusive of overtopping failures). This event includes all other failures and it models all independent levee/floodwall sections. This event is treated using conditional probabilities as provided in Figure 6.

Risk Quantification

Functional Modeling and Computational Considerations. Although the primary purpose of the HPS is to prevent water from entering protected areas during hurricanes, water may also enter the system during rainfall events and from groundwater. The protected areas of the HPS are subdivided into basins and sub-basins. This partitioning is based on the internal drainage and pumping system within each basin. Figure 1 shows these basins and their sub-basins. Basins and sub-basins are divided into sections, or reaches, that have similar cross sections, material strength parameters, and foundation conditions.

The quantification of risk associated with the HPS requires the determination of the amount of water that is expected to reach the protected areas for a particular hurricane. The water entering the protected areas was determined to be the as a result of one or more of the following cases:

- Non-breach events producing overtopping water volume, water volume entering through closures (i.e., gates) that are left open, precipitation, and potential backflow from pumping stations
- Breach events leading to water elevations in protected areas
- Rainfall during hurricane events.

The risk quantification framework was, therefore, based on obtaining estimates of water volumes and elevations entering the HPS due to one of these cases.

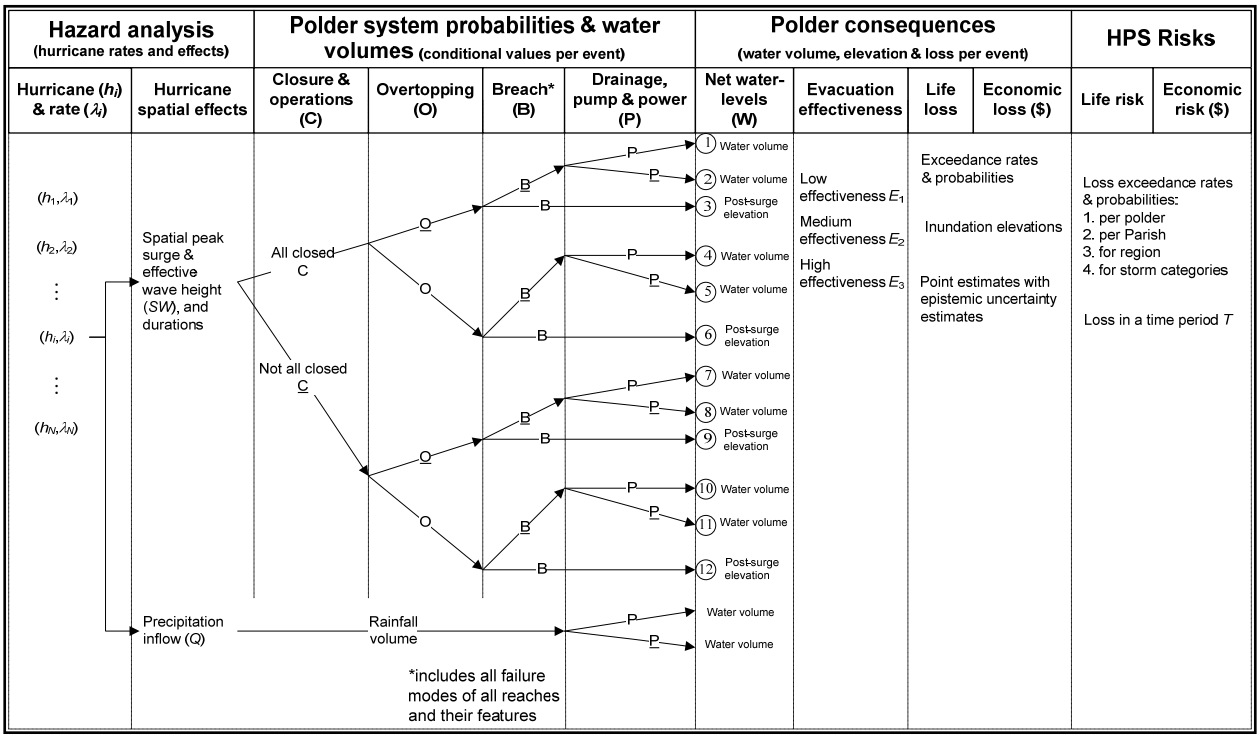

Figure 6. Event tree for quantifying risk. Underlined events (i.e., C, P, O, and B) are the complements of the respective events (i.e., C, P, O, and B).

The event tree presented in Figure 6 shows the two quantities of interest in the net water levels column: water volumes resulting from overtopping, precipitation and open closures, and the post-surge elevation that would result in breaching cases. Potential backflow from pumping stations in non-breach cases was not considered. The branches of the rainfall volume are added to all the other branches for a particular hurricane. Figure 6 shows a total of twelve branches that are constructed per hurricane. The computations needed to quantify risk are presented in a manner that corresponds to the events shown in Figure 6 and were modeled in a spreadsheet to perform the computations. The sections that follow provide the background information and bases behind the approaches used for these computations.

Definition of Basins, Sub-basins, Reaches, and Features. The HPS is divided into basins, sub-basins, reaches, and features. The HPS perimeter is discretized into reaches that define sections of similar physical and engineering characteristics. Initially, the reaches were defined using the beginning and ending stations shown in the original design memoranda. The stations were then adjusted based on examinations of the subsurface material information to form reaches that were expected to have similar performance (reliability). Table 2 illustrates the information structure used to define reaches. Table 2 shows for each reach its unique reach number, length, elevation, design water elevation, reach type (levee, wall, or transition), applicable weir coefficient, and a sub-basin identification. A full description of all the reaches, features and transitions identified in the risk model are shown in Appendix 14.

Table 2. Definition of Reaches						
Reach No.	Length (ft)	Elevation (ft)	Design Water Elevation (ft)	Reach Type	Reach Weir Coefficient	Sub-basin Reference
1	5,000	14.00	8.00	Levee	2.6	Basin1-1
2	10,000	15.00	9.00	Floodwall	3.0	Basin1-2
3	22,500	16.00	11.00	Levee	2.6	Basin1-3
4	6,000	14.00	10.00	Floodwall	3.0	Basin1-4
5	9,000	18.00	13.00	Levee	2.6	Basin1-5
6	7,000	14.00	8.00	Levee	2.6	Basin2-1
7	11,000	15.00	9.00	Floodwall	3.0	Basin2-2
8	7,500	16.00	11.00	Levee	2.6	Basin2-3
9	500	11.00	8.00	Transition	3.0	Basin3-1
10	400	12.00	8.00	Transition	2.6	Basin3-2

The elevations of the tops of walls and levees, adjusted to the current datum, of the entire New Orleans area HPS were developed for use in the suite of hurricane simulations and the risk assessment model calculations of water volumes from overtopping and breaching.

Table 3 lists features that consist of gates and closures within each reach. For each feature, the following information is needed:

- Feature number for unique identification
- Reach in which the feature is located
- A reference value for correlated features that could have different probabilities of closure; however, a set of gates of the same reference value are either all closed or all open
- Length of water inflow when gates are left completely open
- Bottom elevation of gates
- Probability of not closing gates

Data were collected from design documents, construction drawings, and studies conducted by other IPET teams to develop detailed descriptions of the basins. Maps were assembled from aerial photos that included latitude/longitude data, geotechnical profiles and boring logs, crest elevations, stationing used to define reaches, and the locations of critical features such as closure gates and pump stations. The information on these maps was confirmed by field surveys of the entire system. Photos, global positioning coordinates, and notes were taken during these surveys to document each feature and reach used in the risk model. This process has resulted in a comprehensive description of the HPS.

Hurricane Hazard Analysis. The hurricane hazard analysis method parameterizes hurricanes using their characteristics at landfall. The following parameters were considered:

- Central pressure deficit at landfall
- Radius to maximum winds at landfall
- Longitudinal landfall location relative to downtown New Orleans
- Direction of storm motion at landfall
- Storm translation speed at landfall

- Holland's radial pressure profile parameter at landfall (Holland 1980)

Using these values and historic events, the recurrence rate is estimated for hurricane events in a neighborhood of the region of interest, the joint probability density function of the hurricane parameters in that neighborhood. The possible combinations of winds, surges, and waves would be computationally demanding if every combination was run through the ADCIRC models (ADCIRC, 2006). To reduce the number of runs, a response surface approach was used. In this approach, a relatively small number of hurricanes are selected and used to calculate the corresponding surge and wave levels at the sites of interest. Then a response surface model is fitted to each response variable (surge or wave level at a specific site). Finally, a refined discretization of parameter space is used with the response surface as a proxy model in place of the range of possible events to represent the hurricane hazard. The outcomes of these computations are combined surge and effective wave values at particular locations of interest along the hurricane protection system, e.g., representative values at the reaches.

Table 3. Definition of Gate and Closure Features with Respective Reaches

Feature No.	Reach No.	Correlated Features	Length (ft)	Bottom Elevation (ft)	Not-closed Probability
1	1	1	500	5.00	0.10
2	1	1	500	5.00	0.15
3	2	3	400	6.00	0.10
4	2	3	400	7.00	0.20
5	2	3	400	5.00	0.10
6	3	3	600	5.00	0.15
7	4	7	600	7.00	0.20
8	4	8	600	6.00	0.10
9	5	9	500	6.00	0.10
10	5	9	500	5.00	0.01

The water elevation required by risk model as a loading is taken as a hydrograph of the surge elevation plus wave setup and runup at each reach in the system. Table 4 illustrates information and results related to hurricane simulations that include the following:

- Hurricane run numeric identification
- Hurricane rates
- Reach overtopping volume mean value and standard deviation with computational models based on hydraulic engineering provided in subsequent sections

Hurricane rate modeling and prediction methods are then used to compute the corresponding exceedance rates to h_i values and are denoted as λ_i in Figure 6. Also, the water elevation in a basin after a breach is termed the post-surge elevation. This post-surge elevation in a basin could be higher than the applicable lake or river water level. A breach model was developed to compute this elevation as provided in subsequent sections.

The epistemic uncertainties in both the surge/wave elevation and the rates are considered. Figure 7 illustrates surge water elevation as a function of time, i.e., hydrographs, at stations defining the HPS for one storm.

Overtopping Flow Rate, Volume Models, and Probabilities. The *overtopping rate* can be computed using the rectangular weir formula (Daugherty et al. 1985). The overtopping water flow has the elevation H and width L. If the water is assumed to be an ideal liquid, it can be shown using the energy conservation law that the flow rate Q (L^3/T) is given by the following equation:

$$Q = \frac{2}{3}(2g)^{1/2} LH^{3/2} \tag{4}$$

where g is the acceleration of gravity. The actual flow rate over the weir is known to be less than ideal (Daugherty et al. 1985) because the effective flow area is considerably smaller than the product LH.

The model can be enhanced further for engineering applications by replacing the term $2/3\ (2g)^{1/2}$ in Equation 4 by the empirical coefficient, known as the weir coefficient C_w, so that Equation 4 takes on the following form:

$$Q = C_W LH^{3/2} \tag{5}$$

where

$$C_W = \begin{cases} 3.33 & \text{if } L \text{ and } H \text{ are given in inch-pound units} \\ 1.84 & \text{if } L \text{ and } H \text{ are given in SI units} \end{cases} \tag{6}$$

Note that the C_w for the ideal fluid case is $2/3\ (2g)^{1/2}$ which is equal to 2.95 m/s^2. This coefficient is assumed to have a coefficient of variation (COV) of 0.2. C_W takes a value of 3.0, 2.6, and 2.0 for floodwalls, levees, and gates, respectively, with an assumed COV of 0.2 in inch-pound units (L and H in feet).

For the application considered, the mean volume of the overtopping (OT) water μ_V for a given reach can be calculated as

$$\mu_V = C_w L \int \left[\max\left(X_s h_s(t) - H_r, 0 \right) \right]^{3/2} dt \tag{7}$$

where a surge hydrograph is represented by $h_s(t)$ as illustrated in Figure 7; H_r is the reach height; L is the reach length; C_w is the weir coefficient with a COV of 0.2, and a mean of 3.0, 2.6, and 2.0 for floodwalls, levees, and gates, respectively; X_s is an aleatory uncertainty random factor with a lognormal distribution (0.20 log standard deviation and a median of 1.0) that accounts for variability in surge height.

Table 4. Hurricane Runs, Rates, and Reach Overtopping Volume Results							
Hurricane Run No.	Hurricane Rate (events/year)	Overtopping Volume (ft^3)					
		For Basin1-1		For Basin1-2		For Basin2-1	
		Mean	Standard Deviation	Mean	Standard Deviation	Mean	Standard Deviation
1	1.00E-01	0.00E+00	0.00E+00	0.00E+00	0.00E+00	8.28E+07	1.66E+07
2	5.00E-02	0.00E+00	0.00E+00	0.00E+00	0.00E+00	1.07E+08	3.31E+07
3	1.00E-02	6.57E+07	1.22E+07	8.28E+07	1.66E+07	8.28E+07	1.66E+07
4	1.00E-02	7.87E+07	2.11E+07	8.28E+07	1.66E+07	8.28E+07	1.66E+07
5	1.00E-02	0.00E+00	0.00E+00	0.00E+00	0.00E+00	9.67E+07	3.30E+07
6	1.50E-01	0.00E+00	0.00E+00	0.00E+00	0.00E+00	7.92E+07	1.89E+07
7	5.00E-03	1.24E+08	2.39E+07	1.90E+08	3.76E+07	1.90E+08	3.76E+07
8	9.00E-02	8.69E+07	2.99E+07	7.99E+07	1.99E+07	6.78E+06	1.79E+07
9	1.00E-02	0.00E+00	0.00E+00	0.00E+00	0.00E+00	1.03E+08	2.43E+07
10	5.00E-02	0.00E+00	0.00E+00	0.00E+00	0.00E+00	1.03E+08	3.21E+07

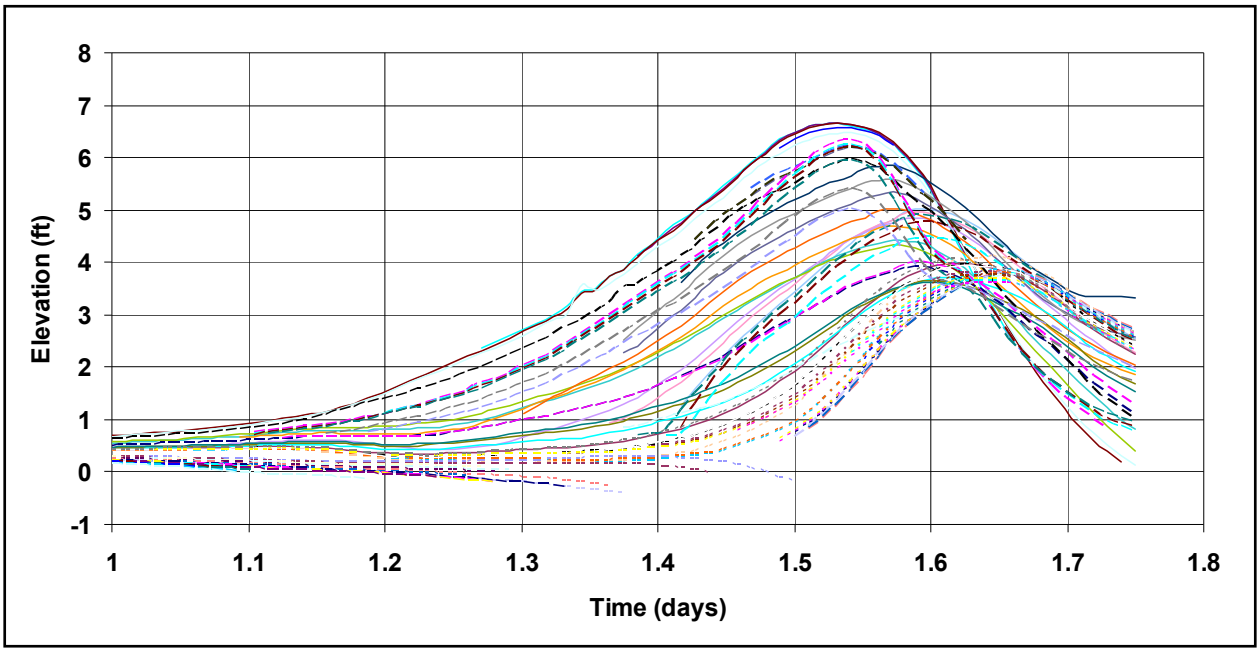

Figure 7. Hydrographs at selected stations defining the hurricane protection system for a national storm.

The variance of the water volume for each case is computed based on the coefficient of variation (δ) of the weir coefficient as follows:

$$\sigma_{Vi}^2 = (\mu_{Vi}\delta_{Cw})^2 \tag{8}$$

where μ_{Vi} is provided by Equation 7, and the coefficient of variation (δ_{Cw}) of the weir coefficient is taken as 0.2.

The cumulative distribution function (CDF) of the total water volume for a sub-basin of n reaches can be computed as follows:

$$F_V = \sum_{i=1}^{n} p_i F_{V_i} \tag{9}$$

where p_i = a overtopping probability, and F = CDF of the total water volume. The overtopping probability can be treated as a binary variable and Equation 9 is still valid. Equation 13 is also based on the assumption of perfectly correlated overtopping volume over the length of a reach, but non-correlated among reaches. Once the total volume is obtained from all overtopping and breach cases, the net volume (as a random variable) needed for consequence analysis can be computed by adding to it water volume from rainfall and wave runup minus the effect of pumping. The pumping system in New Orleans is designed to remove rainfall from tropical storms up to a 10-year event. The effect of pumping on sub-basin inflow water volumes can be approximated by subtracting a portion of the 10-year rainfall that considers degraded pump reliabilities and efficiencies as a function of water level accumulated in a sub-basin.

As was stated previously, Table 4 provides typical results for a reach. Several hypothetical reaches are listed, and overtopping results that were aggregated by sub-basins are illustrated in Table 5. In this example, the basin is assumed to contain one or more sub-basins. The overtopping results for this sub-basin include the overtopping volume based on an overtopping condition, i.e., $V|O$. The overtopping (O) probability, i.e., $P(O)$, can be computed using system reliability concepts as:

$$P(O) = 1 - \prod_{i=1}^{m} (1 - P_i(O)) \tag{10}$$

where $P_i(O)$ is the probability of overtopping of reach i in a sub-basin with m reaches. Thus, Equation 10 expresses the probability that one or more reaches will experience overtopping in a given sub-basin.

The HPS includes *features* that could contribute to water volume making its way to the protected areas during a hurricane. These features include closure structures, i.e., gates, that are left open or failed to close; and localized changes in levee or floodwall elevations that create a transition in the HPS.

These features are identified within each reach and assigned to sub-basin in case of nonperformance. For the closure structures case, the water volume resulting from the closure structure for a given hurricane can be computed based on respective gate non-closure probabilities, width of the closure structure, elevation of the bottom of the structure, and Equation 7. The water volume associated with the localized changes in levee or floodwall elevations requires identifying the changes in elevation and the lengths over which the elevation varies, and the volume is computed using Equation 7 treating the transition as a reach. Table 5 shows a tabulated structure for computing volumes associated with features.

Breach Elevation and Volume Models. Three cases of breach failure within reaches are considered. The risk quantification was effectively performed by examining three cases of breach failure that correspond to branches presented in the event tree of Figure 6. The three cases are breach given overtopping, breach given no overtopping, and breach due to transition failure. A full description of the breach model is presented in Appendix 9.

The first case of breach given overtopping is primarily driven by erosion resulting from overtopping water flow. Fragility curves for these cases were developed expressed as failure probabilities as functions of water depth starting from zero to overtopping. An example fragility curve is shown in Figure 8.

Table 5. Tabulated Structure for Scenario Water Volumes for a Hurricane by Sub-basin

Sub-basin Identifier	Overtopping Volume (ft^3)		Precipitation Volume (ft^3)		Closure Related Volume (ft^3)		Breach Volume (ft^3)		Total Volume (ft^3)	
	Mean	Standard Deviation	Mean	Standard Deviation	Mean	Standard Deviation	Mean	Standard Deviation	Mean	Standard Deviation
Basin 1-1	0.00E+00	0.00E+00	6.67E+05	4.67E+05	1.33E+05	2.67E+04	4.00E+05	8.01E+04	1.20E+06	4.75E+05
Basin 1-2	0.00E+00	0.00E+00	6.57E+05	4.60E+05	1.31E+05	2.63E+04	3.94E+05	7.89E+04	394272	4.67E+05
Basin 1-3	6.90E+07	1.28E+07	6.90E+06	4.83E+06	1.38E+06	2.76E+05	4.14E+06	8.27E+05	4137210	1.37E+07
Basin 1-4	8.69E+07	1.74E+07	8.69E+06	6.08E+06	1.74E+06	3.48E+05	5.21E+06	1.04E+06	5213880	1.84E+07
Basin 1-5	8.69E+07	1.74E+07	8.69E+06	6.08E+06	1.74E+06	3.48E+05	5.21E+06	1.04E+06	5213880	1.84E+07
Basin 2-1	8.69E+07	1.74E+07	8.69E+06	6.08E+06	1.74E+06	3.48E+05	5.21E+06	1.04E+06	5213880	1.84E+07
Basin 2-2	9.12E+07	3.14E+07	9.12E+06	6.39E+06	1.82E+06	3.65E+05	5.47E+06	1.09E+06	5474700	3.20E+07
Basin 2-3	8.38E+07	2.09E+07	8.38E+06	5.87E+06	1.68E+06	3.35E+05	5.03E+06	1.01E+06	5030550	2.17E+07
Basin 2-4	7.12E+06	1.88E+07	7.12E+05	4.98E+05	1.42E+05	2.85E+04	4.27E+05	8.54E+04	427140	1.88E+07

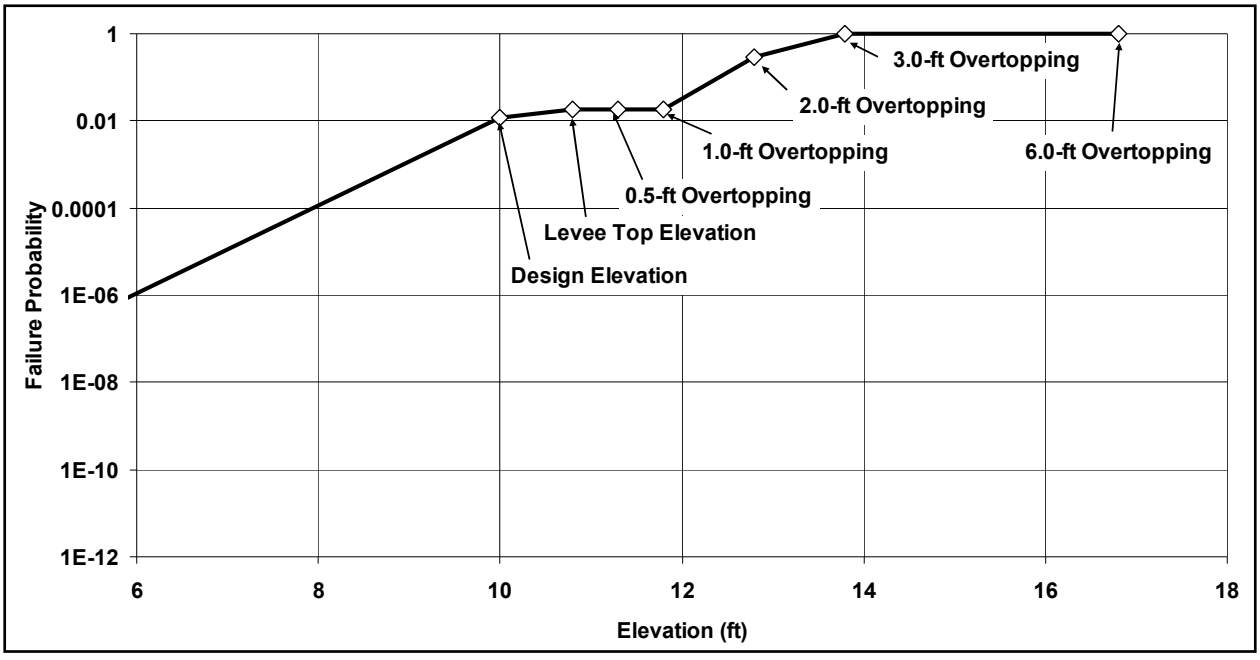

Figure 8. Typical fragility curve for a levee, floodwall, or transition

The breaching scenarios require knowledge of the average breach length and depth and of the surge hydrograph at the breach location in order to determine basin inflows. The HPS condition after Katrina was reviewed to identify basic characteristics of the major breaches in order to develop general rules to use in the risk model for estimating breach dimensions. One critical characteristic that determines the volume of water flowing through a breach is the duration of time that the breach is open. During Katrina, the breaches could not be repaired in time to have an effect on the level of water achieved inside the basins. The duration that the breach is open was, therefore, assumed to have no effect on inflow volumes and water elevations.

The London Avenue and 17th Street Canal breaches of New Orleans that occurred during Katrina before the water level in the canals reached the top of wall and appear to have been the result of the deflection of floodwalls, seepage, or foundation failure. This case is an example of a breach given no overtopping scenario in the risk analysis. The high water marks (HWM) experienced during Katrina inside the Orleans basin where the canal breaches occurred and the length of time that surge elevations exceeded lake levels in the canals were examined. The HWM experienced during Katrina in the basins were very close (within about 1 ft) to the peak surges in the canals. For example, the London Avenue South breach occurred when the canal water level was at about 7 to 8 ft, or 3 ft or so below the top of wall. The peak surge in the area was about 10 to 11 ft and HWM is also about 10 ft. The hydrographs experienced in those areas show that the duration of the surge elevation exceeding the elevation at failure was on the order of several hours. The water elevations inside the basin, therefore, closely followed the surge levels. The inverts of the canal breaches were at or below the normal lake level; therefore water flowed back into the lake after the surge passed. Based on this case and other similar cases, the peak surge level can be used as the water elevation achieved inside the basin when a catastrophic breach (full levee height) occurs during a non-overtopping event, and the following non-overtopping breach assumptions can be used:

- All non-overtopping breaches that are a result of a structural or foundation failure would be catastrophic (full depth of levee or floodwall).

- The breach depth would extend to or below lake or river level.

- The maximum interior water levels caused by the breach would be the same as the maximum surge level experienced adjacent to the breach.

For the case of a breach during an overtopping event, a probabilistic model for overtopping erosion was developed such that a levee (or a floodwall) is expected to show different breach inverts based on the amount of overtopping from surge or waves and the soil type at the levee's protection side. In the case where the breach invert is higher than lake or river level, the depth and length of the breach, the duration of time that the surge exceeds the breach invert, and the weir coefficient through the breach are required to calculate inflow volumes. The breach widths for the levees and floodwalls could also be expected to be similar to that experienced during Katrina. Breach widths at the major canal breaches varied (from about 450 to 1,000 ft) but were all on the order of several hundred feet. At the Industrial Canal of New Orleans where overtopping did occur, the two Lower Ninth Ward breaches were similar in width to the other canals where overtopping did not occur, and the depths of the breaches were below the normal

canal water levels so water also flowed back through these breaches when the surge passed. Based on these observations, using the peak surge level as the maximum water elevation achieved inside the basin would be appropriate when a catastrophic breach (full levee height) occurs during an overtopping event. Therefore, for a breach that occurs during an overtopping event, the following assumptions are used in the risk model:

- Breaches result from an erosion or seepage failure mode due to overtopping from surge and/or waves.
- The depth of overtopping required to cause a breach is dependent upon soil properties, and the breach size is also dependent upon soil properties as assumed in Table 6.
- Durations of overtopping are based on the surge hydrographs.
- Breach sizes for transitions can be estimated using the same values provided in Table 6.

Failure modes, performance functions, basic random variables, and computational procedures of failure probability can be performed according to Equations 9 to 12. The failure probabilities of n failure modes for all reaches in a basin are denoted as $p1, p2, \ldots, p_n$. The breach failure probability for a sub-basin (P_B) can be computed as (assuming that the reach failures are statistically independent events)

$$P_B\left(\text{Sub-basin}\right) = 1 - \prod_{i=1}^{n}\left(1 - P_i\right) \tag{11}$$

Thus, Equation 11 gives the probability that one or more reaches within a sub-basin will suffer a breach. Equation 11 can be used for the cases of probability of breach given overtopping, the probability of breach given non-overtopping, and the probability of breach for transitions.

The surge and wave hydrograph produced by a hurricane is used to compute the water volume entering a basin during levee overtopping or breaching and the maximum water elevation within the basin. In the case of levee overtopping, the water elevation within a basin is based on a water volume computed and the duration of overtopping. If a breach occurs and the invert of the breach is below the final elevation of the adjacent body of water, the water elevation is the elevation of that body of water. If the breach invert is above the final elevation of the adjacent body of water, the water elevation is based on a water volume entering the basin computed using the duration that the surge is above the breach invert. The topography of the basin, and the drainage and pumping models were used to construct this relationship. An example of one of these relationships is shown for New Orleans East basin Figure 9 for the sub-basins shown in Figure 1. For the purposes of the risk model, rather than using fitted curves, stage-storage relationships were numerically evaluated and tabulated in increments of 1 ft of elevation and linear interpolation was used.

Table 6. Breach Size Due to Overtopping							
Material	Symbol	Overtopping Depth (ft)					
		0 to 2 ft		2 ft to 5 ft		>5 ft	
		Depth (ft)	Width (ft)	Depth (ft)	Width (ft)	Depth (ft)	Width (ft)
Hydraulic Fill	H	1.569E+01	3.435E+02	1.680E+01	4.005E+02	1.766E+01	4.305E+02
Clay	C	8.334E+00	4.515E+01	8.787E+00	1.350E+02	1.250E+01	1.350E+02
Sand	S	1.529E+01	3.000E+02	1.765E+01	3.450E+02	1.845E+01	3.795E+02
Unknown (Average)	U	1.503E+01	2.296E+02	1.590E+01	2.935E+02	1.724E+01	3.150E+02
Wall	W	1.503E+01	2.296E+02	1.590E+01	2.935E+02	1.724E+01	3.150E+02

Water Interflow among Basins and Sub-basins. As illustrated in Figure 1, several basins of the HPS can be divided into several sub-basins. Consequently, the water entering a sub-basin may, under certain conditions, overflow into adjacent sub-basins. Thus, prior to calculating the final volume of water in the sub-basins and basins for each of the twelve branches in the event tree of Figure 6, the interflow among sub-basins in a basin needs to be considered.

Given a basin consisting of m interconnected sub-basins with mean pre-interflow water volumes V_i, i=1, 2, …, m, the post-interflow water volumes can be computed as:

$$[V_{f,1}, V_{f,2}, \ldots, V_{f,m}] = \text{Interflow}\ (V_1, V_2, \ldots V_m) \tag{12}$$

where $V_{f,i}$ is the mean final post-interflow volume in sub-basin i, and the function "Interflow" is represented by the algorithm illustrated in Figure 10. For simplicity, the COV on water volume in a sub-basin is preserved through the interflow function, i.e., the COV on the post-interflow volume for a given sub-basin equals the pre-interflow COV.

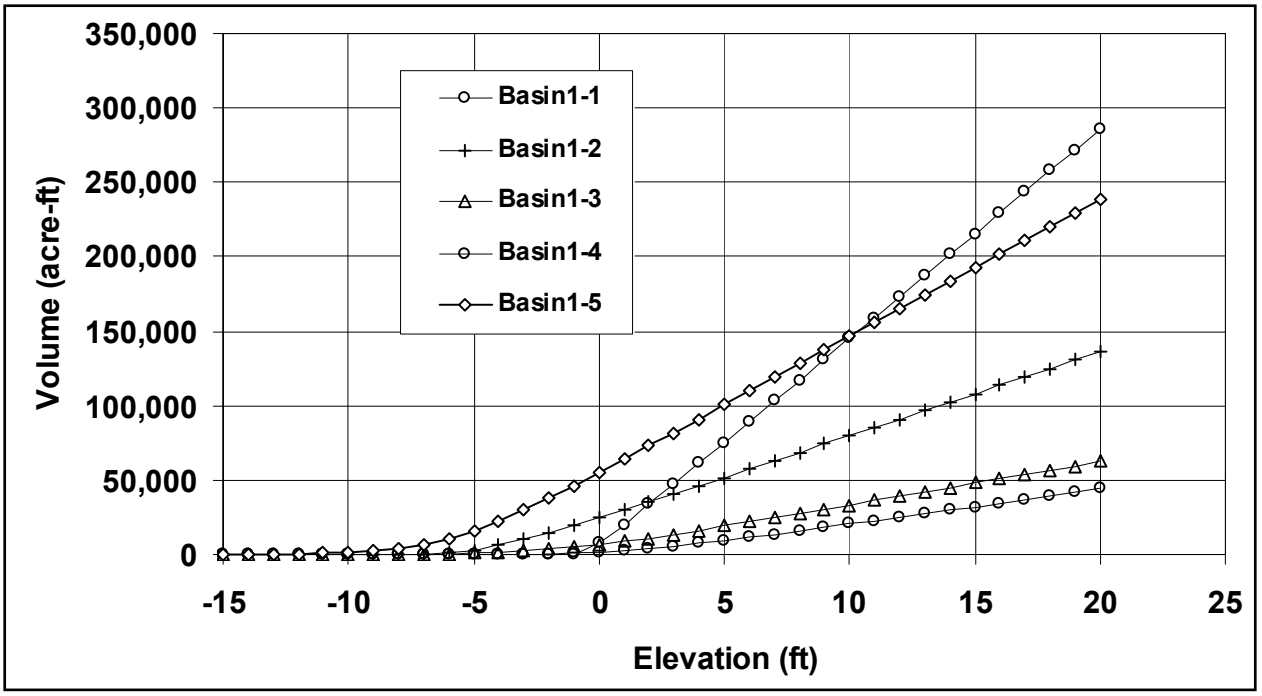

Figure 9. Stage-storage relationships of sub-basins and basin New Orleans East (1 acre-ft = 43,560 ft^3).

Expressed in terms of elevations, the post-interflow elevation of water in a sub-basin, E_f, can be obtained as:

$$E_f = g(V_f) \tag{13}$$

where the function g defines the stage-storage relationship for the sub-basin, i.e., water elevation (stage) as a function of water volume (storage). Typical stage-storage curves are illustrated in Figure 10. Using first-order approximation for uncertainty propagation, the variance of the final water elevation can be obtained as

$$\sigma_{Ef}^2 = \left(\left. \frac{dg}{dV} \right|_{V_f} \right)^2 \sigma_{Vf}^2 \tag{14}$$

where the derivative of the stage-storage relationships with respect to a change in volume evaluated at V_f can be determined numerically.

Event Tree Branch Probabilities and Water Elevations. The event tree of Figure 6 consists of 12 branches per hurricane. This section develops and summarizes the probabilities for these branches.

The event tree includes the following primary independent sub-basin-level events:

- C is the event that all gates within a sub-basin are closed.
- P is the event that all pumps in the sub-basin operate during the hurricane.
- B is the event that at least one reach (or one of its transition features) in a sub-basin is breached.

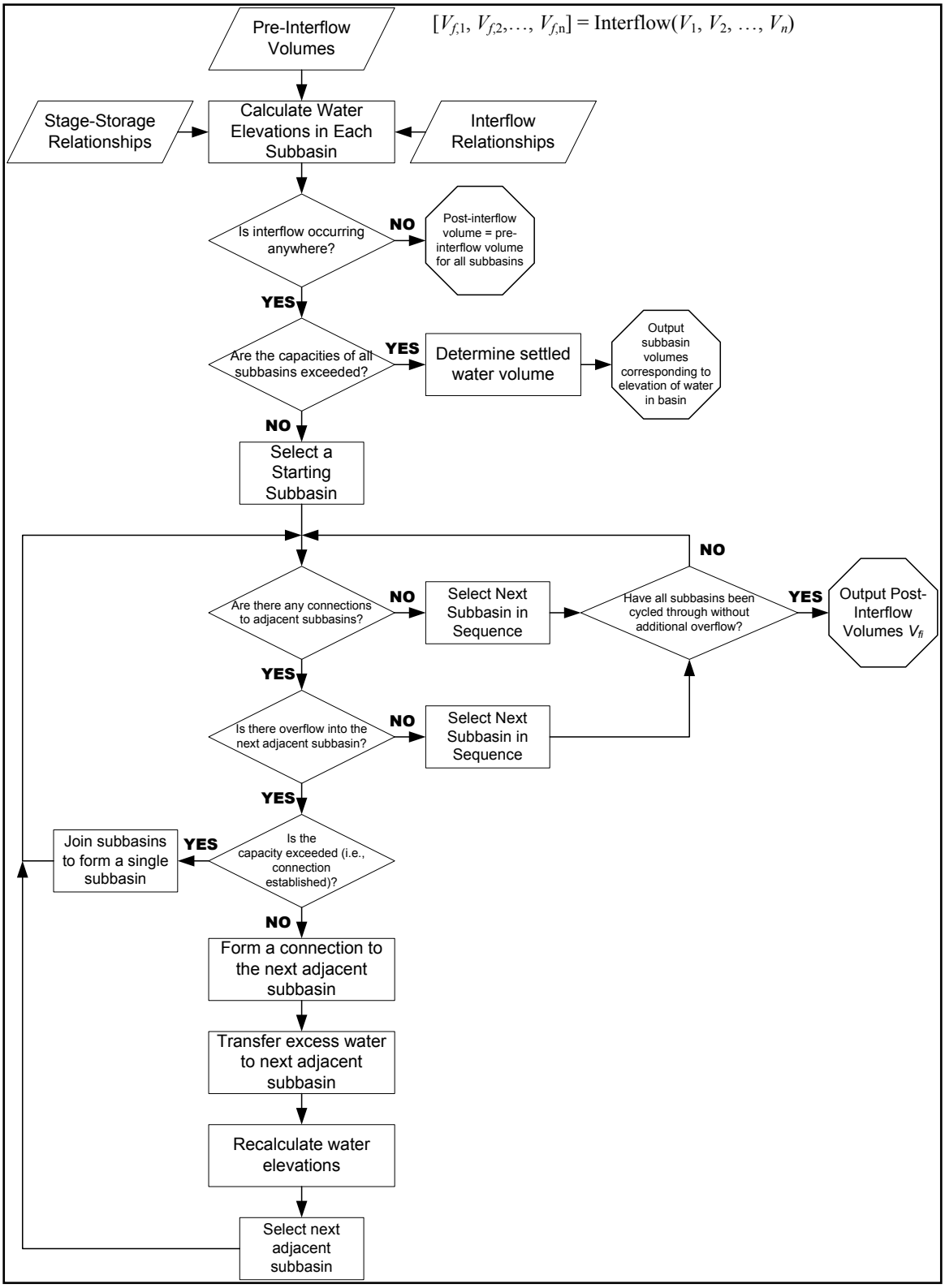

Figure 10. Algorithm for sub-basin interflow function.

These events were used to construct Table 7 that summarizes the expanded expressions for the probability of each branch in the event tree of Figure 6. Table 8 summarizes the respective procedures for water volume and elevation computation. It should be noted that the water volume associated with the branches involving *not-all-gates closed* requires a procedure to account for all possible combinations of not-all-gates closed. Let i be the index denoting a unique scenario among the set of 2^n scenarios of gate open/closed combinations (n = number of uncorrelated gates). The mean water volume (μ) for use in the not-all-gates closed branches is

$$\mu_{\underline{C}} = \frac{\sum_{i=1}^{2^n} p_i \mu_{\underline{Ci}}}{(1 - p_C)} \tag{15}$$

where p_c is the probability of all gates closed, $\mu_{\underline{Ci}}$ the mean volume associated with not-closing gates according to the i^{th} scenario, and p_i the multinomial probability of the i^{th} scenario. The volume variance for use in the not-all-gates closed branches is:

$$\sigma^2_{\underline{C}} = \frac{\sum_{i=1}^{2^n} p_i^2 \sigma^2_{\underline{Ci}}}{(1 - p_C)^2} \tag{16}$$

where $\sigma^2_{\underline{Ci}}$ is the volume variance associated with not-closing gates according to the i^{th} scenario.

The sub-basin interflow analysis as previously described is performed subsequent to Table 8 procedures. Uncertainty propagation from the volume (V) moments (μ_V and σ_V^2) to elevation (E) moments (μ_E and σ_E^2) using the tabulated stage-storage relationship for a sub-basin can be based on linear interpolation. Linear interpolation is used to define this relationship since the increment size of 1 ft for tabulation has been selected relatively small for this purpose.

The results produced so far can be summarized by sub-basin, and for all storms and the branches of the event tree in the form of water elevation (mean and variance) and occurrence rate. These results can be used to evaluate elevation-exceedance rate for a sub-basin at selected e values as follows:

$$\lambda(E > e) = \sum_{All\ storms\ \&\ branches} \lambda P(h) P(S \mid h) P(E > e \mid h, S) \tag{17}$$

Table 7. Computational Summary for Branches of the Event Tree of Figure 6 for a Hurricane and a Basin

Branch	Branch Probability (See Figure 6)
1. Non-Breach	$P(C)P(P)P(\underline{B}\cap\underline{O}) = P(C)P(P)\left(\prod_i (1-P_i(B\mid\underline{O}))P_i(\underline{O})\right)$
2. Non-Breach	$P(C)P(P)P(\underline{B}\cap\underline{O}) = P(C)P(\underline{P})\left(\prod_i (1-P_i(B\mid\underline{O}))P_i(\underline{O})\right)$
3. Breach	$P(C)P(B\cap\underline{O}) = P(C)\left(1-\left(\prod_i (1-P_i(B\mid\underline{O}))P_i(\underline{O})\right)\right)$
4. Non-Breach	$P(C)P(P)P(\underline{B}\cap O) = P(C)P(P)\left(P(\underline{B})-P(\underline{B}\cap\underline{O})\right) =$ $P(C)P(P)\left(\prod_i ((1-P_i(B\mid O))P_i(O)+(1-P_i(B\mid\underline{O}))P_i(\underline{O}))-\prod_i (1-P_i(B\mid\underline{O}))P_i(\underline{O})\right)$
5. Non-Breach	$P(C)P(\underline{P})P(\underline{B}\cap O) = P(C)P(P)\left(P(\underline{B})-P(\underline{B}\cap\underline{O})\right) =$ $P(C)P(\underline{P})\left(\prod_i ((1-P_i(B\mid O))P_i(O)+(1-P_i(B\mid\underline{O}))P_i(\underline{O}))-\prod_i (1-P_i(B\mid\underline{O}))P_i(\underline{O})\right)$
6. Breach	$P(C)P(B\cap O) = P(C)\left(1-P(\underline{B})-P(\underline{B}\cap\underline{O})\right) =$ $P(C)\left(1-\prod_i ((1-P_i(B\mid O))P_i(O)+(1-P_i(B\mid\underline{O}))P_i(\underline{O}))-\prod_i (1-P_i(B\mid\underline{O}))P_i(\underline{O})\right)$
7. Non-Breach	$(1-P(C))P(P)P(\underline{B}\cap\underline{O}) = (1-P(C))P(P)\left(\prod_i (1-P_i(B\mid\underline{O}))P_i(\underline{O})\right)$
8. Non-Breach	$(1-P(C))P(\underline{P})P(\underline{B}\cap\underline{O}) = (1-P(C))P(\underline{P})\left(\prod_i (1-P_i(B\mid\underline{O}))P_i(\underline{O})\right)$
9. Breach	$(1-P(C))P(B\cap\underline{O}) = (1-P(C))\left(1-\left(\prod_i (1-P_i(B\mid\underline{O}))P_i(\underline{O})\right)\right)$
10. Non-Breach	$(1-P(C))P(P)P(\underline{B}\cap O) = P(C)P(P)\left(P(\underline{B})-P(\underline{B}\cap\underline{O})\right) =$ $(1-P(C))P(P)\left(\prod_i ((1-P_i(B\mid O))P_i(O)+(1-P_i(B\mid\underline{O}))P_i(\underline{O}))-\prod_i (1-P_i(B\mid\underline{O}))P_i(\underline{O})\right)$
11. Non-Breach	$(1-P(C))P(\underline{P})P(\underline{B}\cap O) = P(C)P(P)\left(P(\underline{B})-P(\underline{B}\cap\underline{O})\right) =$ $(1-P(C))P(\underline{P})\left(\prod_i ((1-P_i(B\mid O))P_i(O)+(1-P_i(B\mid\underline{O}))P_i(\underline{O}))-\prod_i (1-P_i(B\mid\underline{O}))P_i(\underline{O})\right)$
12. Breach	$(1-P(C))P(B\cap O) = P(C)\left(1-P(\underline{B})-P(\underline{B}\cap\underline{O})\right) =$ $(1-P(C))\left(1-\prod_i ((1-P_i(B\mid O))P_i(O)+(1-P_i(B\mid\underline{O}))P_i(\underline{O}))-\prod_i (1-P_i(B\mid\underline{O}))P_i(\underline{O})\right)$
Combined Branches 3 and 9	$\left(P(C)+P(\underline{C})\right)\left(P(P)+P(\underline{P})\right)(B\cap\underline{O}) = 1-\left(\prod_i (1-P_i(B\mid\underline{O}))P_i(\underline{O})\right)$
Combined Branches 6 and 12	$\left(P(C)+P(\underline{C})\right)\left(P(P)+P(\underline{P})\right)\left(1-P(\underline{B})-P(\underline{B}\cap\underline{O})\right) =$ $1-\prod_i ((1-P_i(B\mid O))P_i(O)+(1-P_i(B\mid\underline{O}))P_i(\underline{O}))-\prod_i (1-P_i(B\mid\underline{O}))P_i(\underline{O})$

Table 8. Computational Summary for Water Volumes Associated with the Branches of the Event Tree of Figure 6 for a Hurricane and a Basin	
Branch	**Branch Water Volume (See Figure 6)**
1. Non-Breach	Use precipitation volume, with pumping
2. Non-Breach	Use precipitation volume no pumping
3. Breach	Use post-surge breach water elevation, no pumping
4. Non-Breach	Use overtopping and precipitation volume, with pumping
5. Non-Breach	Use overtopping and precipitation volume no pumping
6. Breach	Use post-surge breach water elevation, no pumping
7. Non-Breach	Use precipitation and not-all-closed-closure volume, with pumping
8. Non-Breach	Use precipitation and not-all-closed-closure volume no pumping
9. Breach	Use post-surge breach water elevation, no pumping
10. Non-Breach	Use overtopping, precipitation and not-all-closed-closure volume, with pumping
11. Non-Breach	Use overtopping, precipitation and not-all-closed-closure volume no pumping
12. Breach	Use post-surge breach water elevation, no pumping

Risk Profile by Basin and Storm Categories. Economic and life losses were estimated and results were provided as elevation-loss curves per sub-basin. Figure 11 provides results using notional data for hypothetical sub-basins for the purpose of illustration. Using results from Equation 21 and elevation-loss curves per sub-basin, loss-exceedance curves can be easily developed.

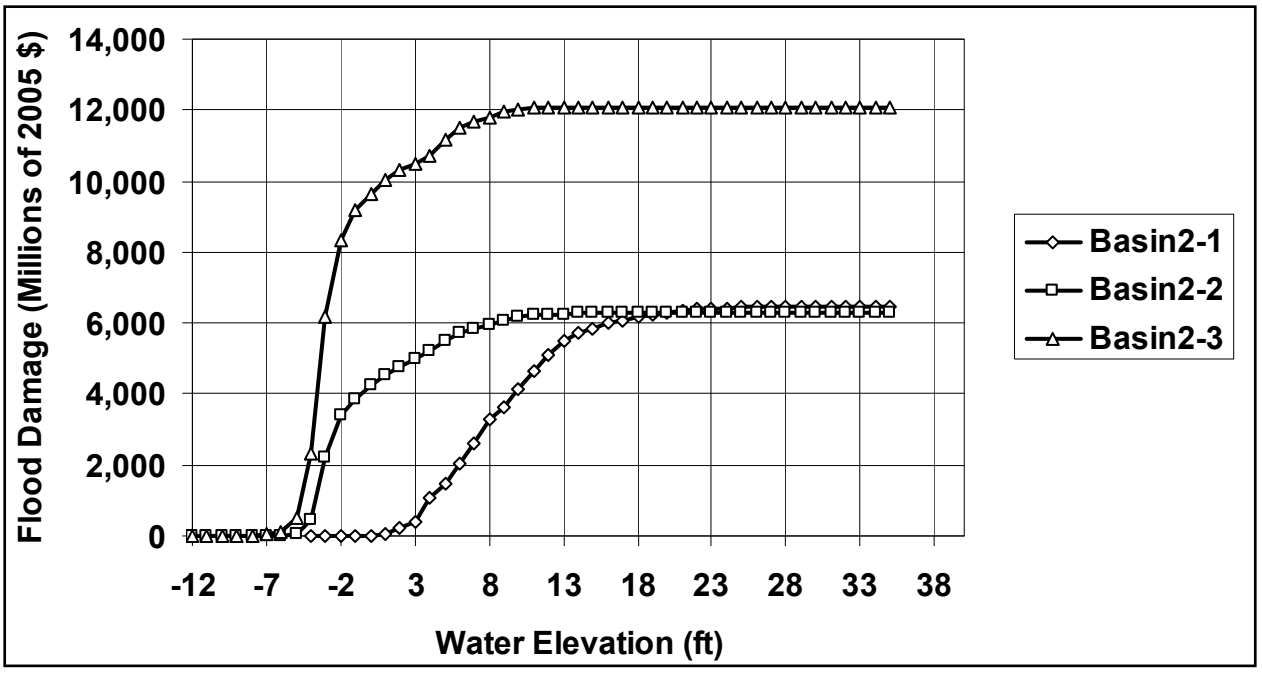

Figure 11. Elevation-loss curves for hypothetical sub-basins.

The risk profiles for basins and storm categories were evaluated by performing the corresponding aggregation similar to what is done for the sub-basins, and results were displayed using curves similar to those provided in Figure 12. The risk profile for the HPS is expressed in

direct economic (as illustrated by Figure 13) and life loss consequences (as illustrated in Figure 14) based upon the stage-damage curves. Inundation maps can be developed as illustrated in Figure 15. The inundation maps can be supplemented with return periods corresponding to respective elevations. This risk profile requires that all storms be evaluated for all possible combinations of all the branches for all the basins with dependency modeling. The number of combination per storm for 8 basins and 12 branches of the event tree is 68,719,476,736. Dependency among the basins has not been examined in order to reduce the number of possible combinations; however, the risk results obtained by examining the individual basins are considered to be adequate for evaluating the relative risks and vulnerabilities of the HPS.

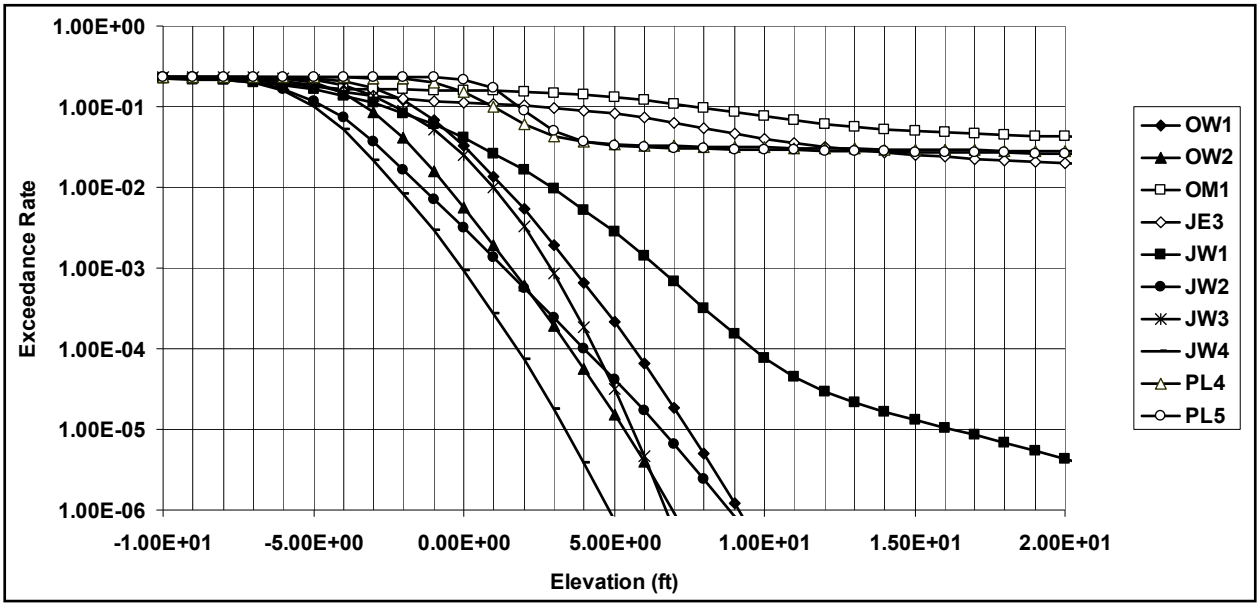

Figure 12. Illustrative overtopping risk profile for hypothetical sub-basin.

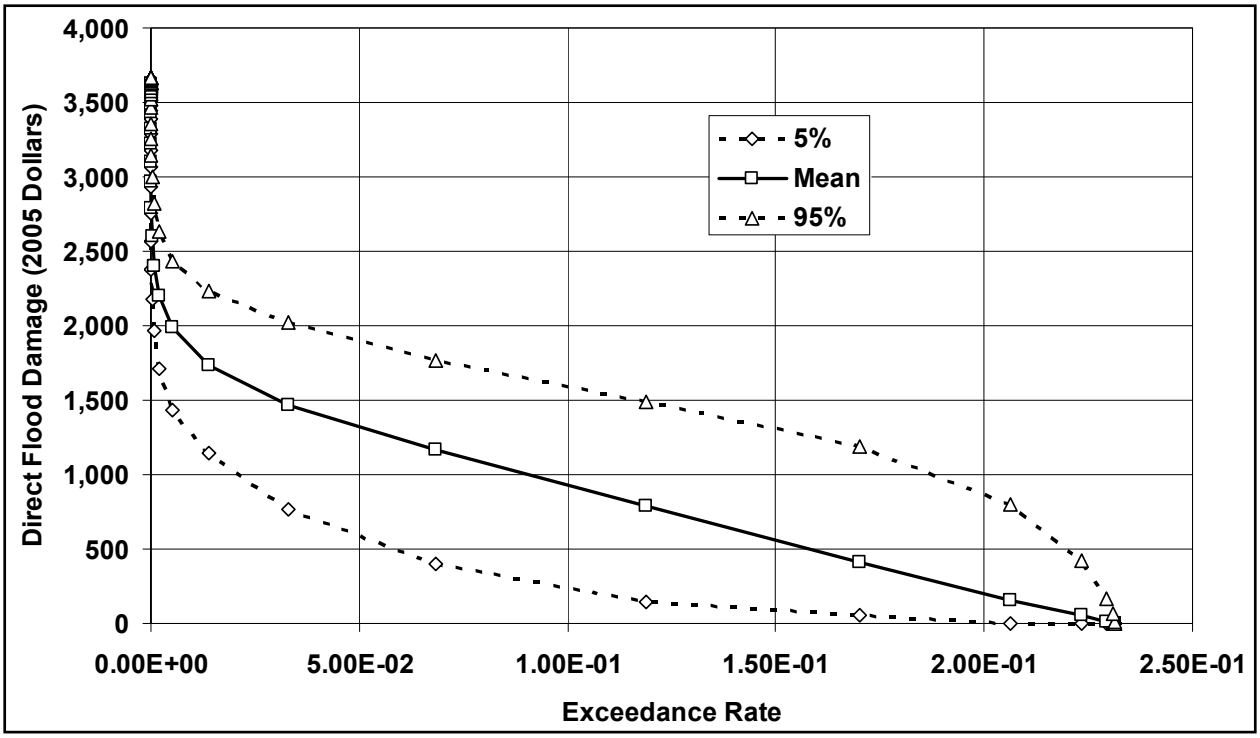

Figure 13. Illustrative direct flood damage risk profile in 2005 dollars for a sub-basin.

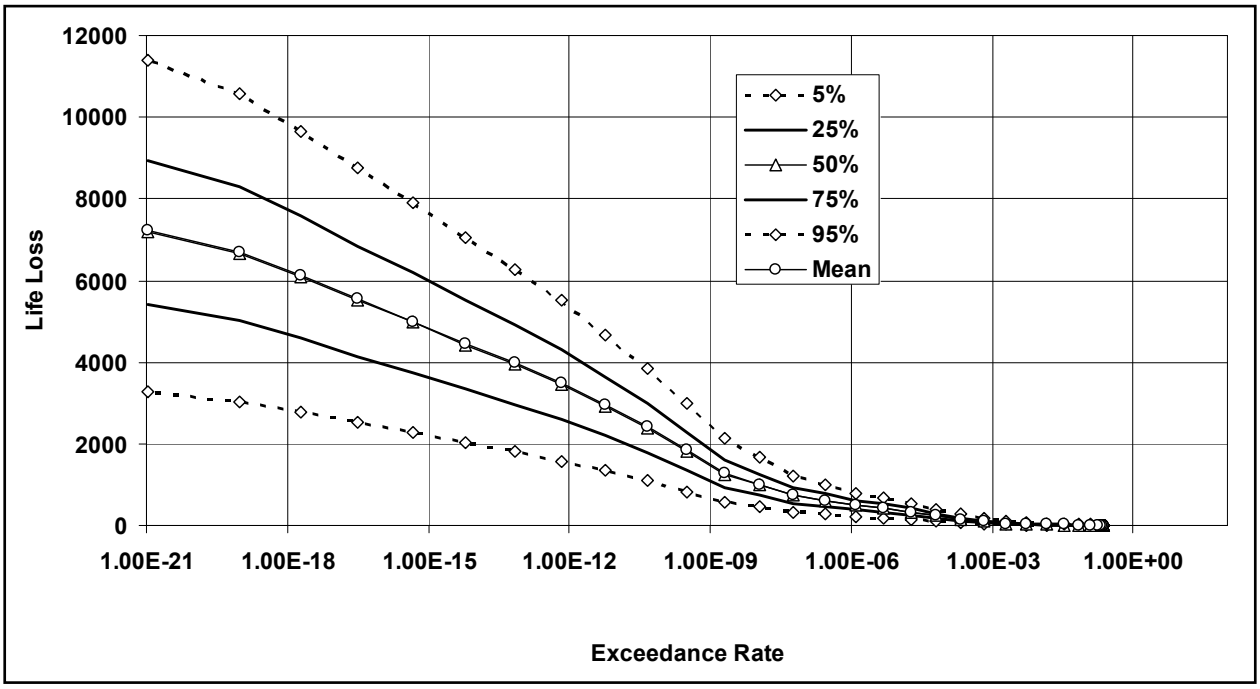

Figure 14. Illustrative direct flood life loss risk profile for a sub-basin.

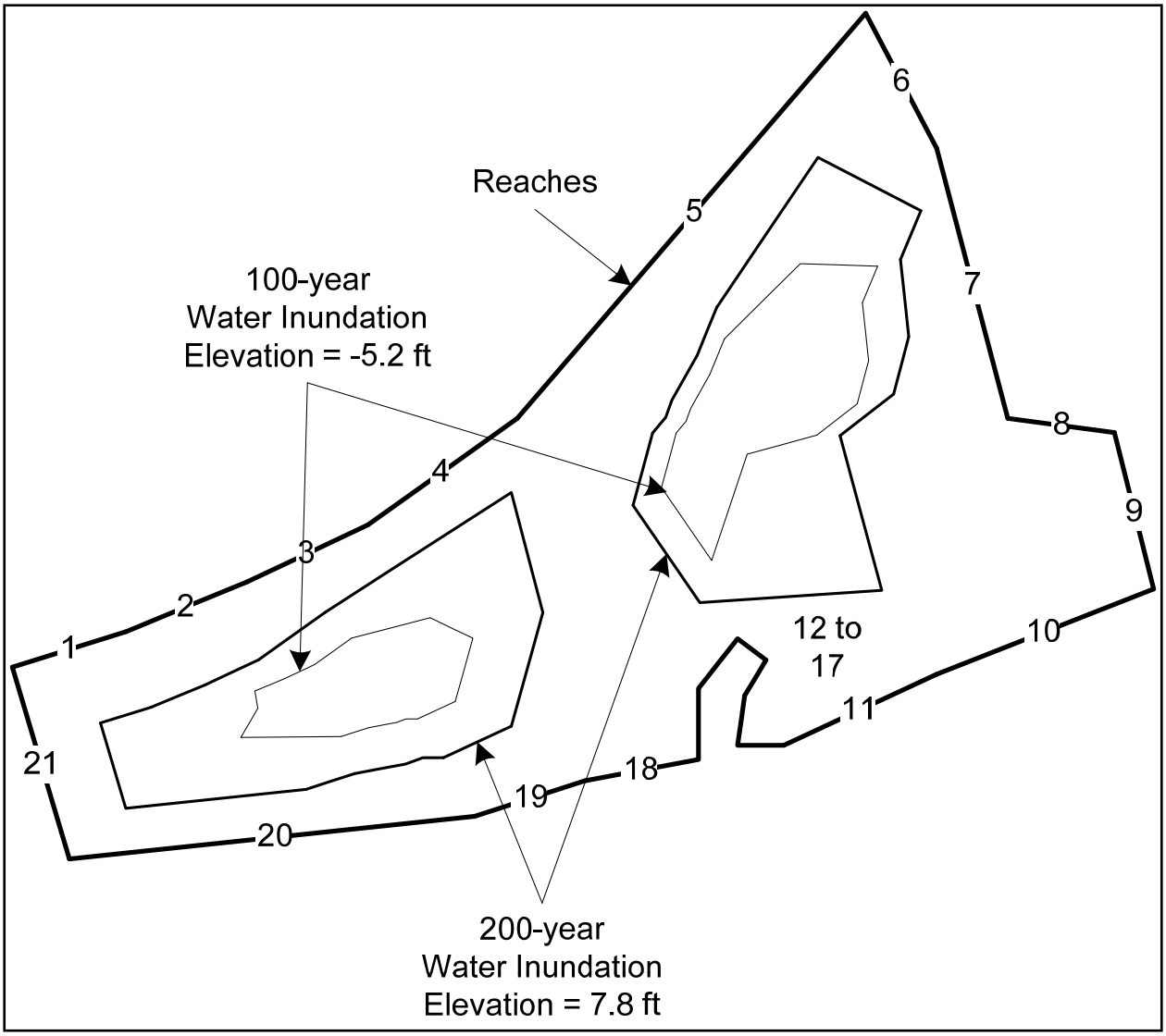

Figure 15. Illustrative inundation map using hypothetical information.

Hazard Analysis[1]

The initiating events selected for study in the risk analysis were based upon the range of hurricanes considered to be possible in the New Orleans area that would be capable of causing widespread damage and flooding. The Risk Analysis Team relied upon the analysis techniques and procedures used by the Storm Team to conduct the hindcast of the Katrina event; however, the approaches were modified to account for the large number of storms that were required to be studied in a probabilistic hazard analysis. Several methods have been used in other studies to quantify hurricane hazard, typically in the context of wind-related risk. The methods available to conduct probabilistic hurricane surge and wave predictions in the context of a risk analysis are limited. These methods are generally classified into three main types: historic (HI), joint probability (JP), and Monte Carlo (MC) simulation methods. Details of the hazard analyses are provided in Appendix 8.

Historical Methods. Historical methods quantify the hazard based on the rate at which the effect of interest (e.g., wind speed or surge or loss) has occurred in the historical record. These methods are fundamentally nonparametric, i.e., they do not assume a specific analytic form for the recurrence rate of the hurricanes or their effects. The primary limitation of purely nonparametric historic approaches is their sensitivity to sample error. Hurricanes are both sporadic and spatially limited so that the flood record over a region can be highly granular despite climatic homogeneity. This granularity derives from both the small number of hurricane parameters experienced in the sample (e.g., intensity) and the randomness of the storm tracks, so that some areas are affected much more strongly than other nearby areas. Consequently, the record at any given site may be unrepresentative of the underlying population, likely being either significantly more or significantly less severe than should be expected.

To reduce the impact of local sample error, some historic approaches include smoothing procedures. For example, the empirical simulation technique (EST) of Sheffner et al. (1996) attempts to smooth the storm parameter granularity through consideration of hypothetical storms obtained by resampling from the historic record, with a random variation of the storm parameters. Similarly, spatial granularity is addressed by adopting alternate hypothetical tracks for the historical storms. Bootstrap resampling in EST also simulates an extended period of record, allowing estimates at recurrence intervals much greater than the actual period of record; this is needed since the nonparametric frequency estimates are based on a plotting position formula. Other smoothing methods introduce parametric assumptions and fit a specific distribution to the hurricane effects L_i calculated from the historic events. An example of the latter type is the 1987 version of the National Hurricane Center Risk Analysis Program HURISK (Neumann 1991). The EST method has been extensively used by USACE and FEMA to identify design events with return periods up to 100 years. Confidence intervals on the results are usually obtained through bootstrapping (resampling) techniques over a large number of life cycles.

Joint Probability Methods (JPM). Joint probability methods attempt to circumvent the vagaries of the local historical record by first determining the local population characteristics of

[1] The hurricane hazard analysis used in the risk studies was developed by the Storm Team and is reported in IPET Volume IV.

a set of parameters that are taken to define the physics of a storm (abstracted from a study of the regional climatological record), and, second, using that knowledge to simulate all significant storms through the use of hydrodynamic models. The number of parameters has, conventionally, been limited to a small number of factors deemed significant in the specification of a storm's wind and pressure fields. The number of parameters must also be held to a minimum in order to avoid the excessively large number of simulations needed to cover a higher-dimensional parameter space. Conventionally, the essential storm parameters considered in a JPM approach include the following: 1) the central pressure depression, measuring storm intensity; 2) a measure of storm size, such radius to maximum winds; and 3-5) three kinematic parameters describing the track (forward speed, direction of motion, and a position, such as coastal crossing point). Additional parameters are introduced as necessary to better describe the flooding mechanisms. For example, the adopted wind model may involve a shape factor (Holland's B) affecting the wind gradients, whereas non-storm parameters such as local astronomic tide amplitude and phase could also be counted as additional JPM parameters. Given a knowledge of local storm occurrence rate coupled with probability distributions for the several parameters, it is possible to integrate over the entire parameter space, attaching vectors in that space to the resulting local surge elevations through hydrodynamic simulations, and in this way obtain the frequency distribution of surge elevation.

Monte Carlo (MC) Simulation Methods. Monte Carlo simulation methods differ in that the possible parameter space is not explicitly integrated, as in JPM, but is instead randomly sampled. These methods use a stochastic representation of the origin, characteristics, and temporal evolution of hurricanes in the general region of interest. Random trajectory and parameter evolution may be represented through Markov processes of suitable order, discrete in time but continuous in state. The state-transition parameters vary spatially and are estimated from the historical record. A large number of hurricane events are derived using this random sampling dynamic model, and the sample is trimmed to retain only those events that are considered to be significant to the region. Hydrodynamic modeling of those events yields a synthetic record that can be evaluated using conventional methods of historical frequency analysis. As with the JPM, if the number of simulations necessary to obtain accuracy is too large, it may be necessary to use a parsimonious combination of high-accuracy runs with supplementary methods such as interpolation and inference from simplified methods. The Empirical Track Model is a MC simulation method proposed by Vickery et al. (2000); other recent studies that use MC simulation include, for example, Powell et al. (2005).

Adopted Approach

The attractiveness of a method depends in general on both the amount of data and the computational resources available, as well as on the objective of the analysis. Regarding the latter, it matters whether (1) interest is in frequent or rare events, (2) the objective is to identify design events with given return periods (return-period analysis) or to find the rate at which certain consequences are exceeded (risk analysis), and (3), in the case risk analysis, whether the losses occur in a small geographical region that may be considered uniformly impacted by any given hurricane or over an extended region where spatial homogeneity of the hurricane loads cannot be assumed. For flood hazard, return-period analysis is generally easier than risk analysis

because hurricane severity may be ranked using surrogate quantities (such as a rough estimate of maximum surge) that are much easier to calculate than the flooding conditions themselves.

The present risk analysis relies primarily on the methods and results of the IPET Storm Team for hazard analysis input. Since medium to long return periods are of interest, historical methods based on limited local samples were deemed unreliable. One might consider the pre- and post-Katrina record in the northern Gulf of Mexico as an example. As noted in a white paper by Resio (2007), included in Appendix 8, Katrina was unprecedented in its combination of intensity and size, and so it was not implicitly represented among the storms constituting the prior record. On the other hand, Katrina is now a part of the record. A historical method would produce markedly different results according to which record, pre- or post-Katrina, was used. In principle, either JP or MC methods could be adopted, and would be less sensitive to the specific historical record, since the possibility of Katrina-like storms combining high intensity and large size would be accounted for in either case, with neither parameter, separately, falling outside the range of prior observations. Monte Carlo approaches, however, may be relatively inefficient, contending with the problem of selecting the potentially damaging events from large suites of simulated hurricane scenarios. This is a difficult problem for the geographically extended and differently vulnerable system being considered. For these reasons, the joint probability approach was selected.

The particular implementation of the JPM analysis used here is fully described in a whitepaper by Resio (2007) that is included here in Appendix 8. This is a primary reference for this section, and for convenience will be abbreviated as R2007; note that R2007, itself, contains several appendices, all of which are also part of Appendix 8. The method is termed JPM-OS, denoting *Optimum Sampling*. The intent of optimum sampling (of the parameter space) is to reduce the number of storm simulations to an acceptable minimum, while adequately covering the range of possibilities. This is a critical requirement, since the hydrodynamic storm surge simulations (using the ADCIRC model with a very high resolution bathymetric and topographic grid) are extremely time consuming, even on large parallel-computer clusters, possibly requiring hundreds of hours. The following sections provide an overview of the JPM-OS approach that was used; R2007 should be consulted for more details.

To implement a joint probability analysis of hurricane flood hazards, it is necessary to select the minimum set of parameters required to accurately describe the flood producing mechanisms. For this work, the primary hurricane description included statistical representations of the following six parameters:

ΔP = central pressure deficit at landfall (mb)
R_{max} = radius to maximum winds at landfall (km)
X = longitudinal landfall location relative to downtown New Orleans (positive if east of New Orleans) (km)
θ = direction of storm motion at landfall, ($\theta = 0$ for tracks pointing north, increasing clockwise) (degrees)
V = storm translation speed at landfall (m/s)
B = Holland's radial pressure profile parameter at landfall (Holland 1980)

In addition to these parameters, the local storm population is also characterized by an overall spatial-temporal storm density or rate of occurrence λ defined as the number of storms occurring per unit distance per unit time within the region.

Although the variation of the storm parameters before and after landfall is also of interest, the fundamental characterization of hurricanes was, by their properties at landfall, defined as crossing the representative landfall line shown in Figure 16 of R2007.

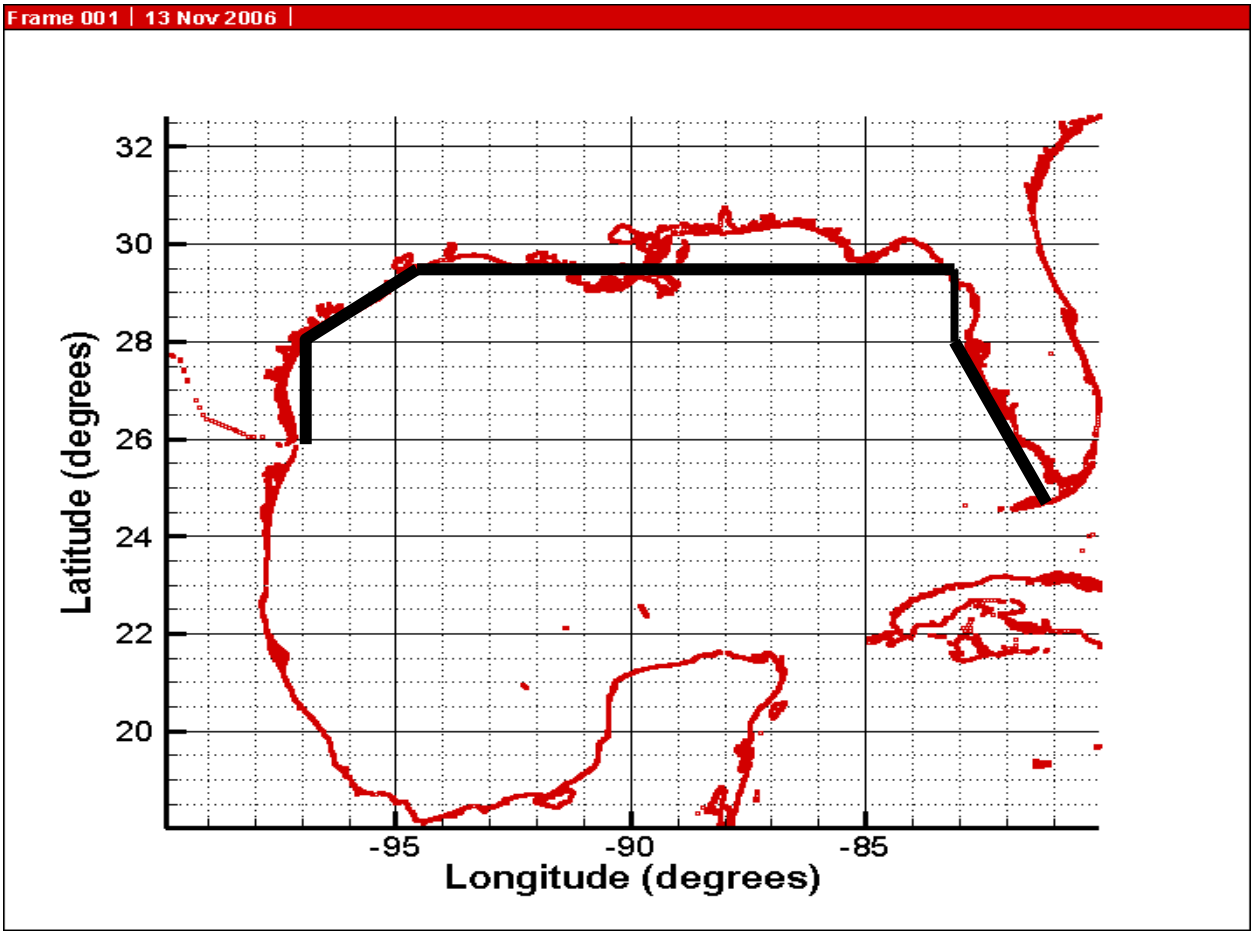

Figure 16. Location of line for analysis of hurricane landfalling characteristics.

Pre- and post-landfall variations relative to the chosen line were based on observed average behavior. For example, storms were taken to weaken at specified rates just prior to and after landfall, with associated variations of storm size. Hence, the main tasks of the hazard quantification for the initiating events in the risk analysis were the estimation of the hurricane recurrence rate and the evaluation of the wave and surge loads over suitable ranges of the characteristic parameters.

Hurricane Recurrence and Parameter Distributions

The period of record for the determination of the necessary parameter distributions was limited to 1941 and later. The reasons for this choice are discussed at length in R2007 but they are basically two-fold. First, the WWII era marked the beginning of high-quality storm data acquisition, thanks in part to advances in military reconnaissance. Second, there is some, not necessarily decisive, indication of decadal variations in hurricane climatology, and the post-1941 choice may properly cover complete cycles (as discussed in the Appendix 8 of this volume), thereby lessening the chance of bias from this source. Furthermore, since only extreme events are of interest, it is not necessary to consider storms too weak to produce the conditions of interest. Consequently, after review of the data, a basic data set consisting of 22 hurricanes with central pressures of 955 mb or less was selected for analysis.

Techniques generally following Chouinard et al. (1997) were used for storm parameter sampling, with an optimum kernel size of 160 to 200 km being indicated. Using this approach, the central pressure distribution was found to be adequately described by a Gumbel distribution

$$F\left(\Delta P \mid x\right) = \exp - \left\{ \exp - \left[\frac{\Delta P - a_0(x)}{a_1(x)} \right] \right\}$$

in which x denotes position along the longitudinal baseline, ΔP is the central pressure depression in megabytes (mb), and (a_0, a_1) are the parameters of the distribution.

The storm radius is taken to be conditional upon central pressure, with large radii being less likely for large pressure deficits. As shown in Appendix A of R2007, observed radii bracket a mean value depending upon ΔP in an approximately Gaussian fashion:

$$P(R_p \mid \Delta p) = \frac{1}{\sigma(\Delta p)\sqrt{2\pi}} e^{-\frac{x^2}{2}}$$

where:

$$x = \left(\frac{R_p - \overline{R}_p(\Delta p)}{\sigma(\Delta p)} \right)$$

with the mean at ΔP given by the linear regression ($\overline{R}_p = 14.0 + 0.3 * (110.0 - \Delta p)$ in which R_p and $\overline{R}_p$ are in nautical miles and Δp is in millibars. Note that R_p is the storm *scaling* radius, which differs slightly from the radius to maximum winds, R_{max}. The standard deviation for the Gaussian spread around the varying mean was taken to be $\sigma(\Delta p) = 0.44\overline{R}_p(\Delta p)$.

The most significant storm tracks for the region during the period of record have followed tracks similar to those shown in Figure 17 (Figure 12 of R2007). This track pattern has been given the name *RICK fan*, corresponding to Hurricanes Rita, Ivan, Camille, and Katrina which

suggested this typical path arrangement. Other track patterns at ±45 degrees to this fundamental pattern are shown in Figures 13 and 14 of R2007. Use of a reasonable track shape – beyond simple straight-line tracks at shore crossing – was thought to be appropriate for the study, owing to the possible significance of wind waves. While the basic storm surge develops over a nearshore zone for which track shape might not be too significant, waves are generated over a larger area for a longer time. Waves contribute a secondary component to the total flood level through the mechanism of wave setup. The use of these typical RICK fan tracks is thought adequate to account for the secondary wave effects; in any case, the introduction of additional parameters into the JPM analysis to account for track curvature would be both prohibitive and of little additional value.

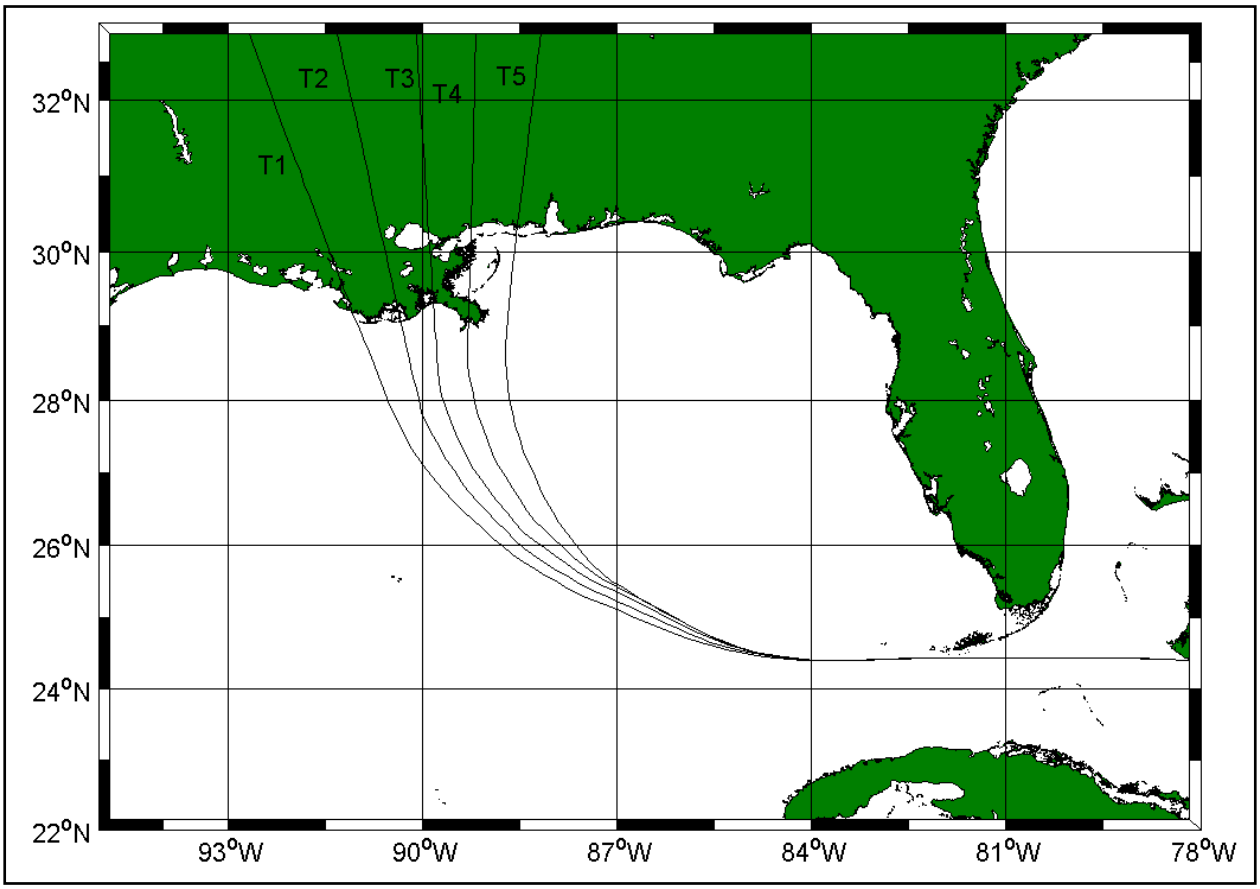

Figure 17. Dominant track pattern (the RICK fan). Tracks oblique to these were also modeled.

As shown in Figure 9 of R2007, the probability distribution of track angle at the time of shore crossing is taken to be normally distributed around a longitude-dependent mean. As shown in that figure, the mean heading is approximately 10 degrees west of north over the region, with a spread characterized by a standard deviation of approximately 20 degrees. Using this Gaussian description, each of the RICK fan and related oblique tracks is assigned a relative probability, discretizing and allocating the directional distribution probability mass among the selected tracks.

Observations regarding forward speed are shown in Figures 10 and 11 of R2007. Figure 10 (R2007) suggests that forward speed is effectively uncorrelated with central pressure. However, Figure 11 (R2007) indicates some dependence of speed upon direction of motion, with storms recurving to the east moving somewhat faster than those persisting to the west. This behavior has been accounted for by use of a Gaussian distribution for forward speed, conditional upon shore crossing angle, as specified in R2007.

The remaining parameters are position and Holland's B, as well as astronomic tide if considered within the JPM context. Position is taken to be uniformly distributed with longitude over the region of the study. Holland's B and astronomic tide, however, are treated differently from all other parameters, as is discussed below. First, however, it is necessary to indicate how the probability distributions discussed to this point are implemented in the determination of surge frequency.

Calculating Hurricane Frequencies

Each storm considered in the ADCIRC simulation set is envisioned to represent a region of the storm parameter space around that particular storm. In other words, the entire space is subdivided into a small number of facets, each of which is assigned a fraction of the total storm rate according to the joint probability of the several parameters. For this study, the approach was to first construct a response surface giving surge elevation as a function of storm parameters and location. This was done through simulation of 152 storms, as specified in Appendix D of R2007. Subsequently, this response surface was discretized through selection of a subset of storms adequately covering the surface. A set of 77 storms was selected, with a rate assigned to each (Resio, personal communication, 2007) so as to cover the entire space. The parameters used to model the 152 storm are presented in Table 9. Note that only the 77 storms with frequencies are used in the risk analysis.

Table 9
Hurricane Parameters for Hazard Analysis

IPET Storm No.	Central Pressure	Radius Max Winds	Forward Speed	Hollands B	Angle	Track	LAT 1	LON	Lacpr Storm No.	Storm Frequency
1	960	11	11	1.27	0	1	24.43	-79.1	1	7.90E-04
2	960	21	11	1.27	0	1	24.43	-79.1	2	9.19E-04
3	960	35.6	11	1.27	0	1	24.43	-79.1	3	4.92E-04
4	930	8	11	1.27	0	1	24.43	-79.1	4	2.50E-03
5	930	17.7	11	1.27	0	1	24.43	-79.1	5	2.73E-03
6	930	25.8	11	1.27	0	1	24.43	-79.1	6	2.30E-03
7	900	6	11	1.27	0	1	24.43	-79.1	7	1.13E-03
8	900	14.9	11	1.27	0	1	24.43	-79.1	8	1.39E-03
9	900	21.8	11	1.27	0	1	24.43	-79.1	9	3.46E-04
10	960	11	11	1.27	0	2	24.42	-78.6	10	7.90E-04
11	960	21	11	1.27	0	2	24.42	-78.6	11	9.19E-04
12	960	35.6	11	1.27	0	2	24.42	-78.6	12	4.92E-04
13	930	8	11	1.27	0	2	24.42	-78.6	13	2.50E-03
14	930	17.7	11	1.27	0	2	24.42	-78.6	14	2.73E-03

Table 9
Hurricane Parameters for Hazard Analysis

IPET Storm No.	Central Pressure	Radius Max Winds	Forward Speed	Hollands B	Angle	Track	LAT 1	LON	Lacpr Storm No.	Storm Frequency
15	930	25.8	11	1.27	0	2	24.42	-78.6	15	2.30E-03
16	900	6	11	1.27	0	2	24.42	-78.6	16	1.13E-03
17	900	14.9	11	1.27	0	2	24.42	-78.6	17	1.39E-03
18	900	21.8	11	1.27	0	2	24.42	-78.6	18	3.46E-04
19	960	11	11	1.27	0	3	24.42	-78.5	19	7.90E-04
20	960	21	11	1.27	0	3	24.42	-78.5	20	9.19E-04
21	960	35.6	11	1.27	0	3	24.42	-78.5	21	4.92E-04
22	930	8	11	1.27	0	3	24.42	-78.5	22	2.50E-03
23	930	17.7	11	1.27	0	3	24.42	-78.5	23	2.73E-03
24	930	25.8	11	1.27	0	3	24.42	-78.5	24	2.30E-03
25	900	6	11	1.27	0	3	24.42	-78.5	25	1.13E-03
26	900	14.9	11	1.27	0	3	24.42	-78.5	26	1.39E-03
27	900	21.8	11	1.27	0	3	24.42	-78.5	27	3.46E-04
28	960	11	11	1.27	0	4	24.4	-77.9	28	7.90E-04
29	960	21	11	1.27	0	4	24.4	-77.9	29	9.19E-04
30	960	35.6	11	1.27	0	4	24.4	-77.9	30	4.92E-04
31	930	8	11	1.27	0	4	24.4	-77.9	31	2.50E-03
32	930	17.7	11	1.27	0	4	24.4	-77.9	32	2.73E-03
33	930	25.8	11	1.27	0	4	24.4	-77.9	33	2.30E-03
34	900	6	11	1.27	0	4	24.4	-77.9	34	1.13E-03
35	900	14.9	11	1.27	0	4	24.4	-77.9	35	1.39E-03
36	900	21.8	11	1.27	0	4	24.4	-77.9	36	3.46E-04
37	960	11	11	1.27	0	5	24.43	-78.9	37	7.90E-04
38	960	21	11	1.27	0	5	24.43	-78.9	38	9.19E-04
39	960	35.6	11	1.27	0	5	24.43	-78.9	39	4.92E-04
40	930	8	11	1.27	0	5	24.43	-78.9	40	2.50E-03
41	930	17.7	11	1.27	0	5	24.43	-78.9	41	2.73E-03
42	930	25.8	11	1.27	0	5	24.43	-78.9	42	2.30E-03
43	900	6	11	1.27	0	5	24.43	-78.9	43	1.13E-03
44	900	14.9	11	1.27	0	5	24.43	-78.9	44	1.39E-03
45	900	21.8	11	1.27	0	5	24.43	-78.9	45	3.46E-04
46	960	18.2	11	1.27	-45	1	24.54	-80.9	46	3.50E-04
47	960	24.6	11	1.27	-45	1	24.54	-80.9	47	3.90E-04
48	900	12.5	11	1.27	-45	1	24.54	-80.9	48	7.16E-04
49	900	18.4	11	1.27	-45	1	24.54	-80.9	49	5.48E-04
50	960	18.2	11	1.27	-45	2	24.83	-80.8	50	3.50E-04
51	960	24.6	11	1.27	-45	2	24.83	-80.8	51	3.90E-04
52	900	12.5	11	1.27	-45	2	24.83	-80.8	52	7.16E-04
53	900	18.4	11	1.27	-45	2	24.83	-80.8	53	5.48E-04
54	960	18.2	11	1.27	-45	3	25.38	-80.8	54	3.50E-04
55	960	24.6	11	1.27	-45	3	25.38	-80.8	55	3.90E-04
56	900	12.5	11	1.27	-45	3	25.38	-80.8	56	7.16E-04
57	900	18.4	11	1.27	-45	3	25.38	-80.8	57	5.48E-04
58	960	18.2	11	1.27	-45	4.1	26.08	-80.8	58	3.50E-04
59	960	24.6	11	1.27	-45	4.1	26.08	-80.8	59	3.90E-04

Table 9
Hurricane Parameters for Hazard Analysis

IPET Storm No.	Central Pressure	Radius Max Winds	Forward Speed	Hollands B	Angle	Track	LAT 1	LON	Lacpr Storm No.	Storm Frequency
60	900	12.5	11	1.27	-45	4.1	26.08	-80.8	60	7.16E-04
61	900	18.4	11	1.27	-45	4.1	26.08	-80.8	61	5.48E-04
	0	0	0	0	0	0	0		62	
	0	0	0	0	0	0	0		63	
	0	0	0	0	0	0	0		64	
	0	0	0	0	0	0	0		65	
62	960	18.2	11	1.27	45	1	21.28	-90	66	
63	960	24.6	11	1.27	45	1	21.28	-90	67	2.50E-04
64	900	12.5	11	1.27	45	1	21.28	-90	68	3.02E-04
65	900	18.4	11	1.27	45	1	21.28	-90	69	2.01E-04
66	960	18.2	11	1.27	45	2	21.3	-90	70	1.54E-04
67	960	24.6	11	1.27	45	2	21.3	-90	71	2.50E-04
68	900	12.5	11	1.27	45	2	21.3	-90	72	3.02E-04
69	900	18.4	11	1.27	45	2	21.3	-90	73	2.01E-04
70	960	18.2	11	1.27	45	3	21.27	-90.1	74	1.54E-04
71	960	24.6	11	1.27	45	3	21.27	-90.1	75	2.50E-04
72	900	12.5	11	1.27	45	3	21.27	-90.1	76	3.02E-04
73	900	18.4	11	1.27	45	3	21.27	-90.1	77	2.01E-04
74	960	18.2	11	1.27	45	4	21.28	-90	78	1.54E-04
75	960	24.6	11	1.27	45	4	21.28	-90	79	2.50E-04
76	900	12.5	11	1.27	45	4	21.28	-90	80	3.02E-04
77	900	18.4	11	1.27	45	4	21.28	-90	81	2.01E-04
78	960	17.7	6	1.27	0	1	24.43	-78.9	82	
79	900	17.7	6	1.27	0	1	24.43	-78.9	83	
80	960	17.7	6	1.27	0	2	24.42	-78.4	84	
81	900	17.7	6	1.27	0	2	24.42	-78.4	85	
82	960	17.7	6	1.27	0	3	24.42	-78.3	86	
83	900	17.7	6	1.27	0	3	24.42	-78.3	87	
84	960	17.7	6	1.27	0	4	24.4	-77.7	88	
85	900	17.7	6	1.27	0	4	24.4	-77.7	89	
86	960	17.7	6	1.27	0	5	24.42	-78.7	90	
87	900	17.7	6	1.27	0	5	24.42	-78.7	91	
88	930	17.7	6	1.27	-45	1	26.94	-80.9	92	
89	930	17.7	6	1.27	-45	2	27.09	-80.9	93	
90	930	17.7	6	1.27	-45	3	27.52	-80.9	94	
91	930	17.7	6	1.27	-45	4.1	28.21	-80.9	95	
	0	0	0	0	0	0	0		96	
92	930	17.7	6	1.27	45	1	20.66	-92.3	97	
93	930	17.7	6	1.27	45	2	20.75	-92.6	98	
94	930	17.7	6	1.27	45	3	20.91	-92.8	99	
95	930	17.7	6	1.27	45	4	21.17	-93	100	
96	930	17.7	17	1.27	0	1	24.43	-79.1	101	
97	930	17.7	17	1.27	0	2	24.42	-78.6	102	
98	930	17.7	17	1.27	0	3	24.42	-78.5	103	
99	930	17.7	17	1.27	0	4	24.4	-77.8	104	

Table 9
Hurricane Parameters for Hazard Analysis

IPET Storm No.	Central Pressure	Radius Max Winds	Forward Speed	Hollands B	Angle	Track	LAT 1	LON	Lacpr Storm No.	Storm Frequency
100	930	17.7	17	1.27	0	5	24.43	-78.9	105	
101	930	17.7	17	1.27	-45	1	23.29	-80.8	106	
102	930	17.7	17	1.27	-45	2	23.68	-80.9	107	
103	930	17.7	17	1.27	-45	3	24.27	-80.8	108	
104	930	17.7	17	1.27	-45	4.1	24.94	-80.7	109	
	0	0	0	0	0	0	0		110	
105	930	17.7	17	1.27	45	1	21.28	-90	111	
106	930	17.7	17	1.27	45	2	21.27	-90.1	112	
107	930	17.7	17	1.27	45	3	21.27	-90.1	113	
108	930	17.7	17	1.27	45	4	21.26	-90.1	114	
109	960	17.7	11	1.27	0	1.5	24.42	-78.8	115	
110	900	17.7	11	1.27	0	1.5	24.42	-78.8	116	
111	960	17.7	11	1.27	0	2.5	24.42	-78.5	117	
112	900	17.7	11	1.27	0	2.5	24.42	-78.5	118	
113	960	17.7	11	1.27	0	3.5	24.41	-78.3	119	
114	900	17.7	11	1.27	0	3.5	24.41	-78.3	120	
115	960	17.7	11	1.27	0	4.5	24.43	-79.1	121	
116	900	17.7	11	1.27	0	4.5	24.43	-79.1	122	
117	960	17.7	11	1.27	-45	1.5	24.76	-81.2	123	
118	960	17.7	11	1.27	-45	1.5	25.15	-81.1	124	
119	960	17.7	11	1.27	-45	2.5	25.79	-81.2	125	
120	900	17.7	11	1.27	-45	2.5	24.76	-81.2	126	
121	900	17.7	11	1.27	-45	3.5	25.15	-81.1	127	
122	900	17.7	11	1.27	-45	3.5	25.79	-81.2	128	
	0	0	0	0	0	0	0		129	
	0	0	0	0	0	0	0		130	
123	960	17.7	11	1.27	45	1.5	21.29	-90	131	
124	900	17.7	11	1.27	45	1.5	21.29	-90	132	
125	960	17.7	11	1.27	45	2.5	21.29	-90	133	
126	900	17.7	11	1.27	45	2.5	21.29	-90	134	
127	960	17.7	11	1.27	45	3.5	21.28	-90	135	
128	900	17.7	11	1.27	45	3.5	21.28	-90	136	
129	960	17.7	6	1.27	0	1.5	24.42	-78.6	137	
130	900	17.7	6	1.27	0	1.5	24.42	-78.6	138	
131	960	17.7	6	1.27	0	2.5	24.42	-78.3	139	
132	900	17.7	6	1.27	0	2.5	24.42	-78.3	140	
133	960	17.7	6	1.27	0	3.5	24.41	-78.1	141	
134	900	17.7	6	1.27	0	3.5	24.41	-78.1	142	
135	960	17.7	6	1.27	0	4.5	24.43	-78.9	143	
136	900	17.7	6	1.27	0	4.5	24.43	-78.9	144	
137	930	17.7	6	1.27	-45	1.5	26.93	-81.3	145	
138	930	17.7	6	1.27	-45	2.5	27.23	-81.2	146	
139	930	17.7	6	1.27	-45	3.5	27.79	-81.2	147	
	0	0	0	0	0	0	0		148	
140	930	17.7	6	1.27	45	1.5	20.71	-92.5	149	

Table 9
Hurricane Parameters for Hazard Analysis

IPET Storm No.	Central Pressure	Radius Max Winds	Forward Speed	Hollands B	Angle	Track	LAT 1	LON	Lacpr Storm No.	Storm Frequency
141	930	17.7	6	1.27	45	2.5	20.83	-92.7	150	
142	930	17.7	6	1.27	45	3.5	21.04	-92.9	151	
143	930	17.7	17	1.27	0	1.5	24.42	-78.8	152	
144	930	17.7	17	1.27	0	2.5	24.42	-78.5	153	
145	930	17.7	17	1.27	0	3.5	24.41	-78.2	154	
146	930	17.7	17	1.27	0	4.5	24.43	-79.1	155	
147	930	17.7	17	1.27	-45	1.5	23.64	-81.3	156	
148	930	17.7	17	1.27	-45	2.5	24.08	-81.1	157	
149	930	17.7	17	1.27	-45	3.5	23.73	-81	158	
	0	0	0	0	0	0	0		159	
150	930	17.7	17	1.27	45	1.5	21.27	-90.1	160	
151	930	17.7	17	1.27	45	2.5	21.27	-90.1	161	
152	930	17.7	17	1.27	45	3.5	21.27	-90.1	162	

In summary, as discussed in R2007, the estimates of joint probability densities can be written as

$$p(c_p, R_p, v_f, \theta_l, x) = \Lambda_1 \cdot \Lambda_2 \cdot \Lambda_3 \cdot \Lambda_4 \cdot \Lambda_5$$

where the five parameters are central pressure, scaling radius, forward speed, track direction, and location; the Λs represent the associated parameter distributions defined above, with Λ_5 being the frequency of storms per year per specified distance along the coast.

Other parameters which affect the surge estimates include Holland's B, astronomic tide, and modeling skill. These factors were considered as variations around the basic estimate, through introduction of a random error term. For example, the Holland B parameter for mature Gulf of Mexico storms appears to fall between 0.9 and 1.6. A basic choice of 1.27 was used in the simulations, and the results were adjusted by a random dispersion around this value. A similar method was used for astronomic tide, track variations, modeling errors, and wind field description limitations, as discussed in R2007. Were this approach not used, it would have been necessary to include the additional parameters within the JPM scheme, greatly increasing the required number of simulations.

Assessment of Hurricane Surge

Finding the environmental loads for each parameter set of interest is the most challenging task of hurricane hazard characterization. It is well known that surge and waves interact (surge affects waves and vice versa). Therefore, these loads should be ideally assessed using a coupled formulation. Sophisticated programs are currently being developed that reflect this coupling, but at the present time such programs are not at a stage that they can be routinely used. An

alternative used here is to follow an iterative approach, outlined below, whereby the surge H(x,y,t) without waves is calculated, the wave field is estimated given this preliminary estimate of the surge, and finally the surge code is re-run considering the influence of the calculated wave field.

The adopted surge model, ADCIRC, uses a triangulated grid with spatially varying resolution, which for the risk analysis application covers the entire Gulf of Mexico and extends into the Atlantic Ocean. The grid domain is illustrated in Figure 18, along with the wave grids to be discussed below.

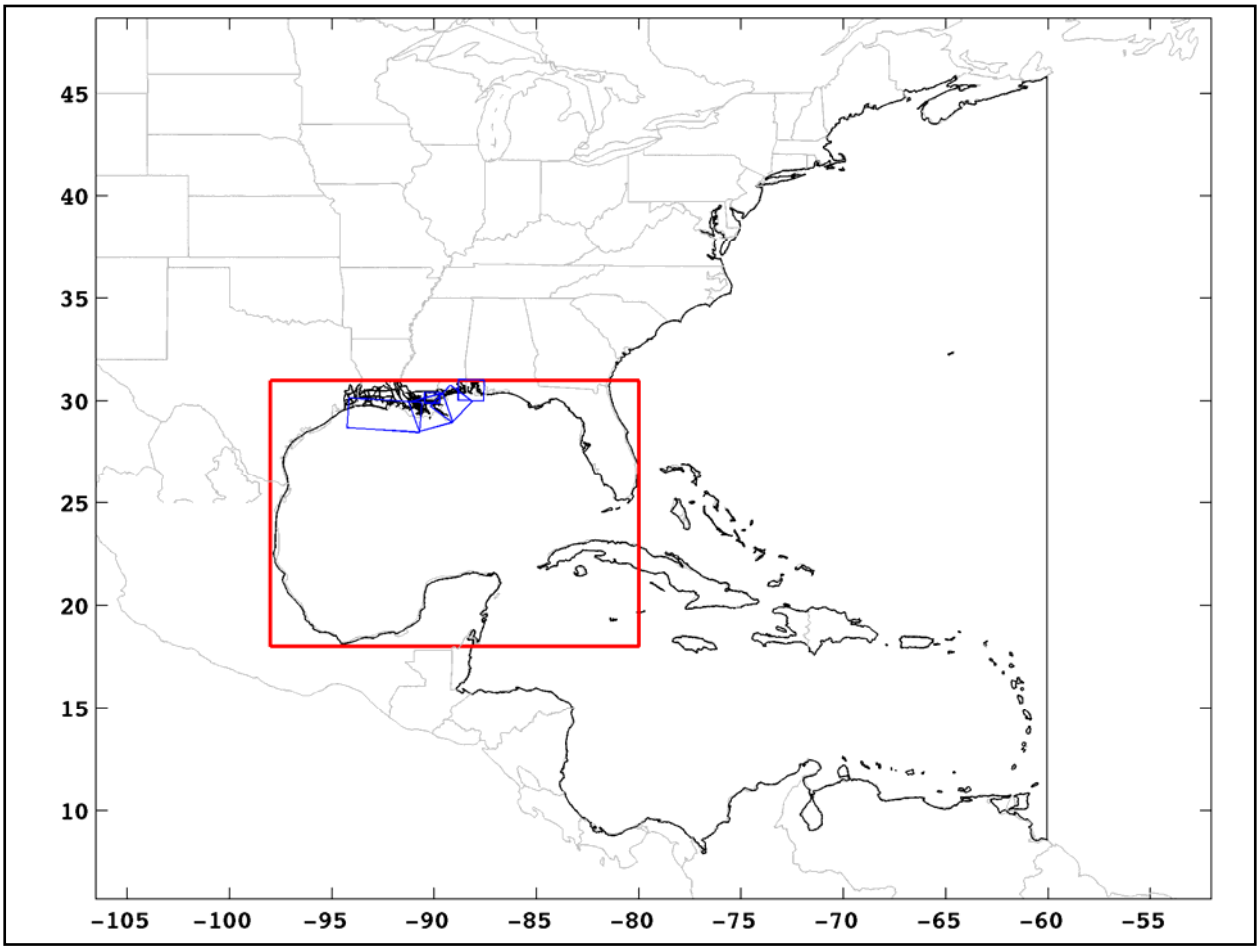

Figure 18. General model grid layouts. The ADCIRC grid extends to the vertical line in the mid-Atlantic. The coarse wave grid is shown in red, and the fine, local wave grids are shown in blue.

The ADCIRC resolution increases in coastal areas, in particular near the Louisiana Coast. The high-resolution ADCIRC grids include millions of nodes and must be run with time-steps on the order of 1 second to avoid numerical problems. Such dense grids produce accurate results and can adequately resolve topographic effects on horizontal scales of tens of meters along the coast. A detailed presentation of the ADCIRC modeling approach is given in IPET Volume IV, *The Storm*; implementation for the risk analysis is discussed in more detail in Appendix 8.

The assessment of hurricane loads is based on a subset of the ADCIRC model runs for a sample of 77 large storms thought to be typical of significant events in the vicinity of New Orleans. The Storm Team selected this sample, determined rates of occurrence for each storm as described above, and generally directed ADCIRC modeling. One or more of these selected storms has approximately a 0.07 probability of occurring in any year. The hazards expressed as surge and wave heights were thus factored by the marginal probability of the event generating them. The individual hurricane paths considered in the risk analysis are given in Appendix 8 of this volume.

For most storms in the sample of ADCIRC runs, the final water levels were taken directly from the simulations. However, for some of the runs, it was necessary to make corrections to adjust for a relative lack of resolution of the grid in limited locations. These corrections are site-specific, depending on the local geometry of the coast, the topography, and the different local land coverage of the ADCIRC grids. The correction further depended on the hurricane parameters; in particular, the correction at a given location will generally depend on landfall position X, direction θ, and possibly storm intensity ΔP, and radius to maximum winds R_{max}.

Hurricane Waves

The effects of waves were accounted for through the multistep simulation procedure mentioned above. Note that the fragilities are defined with respect to the mean water flood levels so that the wave effect of interest is the wave setup, caused by variations in the radiation stresses associated with changes in the wave momentum flux. The effect is to cause an additional elevation of the mean water level within the breaker zone by a small amount, on the order of a few feet. In order to account for the contribution from waves, two wave modeling tools were used. The WAM model (see both Appendix 8 and IPET Volume IV, *The Storm,* for a discussion of the wave models that were employed and their implementations) was run for the Gulf of Mexico to define incident spectral boundary conditions for the more refined STWAVE model, which was used in overlapping nearshore and onshore regions. The domains of these grids are shown in Figure 19; the WAM grid encompasses the entire gulf.

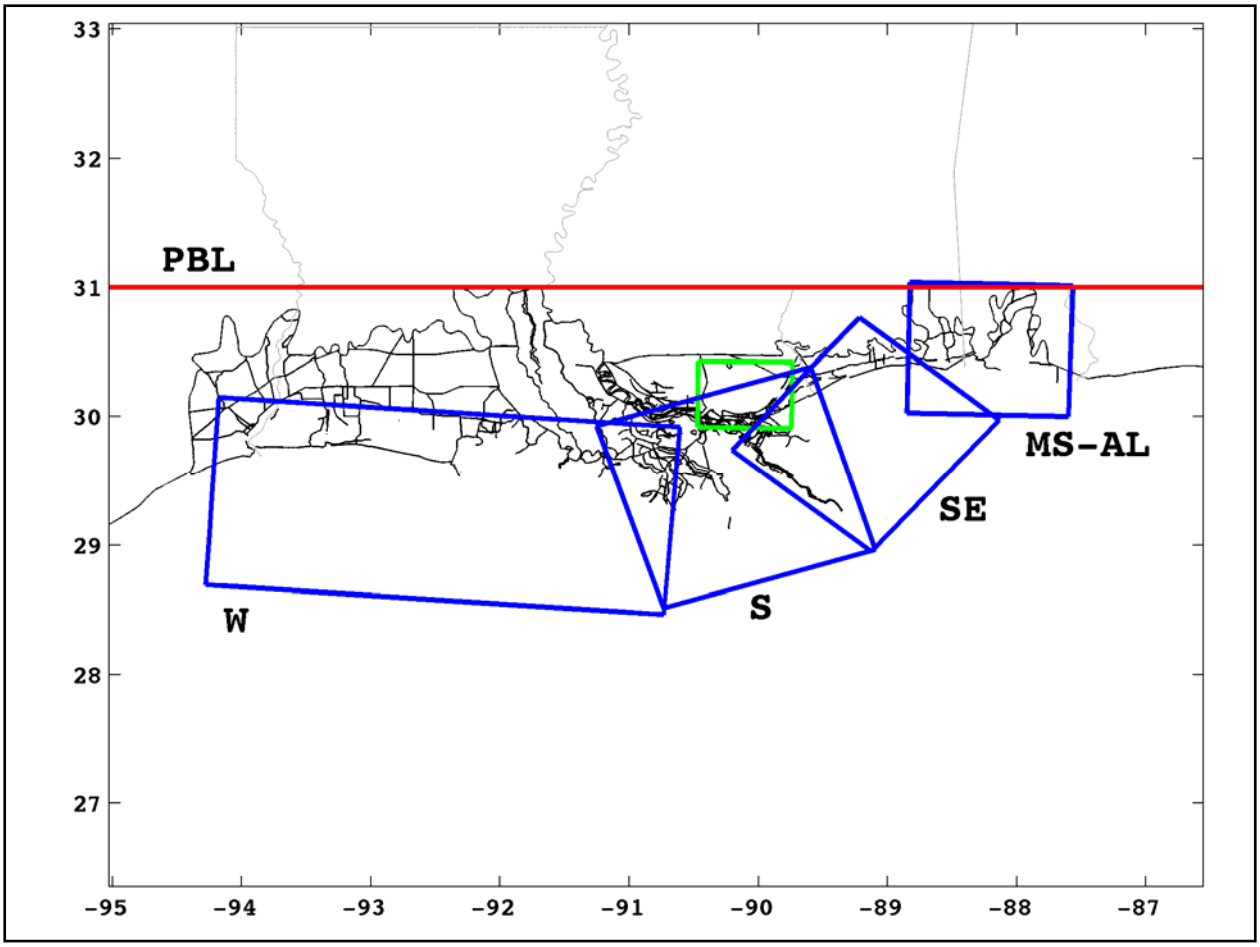

Figure 19. Locations of the five high-resolution local STWAVE grids.

This approach required a significant increase in modeling effort, involving additional iterative steps, fully detailed in Appendix 8. First, because wave behavior depends critically upon water depth, initial ADCIRC runs were made to determine the surge associated with wind and pressure in the absence of waves. The initial conditions (river spinup to account for freshwater inflow to the system), PBL wind and pressure fields, and the wave energy spectra boundary conditions (as computed by WAM) are all required inputs to the system. Given these initial first-order surge determinations, STWAVE is then run over the fine resolution wave grids and the radiation stresses are computed. Then ADCIRC is re-run, including the radiation stresses along with the other (wind and bottom friction) stresses driving the development of the surge.

Rainfall Intensity

Rainfall is among the variables that affect the inundation of the basins. While rainfall is not of primary concern for the hurricane protection system, it is a contributor to the frequency of low-level flood losses. Hence, it was decided that a relatively coarse model of hurricane-induced rainfall would suffice.

Prior to NASA's Tropical Rainfall Measuring Mission (TRMM) (Simpson et al. 1988), information on hurricane rainfall was scanty. The TRMM mission, which started in November 1997, produced vast amounts of rainfall estimates for tropical storms and hurricanes at a spatial scale of about 5 km in various tropical regions, including the Atlantic basin. These rainfall products have been analyzed statistically by Lonfat et al. (2004) and Chen et al. (2006). The model used is based primarily on these two studies and on discussions with Dr. Shuyi Chen at the University of Miami, Florida. The model is described in Appendix 8.

The model adopted relates the rainfall intensity to storm strength and position within the storm. The model first assumes a uniform rainfall rate within the radius to maximum winds and an exponentially declining rate at greater distances. Furthermore, rainfall is taken to be asymmetric, with the more intense rains occurring to the right of the observer, when facing the direction of storm travel. Two sorts of calculations were done using this model. First, the total accumulation into each sub basin for each storm was determined. Second, time dependent intensities for each sub-basin were also calculated.

Uncertainty in the rainfall estimates is large owing to the paucity of data, and it is expressed by a lognormal random variable with mean value 1 and log standard deviation 0.69. This random factor is applied to the entire mean rainfall time-history. In reality, rainfall intensity inside a basin would display significant fluctuations in time and space, which locally could far exceed a factor of 2. However, the above random factor is considered adequate to reflect uncertainty on the total precipitation in a basin during the passage of a hurricane.

Epistemic Uncertainty in Hurricane Loading

Epistemic uncertainty (uncertainty due to limited information and knowledge) affects all aspects of the hazard characterization. While a thorough assessment of these uncertainties is beyond the scope of this project, a rough quantification of uncertainty on the hurricane rates and the loads was made.

The hurricane rates are uncertain due to the limited historical sample size, possible errors in the assumed form of marginal and conditional distributions (especially in the tail regions), and the uncertain near-future hurricane activity due to fluctuations and trends associated with climate changes and multi-decadal cycles. A first-order assessment of uncertainty on hurricane rates is based on the hurricane effects of global warming and shorter-term climatic fluctuations in the North Atlantic.

Causes of epistemic uncertainty on wave and surge levels are hurricane model errors; for example, the wind field idealization, the coefficient of friction with the water surface, the effects of waves on water level, etc., are estimated by hind casting historical events or by comparing results from different modeling assumptions. The use of different models will lead to different estimates, unless one of these models is essentially correct. However, if none of the models captures the physics correctly, the different results are not epistemic uncertainty; they are systematic error.

The potential effect of global warming on the frequency, size, and intensity of tropical cyclones is a hotly debated issue in the technical literature; see Pielke et al. (2005), Emanuel (2005b), and Elsner (2005) for recent reviews. Theoretical analysis, numerical modeling, and historical data analysis have all been used to study the effects of climate variations on various features of tropical cyclones. The main results on hurricane frequency and intensity are summarized below. What determines hurricane size is poorly understood; hence, the possible dependence of R_{max} on global warming.

From the preceding discussion, uncertainty on the hurricane statistics in the Gulf of Mexico during the next 50-100 years is dominated by multi-decadal oscillations. Specifically, considering that the North Atlantic is now experiencing a 50% higher-than-normal activity and that this elevated activity may persist over a number of years and possibly decades, it is reasonable for the next 50-100 years to increase the average historical rate of hurricanes by 20% and allow for an additional 25% uncertainty factor around this corrected rate. The latter factor includes uncertainty on the historical rate due to the finite observation period (16%) as well as uncertainty on the future evolution of the hurricane frequency (judgmentally assessed).

Considering the general consensus and dissenting views on the effect of global warming on hurricane intensity, the historical mean pressure deficit is increased by 3% and an uncertainty factor of 5% is applied to the increased mean value. Since the effects of different factors on hurricane frequency and intensity are poorly understood, these components of epistemic uncertainty are treated as independent.

Reliability Analysis

The *reliability* of a reach, feature, or transition constituting the HPS is the conditional probability of its failure when exposed to a given hurricane loading. The analysis of reliability applied in this work has three steps, described in more detail in Appendix 10 of this volume:

Systems definition: Specify the reaches, point features, and transitions constituting the HPS for each drainage basin. Each drainage basin perimeter was divided into segments, referred to as *reaches*, which were deemed to be homogeneous in three respects: structural cross section, elevations in the cross section, and geotechnical cross section. In addition, localized features exist within most reaches, such as pumping stations, drainage works, pipes penetrating the HPS, and gates. Also points of transition exist within most reaches, as between levee and floodwall, or between features and levees. Each reach typically contains both features and transitions. For the pre-Katrina condition, 135 reaches were identified. For the current condition the same 135 reaches plus three end-of-drainage-canal gates were identified, for a total of 138. For the pre-Katrina and current conditions, 178 point features and 179 transitions were identified.

Limiting states: Define *failure*, and identify failure modes and limit states for each reach, feature, or transition. *Failure* in a general sense is the loss of capacity of the structure or system to fulfill its design intent. Defining *failure* means specifying in a precise way how such loss of capacity could occur. Failure modes are ways in which the structures or systems can fail. For example, one failure mode of a levee is limiting equilibrium strength instability. Limit states are

quantitative criteria for failure. For example, the corresponding limit state to limiting equilibrium strength instability is that the resisting strength of the levee is exceeded by the driving forces to which the levee is subjected.

Fragility curves: Assign conditional probabilities to the failure states of reaches, features, and transitions as a function of hurricane-induced water elevations. These conditional probabilities plotted as a function of the given load are called *fragility curves*. For example, the conditional probability of limiting equilibrium strength instability given a still water elevation at the design level would be assigned some quantitative value based on statistical analysis of strength and load data, on engineering calculations, and on judgment.

Two conditions were analyzed for the reliability of reaches, point features, and transitions:

- Pre-Katrina conditions existing on 28 August 2005
- Current conditions after reconstruction and repair existing on 1 June 2007.

Appendices 2 through 7 contain an inventory of the reaches, point features, and transitions within each drainage basin that were considered in the reliability analysis. Categories of components of the HPS considered in the reliability analysis are shown in Table 9

Systems Definition

The systems definition models for the HPS were developed based on site characterization, engineering design, and construction information as documented in USACE General Design Memoranda (GDM) for the various projects constituting the HPS. This design information was augmented by pre- and post-Katrina high resolutions aerials, the results of post-Katrina field reconnaissance by the Risk Team and studies performed by the IPET Performance Team and the IPET Pump Stations Team (reported in IPET Volume IV, USACE 2006).

A portion of the systems definition for New Orleans East (NOE 5) is shown in Figures 20 and 21. Figure 20 shows dark blue dimension lines that are assigned for multiple design sections from the GDMs in the vicinity of the Lakefront Airport. The red targets and light blue station labels show the location of point features and transitions. This data is transformed into reaches as shown in Figure 21 where the wall reaches are purple and the levee reaches are light green. This figure also includes point features such as gates (red in color) as well as pumping stations (blue lines) and transitions (grey circles). The transitions are changes between levee and floodwall, or between levees and features. Such systems definition was completed for the entire length of the levee and floodwall system.

Table 10. Components in the Hurricane Protection System.	
Component	**Sub-Component**
Levees	Embankment reaches defined by geometry, elevations, base and enlargement materials, and construction Embankment foundation and subsurface geology
Floodwalls	Wall structure and construction Wall foundation including berms
Point Sources	Gate closure structures Position – open or closed
Transitions	Levee and Floodwall transitions Gates Pump stations Ramps

During the course of the study, the entire length of levee and floodwall was inspected by the Risk Team as part of the reconnaissance effort. Geometric and engineering material properties were identified for each reach. Structural cross sections were identified by a review of the corresponding GDM, as-built drawings, aerial photographs, and GIS overlays; and were subsequently confirmed in onsite reconnaissance. Elevations were assessed using hand-held GPS in the same reconnaissance, supplemented by LIDAR and field surveys provided to the Risk Team by the New Orleans District. Final elevations for each reach were confirmed at meetings with New Orleans District personnel Geotechnical cross sections and corresponding soil engineering properties were derived from the original GDMs for the respective project areas of each drainage basin, supplemented by site characterization data collected post-Katrina at levee and floodwall failure sites (reported in IPET Volume IV, USACE 2006).

Systems definition information was summarized in database tables, shown schematically in Table 21**Error! Reference source not found.** for the reaches near the Lakefront Airport. The individual record within a systems definition table provides reach length, elevation, design water elevation, structural type (levee, I-wall, or T-wall), weir coefficient, basin and sub-basin references, erosion modifier coefficient, levee material type (for erosion calculations), and project reference.

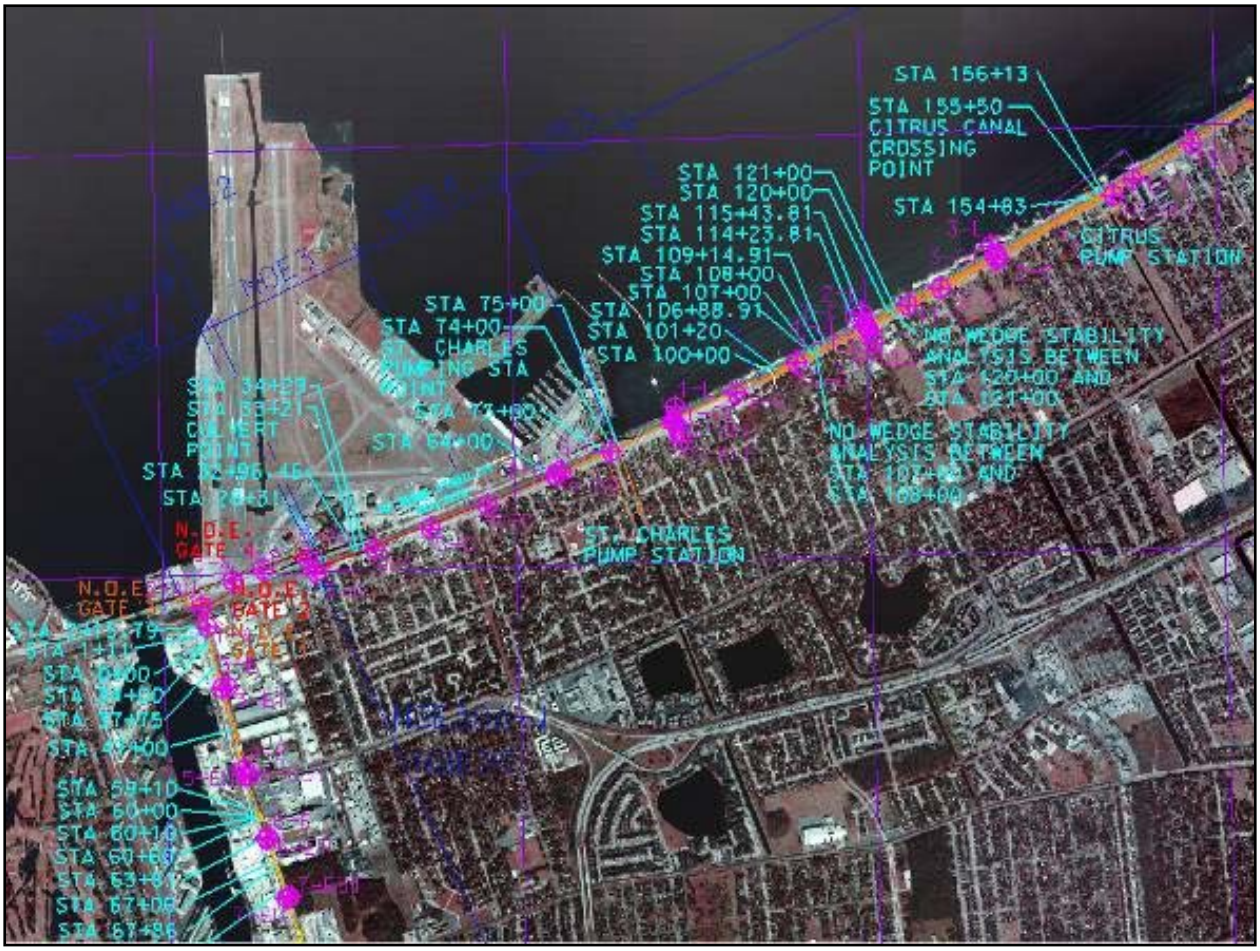

Figure 20. Section of the systems definition for the HPS of New Orleans East.

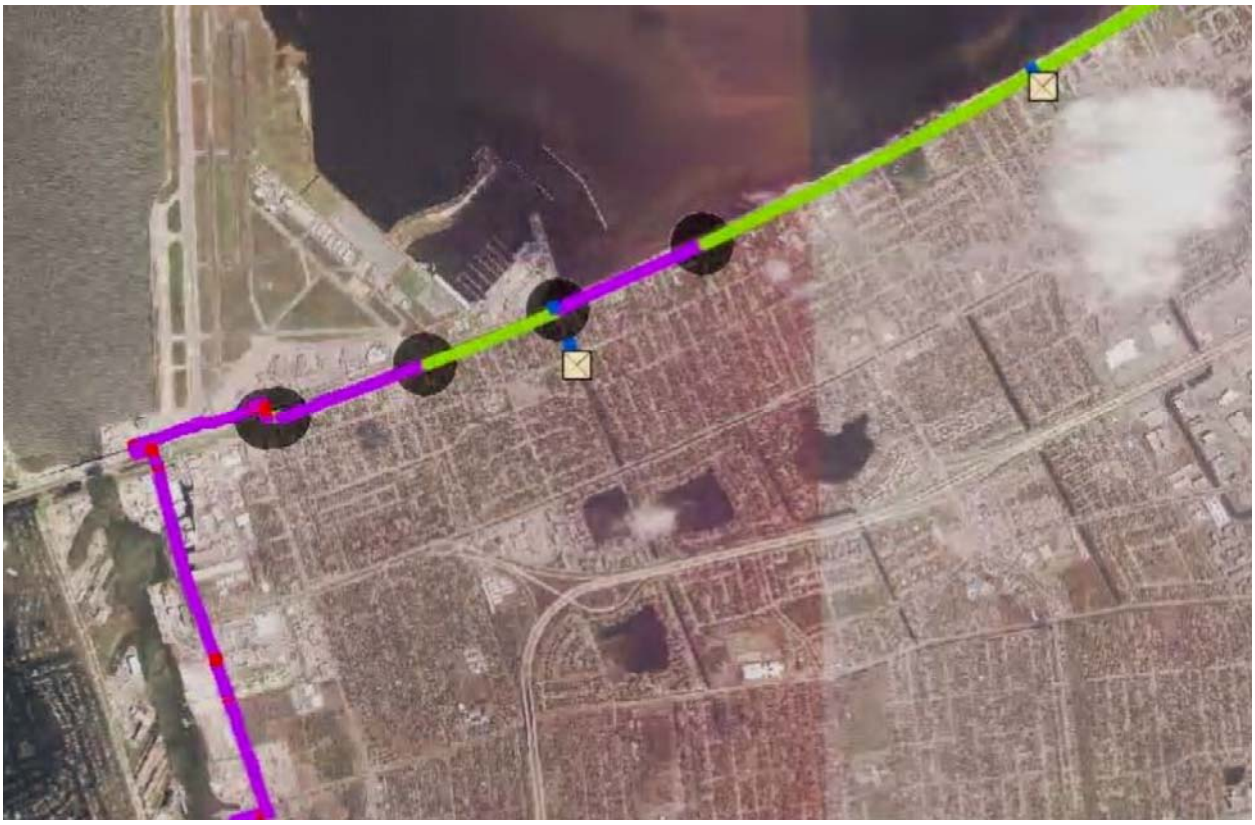

Figure 21. Section of the refined systems definition for the HPS of New Orleans East.

Limiting states

Failures that lead to breach of the drainage basin perimeters were associated with four principal failure modes: (1) levee or levee foundation failure; (2) floodwall or floodwall foundation failure; (3) levee or floodwall erosion caused by overtopping; and (4) failure modes associated with transition features such as levee-wall transitions, gates, pumping stations and ramps. The IPET Performance Team found no failures in the HPS during Katrina that originated in structural failure of floodwall components. All documented failures at flood wall locations were geotechnical in nature, with structural damage resulting from the geotechnical failures.

The HPS for each drainage basin has four components: (1) levees, (2) I-walls (which may be atop levees), (3) point features, and (4) transitions. The reliability analysis examined the performance of each component, separately and in combination. The following structures in the HPS were not independently evaluated for their failure modes: (1) concrete aprons associated with some I-walls under the current system, and (2) sheetpiles with a short (3 to 4 ft) concrete cap. Either could be addressed with failure modes developed for I-walls, but they were not included in the present study. (3) T-walls were included in the HPS but were considered highly reliable due to their pre-stressed concrete pile foundations and successful performance during Katrina.

For each component, a performance level was defined such that its occurrence corresponded to a failure to perform an intended function. The critical components within the HPS, as stated above, are the levees, I-walls, point features and transitions. These components can fail in a variety of modes. For each mode of failure a limit state was defined, which, if it were to occur would result in a failure to keep water out of the drainage basin.

Reach	Length (ft)	Weighted Elevation (ft)	Design Water Elevation (ft)	Reach Type	Reach Weir Coefficient	Basin Reference	Subbasin Reference	Erosion Modifier	Breach Material	High Limit
1	2.290E+03	1.152E+01	9.520E+00	W	3.0	NOE	NOE5	1.0	H	NOE Airport Floodwall
2	9.700E+01	1.327E+01	1.027E+01	L	2.6	NOE	NOE5	1.0	H	Citrus Lakefront Levee
3	2.325E+03	1.350E+01	1.150E+01	W	3.0	NOE	NOE5	1.0	H	Citrus Lakefront Levee
4	2.330E+03	1.325E+01	1.025E+01	L	2.6	NOE	NOE5	1.0	H	Citrus Lakefront Levee
5	2.270E+03	1.372E+01	1.172E+01	W	3.0	NOE	NOE5	1.0	H	Citrus Lakefront Levee
6	1.911E+04	1.293E+01	9.930E+00	L	2.6	NOE	NOE5	1.0	H	Citrus Lakefront Levee
7	1.474E+03	1.212E+01	1.012E+01	W	3.0	NOE	NOE5	1.0	H	Citrus Lakefront Levee
8	2.724E+03	1.264E+01	9.640E+00	L	2.6	NOE	NOE5	1.0	H	Citrus Lakefront Levee
9	3.303E+04	1.864E+01	1.564E+01	L	2.6	NOE	NOE5	1.0	H	NOE Lakefront Levee
10	1.330E+02	1.864E+01	1.564E+01	L	2.6	NOE	NOE1	1.0	H	NOE Lakefront Levee
11	2.767E+04	1.513E+01	1.213E+01	L	2.6	NOE	NOE1	1.0	H	N.O. East Levee
12	8.942E+03	1.672E+01	1.372E+01	L	2.6	NOE	NOE1	1.0	H	N.O. East Levee
13	7.190E+03	1.765E+01	1.465E+01	L	2.6	NOE	NOE1	1.0	H	N.O. East Levee
14	2.226E+04	1.550E+01	1.250E+01	L	2.6	NOE	NOE1	1.0	H	N.O. East Back Levee

Figure 21. Example of a systems definition datasheet for the reliability calculation showing typical levee and floodwall information by reach.

Engineering models of the mechanics of component performance are limited in their ability to explicitly model a failure state. As a result, an analysis is usually carried out for incipient failure by examining the limits of stability. If this state is equaled or exceeded, the structure or component is expected to fail to perform as intended. Incipient failure models were usually similar to design calculations used for the HPS, and in many cases these models were adapted from the GDMs.

For the purpose of evaluating the performance of the levees and floodwalls, *failure* was defined as complete breaching, allowing water to enter the drainage basin. This failure occurs in two ways: (1) loss of levee or wall stability when the strength of the levee or wall and its foundation is insufficient to withstand the forces placed upon the structure for a given water elevation (no overtopping); or (2) overtopping causing the protected side of the levee or wall to erode substantially and resulting in a wall or levee breach, allowing water to flow freely into the drainage basin.

Depending on the performance of individual components in the HPS, various outcomes may result. For purpose of evaluating the performance of the HPS, the outcome of most interest is whether a protected area is flooded or not.

The HPS was assumed to fail if flooding occurred in a protected area, beyond that expected from rainfall and runoff which can be handled by pumping. Given this definition, a failure of the HPS occurs even if the components making up the system do not fail, for example, if levees or

walls are overtopped but not breached. Flooding can occur as a result of chains of events occurring individually or in combination. Among these are the following:

- Levee or floodwall breaching.
- Inflow into an area due to levee or floodwall overtopping that does not result in breeching and which exceeds the capacity of the pumping system.
- Inflow to an area that occurs as a result of rainfall.
- Inflow to an area that occurs when the capacity of the pump system is exceeded or the pump station is shut down, or as a result of backflow through pump houses.

Flooding that occurs as a result of rainfall or transient overtopping in most cases will not be as consequential and may be mitigated by the pumping system. The following failure modes or contributing factors were not considered in the reliability analysis:

- Internal erosion (piping) of levees due to seepage; note, this is in contrast to high pore pressures in sand strata, which was considered, as in the vicinity of the London Avenue Canal or the northern end of the Inner Harbor Navigation Canal (IHNC). Internal erosion may be reconsidered in later studies.
- The effects of maintenance on the HPS capacity over time. Improper maintenance or neglect can lead to reduced capacity of the levees in particular; gates and other moving components also require maintenance. Trees, landscaping, and pools were observed on protected embankments after Hurricane Katrina, indicating a lack of code enforcement and maintenance of the levees. However, there was insufficient information to include maintenance considerations.
- Impact by a barge, floating debris, or other large object on the floodwalls or levees.
- Failure of 3-bulb water stops between I-wall sections.

Fragility Curves

The reliability of the HPS under water loads caused by surge and waves was quantified using structural and geotechnical reliability models integrated within a larger system description of each drainage basin. These structural and geotechnical reliability models are typified by those discussed in Melchers (1999) and Baecher and Christian (2003).

Reliability models were developed and evaluated to determine likely failure modes for each reach in a drainage basin. The reliability models included uncertainties in structural material properties, geotechnical engineering properties, subsurface soil profile conditions, and engineering performance models of levees, floodwalls, and transition points. These are detailed in Appendix 10. Uncertainties due to spatial and temporal variation on the one hand, and due to limited knowledge on the other, were tracked separately in the analysis, providing a best estimate

of the aleatory frequency of failure under given loads, along with a measure of the epistemic uncertainty in that frequency.

Reliability calculations were performed for each reach of the HPS conditioned on given water elevations. A fragility curve was used to describe the conditional probability of failure as a function of water elevation on the reach. These fragility curves were developed separately for levee and floodwall sections and for transitions; and also separately by mode of failure.

Engineering performance models and calculations were adapted from the GDMs. Engineering parameter and model uncertainties were propagated through those calculations to obtain the fragility curves as a function of water height for components of the HPS. These results were calibrated against the analyses of the Performance Team, which applied more sophisticated analysis techniques to similar structural and geotechnical profiles in the vicinity of failures. Failure modes identified by the IPET Performance Team (IPET Volume IV, USACE 2006) were incorporated into the reliability analyses as those results became available.

Reliability assessments for each reach and component of the drainage basin perimeter were combined in the HPS risk model. Each reach within the drainage basin perimeter was analyzed and tracked separately, so that the number of failed reaches and their location around the drainage basin perimeter could be calculated for each branch of the HPS event tree model.

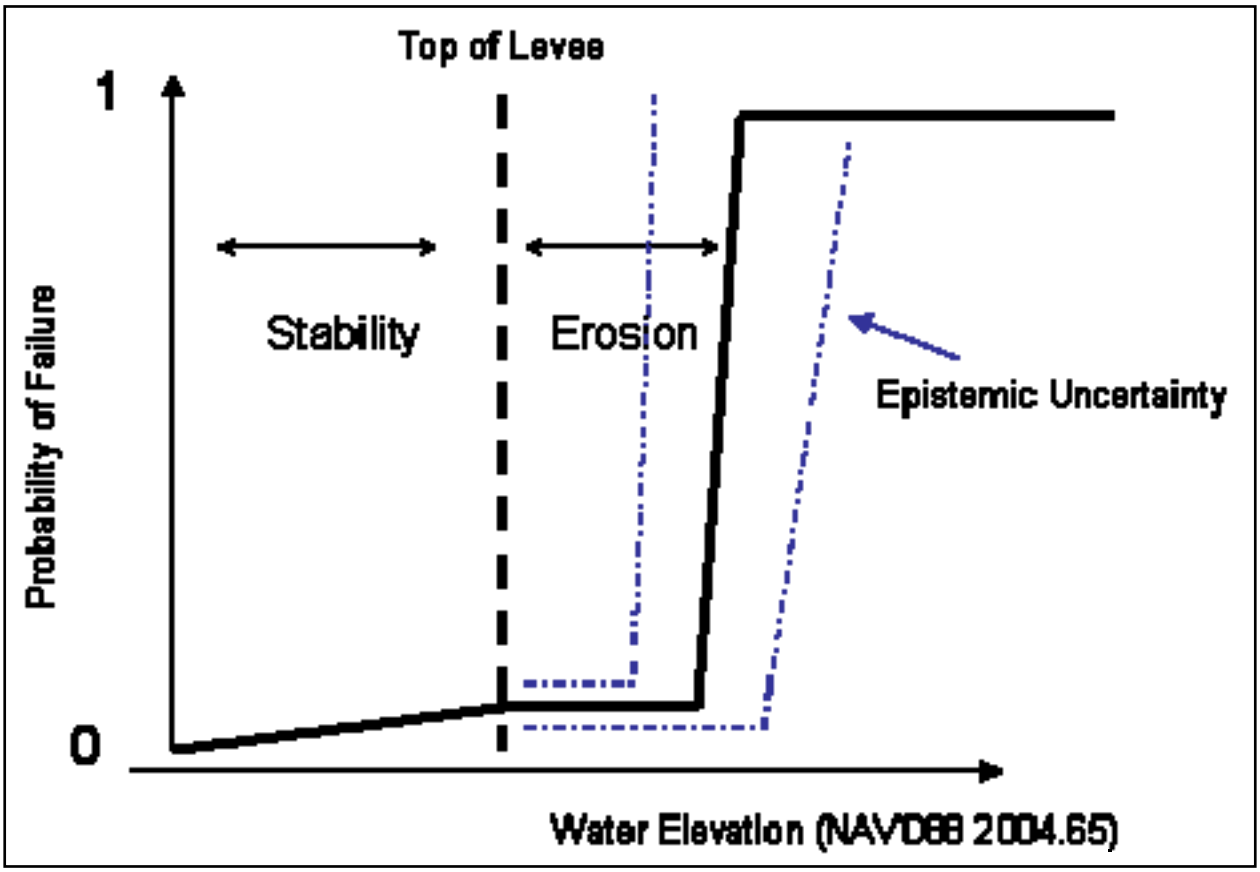

Figure 22. Schematic fragility curve for deep-sliding instability of a levee reach.

Fragility curves summarize the probability of components reaching their respective limit states (i.e., failure), conditioned on water elevations from hurricane conditions. For example, a schematic fragility curve for failure by deep-sliding instability of a levee section is shown in Figure 22 as a function of water height. Design basis water elevation indicates the probability of failure at the design water level (typically 3 ft below levee crest).

Fragility curves for levees and floodwalls were calculated for two conditions: (1) global stability without overtopping, for which reliability was calculated at two water elevations, design elevation and top of levee, and a smooth curve approximated to lower water elevation at mean sea level; and (2) overtopping with subsequent levee erosion, for which reliability was estimated from empirical experience during Katrina at four water elevations of overtopping: 0.5, 1.0, 2.0, and 3.0 ft above the top of levee or floodwall.

Reliability assessments were performed for individual reaches of approximately homogeneous structural type, elevation, geological and geotechnical conditions, and water elevations. This resulted in fragility curves for each reach by mode of failure. Such fragility curves represented the aleatory (i.e., random) uncertainties from one hurricane to another.

Once the fragility curves for each component failure mode were determined, they were input to the HPS risk model, which is based on event tree analysis. For each sequence in the event tree, a "sequence" fragility curve is determined by evaluating the event tree logic at each successive water elevation level. Once each sequence of events has been evaluated, the composite or total fragility for system failure can be determined for each system performance state of interest (e.g., no flooding has occurred in any area protected by the HPS, or flooding occurred as a result of levee or floodwall failure, or flooding occurred as a result of overtopping) by summing the fragility curves for the sequence of events for the same state.

Consequences

One of the primary outputs of the risk modeling of the Risk Team are estimates of the probability distributions of life loss and direct physical damage relating to the performance of the HPS in the Greater New Orleans area. The risk was estimated for the following two scenarios:

- Pre-Katrina (28 August 2005)
- Conditions projected for the 2006 Hurricane Season (1 June 2006).

The Risk Team worked in close collaboration with Consequence Team to obtain estimates of life loss and property loss as a function of maximum inundation elevation in the 27 sub-basins that comprise the following ten basins of the New Orleans HPS:

- East Bank
- New Orleans Metro - Orleans East Bank
- New Orleans East
- St. Bernard Parish
- Jefferson Parish
- St. Charles Parish
- Plaquemines

- West Bank
- Cataouache
- Westwego to Harvey Canal
- Harvey Canal to Algiers Canal
- Algiers Canal to Hero Canal

The numbers of sub-basins that are contained within portions of the following Parishes are indicated in parentheses: Jefferson (7), Orleans (12), Plaquemines (1), St. Bernard (5), and St. Charles (2) Parishes.

The Risk Model was run for hurricane realizations that represent a wide range of hurricane events with different severities, directions, points of landfall, etc. For each of these hurricane realizations, the Risk Model represented the performance of the HPS and estimated the probability that inundation would result from insufficient internal drainage, overtopping of the levees without breaching, and levee breaching. The resulting estimates of maximum inundation depths were used as a basis for interpolation of life loss and property loss estimates using the relationships that were provided by the Consequence Team. Estimates were made for each of the 27 sub-basins and for the Pre-Katrina and 1 June 2006 scenarios. Thus it was necessary that the life loss and property loss estimates covered a range of elevations associated with a range of hurricane events that could impact New Orleans from minor inundation to elevation 36 ft above sea level.

The estimates of life loss were developed as probability distributions and the estimates of property loss were developed as best estimates with an associated 90% confidence interval rather than single-value or point estimates. The probability distributions for life loss and confidence intervals for property losses represent various types of uncertainties in the estimates.

Uncertainty Analysis

One of the principal questions to be addressed in the risk and reliability analysis for the HPS concerns the level of uncertainty associated with estimated levels of flooding that may occur in New Orleans. The uncertainty in the risk analysis results manifests itself in the estimate of the 100-year area (and depth) of inundation. The assessment of the uncertainty takes into account the uncertainties associated with the assessment of hurricane occurrences (how frequently they occur as well as their size) and the estimated surge and wave elevations, and the performance of the HPS (its reliability).

There are two types of uncertainty: aleatory and epistemic uncertainty. The first is attributed to the inherent randomness of events in nature, manifesting as variability over time for phenomena that take place at a single location (temporal variability), or variability over space for phenomena that take place at different locations but at a single time (spatial variability), or as variability over both time and space. These events are predicted in terms of their frequency of occurrence (for example, per year in the case of hurricanes, or per trial in the case of a levee reach that is impacted by a given surge event). Aleatory uncertainty is, in principle, irreducible.

Epistemic or knowledge-based uncertainty is attributed to our lack of knowledge or information (data) about events, or lack of understanding of physical processes that limits our ability to model the natural phenomena (hurricane surges) or events of interest (levee performance). For example, limitations in available data sets (length of record, data quality) impact the assessment of model parameters (shear strength of soils) or the likelihood of an event such as the annual rate of hurricane occurrences. When limited data are available, parameter estimates may be quite uncertain (i.e., statistical confidence intervals on parameter estimates can be large). A second type of knowledge uncertainty is attributed to a lack of understanding or knowledge about physical processes that must be modeled (e.g., the meteorological processes that generate hurricane events). In these instances, expert evaluations are often required to assess the current state of knowledge and to quantitatively evaluate the level of uncertainty.

The distinction between aleatory and epistemic uncertainty can be difficult and is model dependent. Nonetheless, making a distinction between the sources of uncertainty in a logical manner helps insure that all uncertainties are quantified and identified. In principle, epistemic uncertainties are reducible with the collection of additional data or the use/development of improved models.

Uncertainties impact the assessment of each element of the HPS risk and reliability analysis: hurricane and surge analysis, reliability of the HPS, the assessment of flooding/inundation, and the analysis of consequences. To assess or model uncertainties (aleatory and epistemic) a taxonomy of uncertainties can be used to define the various types and to guide their assessment. Aleatory and epistemic uncertainties can be partitioned in terms of models and estimates of model parameters. Modeling uncertainty represents differences between the actual physical process (hurricane, embankment failure) and prediction models. Modeling uncertainty can be estimated by comparing model predictions to actual, observed events/performance. Parameter uncertainty is the uncertainty in the values of model parameters. Parametric uncertainty is quantified by observing the variation in parameters inferred (either in a direct or indirect manner).

The primary uncertainties in the hurricane and reliability parts of the HPS risk analysis have been identified and considered. Table 11 provides a summary of the uncertainties that are considered.

The epistemic uncertainty in the individual parts of the risk analysis are combined to estimate the uncertainty in the analysis products such as the frequency of levee failure in a polder and the frequency of inundation of New Orleans basins and parishes. Figure 22 illustrates the result of the uncertainty analysis for the frequency of HPS system failure. The distribution on the estimate of the frequency of failure is a function of the uncertainty in the hurricane analysis and the fragility of levees and floodwalls. Similarly, implementation of the risk model to estimate inundation in each polder produces an estimate of the uncertainty in the frequency of flooding in each basin.

Appendix 11 of this volume describes the quantification procedure that is used to propagate uncertainties in the HPS risk analysis.

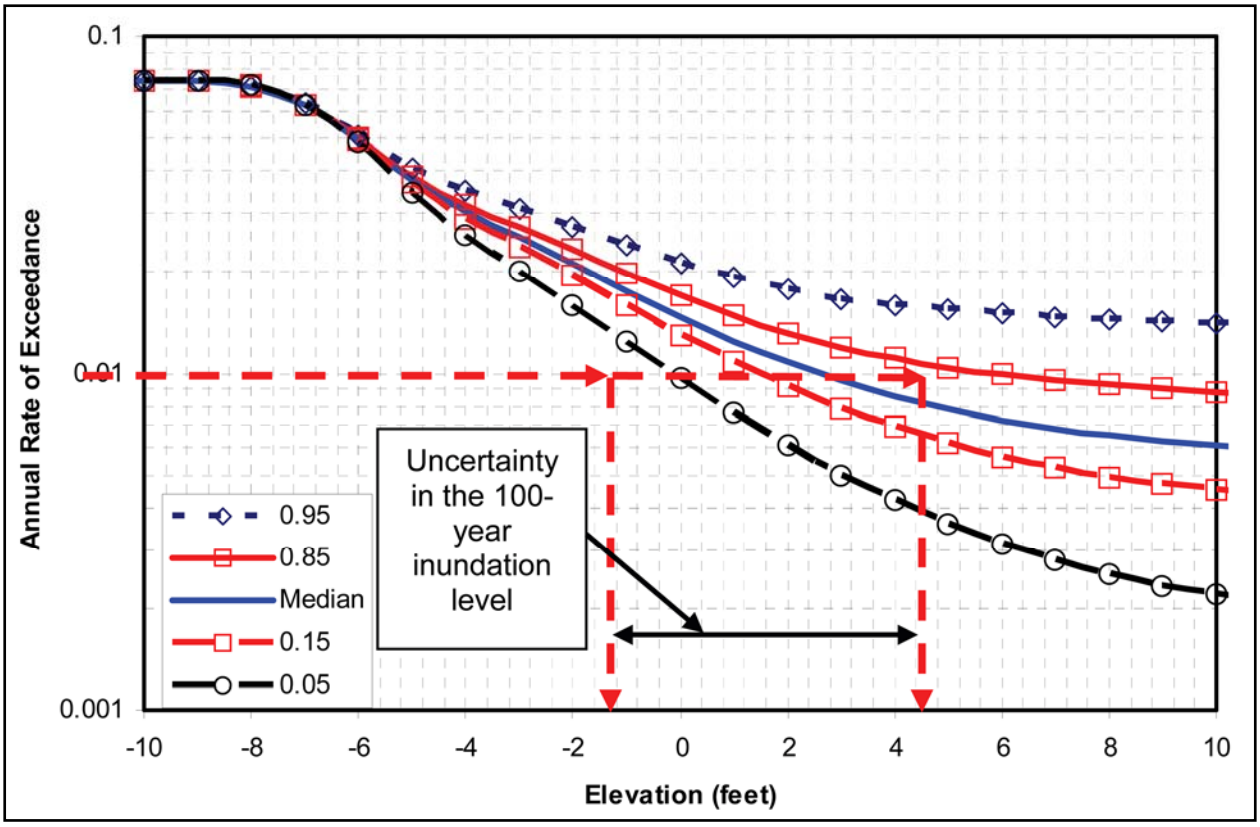

Figure 23. Illustration of the uncertainty in a basin frequency distribution.

Table 11. Summary of Aleatory and Epistemic Uncertainties

Element	Aleatory	Epistemic
Hurricane Analysis	Temporal and spatial hurricane occurrences Hurricane Parameters – central pressure, radius to maximum winds, azimuthal track, translational velocity Inter-event variability in surge/wave elevations Rainfall	Mean temporal rate of occurrence of hurricanes Hurricane prediction model (ADCIRC, etc.) JPM model parameters (c_p, Gumbel distribution)
Levee Reliability	Levee, floodwall reliability Scour potential over space	Geotechnical model uncertainty Limited numbers of borings and soil test data Geological profile uncertainty
Flooding/Inundation	Levee overflow Gate closure reliability Gate flow characteristics	Overflow mean weir coefficient

Table 12. Taxonomy/Partitioning of Uncertainties			
		Risk Analysis	
		Epistemic	Aleatory
Hurricane Hazard Analysis	Modeling	Uncertainty about a model and the degree to which it can predict events (i.e., to what extent model has a tendency to over- or under-predict observations).	Aleatory modeling variability is that variability that is not explained (observations) by a model. For instance, these would be elements of the physical process that are not modeled and, therefore, represent a variability (random differences) between model predictions and observations.
	Parametric	Parametric epistemic uncertainty is associated with the estimates of model parameters given available data, indirect measurements, etc.	This uncertainty is similar to aleatory modeling uncertainty. This storm-to-storm variation in hurricanes is an aleatory variability that may be considered independent from event to event.

Results

The effectiveness of the repairs and improvements made to the HPS can best be measured by comparing the predicted inundation elevation-exceedance relationships for the Pre-Katrina and Current HPS. The risk analysis results show that moderate inundation reductions have been achieved for events of approximately 100-year return periods, but predicted inundation elevations are mostly unchanged for more frequent events (e.g., 50-year return periods) that depend mostly on rainfall, and there is still significant risk of inundation for stronger storms. These results are explained in more detail in Appendix 13.

Figure 24 shows the best estimate (mean) water elevation vs. exceedance probability for each sub-basin associated with the Pre-Katrina HPS as predicted by the risk analysis. Figure 25 shows the best estimate (mean) water elevation vs. exceedance probability associated with the Current HPS. Corresponding results are shown in Figures 26 and 27 for the best estimate water elevations plus the upper uncertainty for the pre-Katrina and Current HPS, respectively.

Pre-Katrina

Rate of HPS Overtopping – Peak surge and wave elevations at each of the 135 reaches in the pre-Katrina HPS for each of the 152 storms developed by the LaCPR unified USACE/FEMA team were compared to the top of levee or wall elevations at each reach. The rates of reach overtopping for the pre-Katrina HPS due to peak surges and waves from the 152 storm set are depicted in Figure 28 and Figure 29. The values shown were determined by counting the number of times that the reach elevation was exceeded by the peak surge in the storm set and then dividing the sum by 152.

Inundation Mapping – Maps have been prepared to depict the following results as determined in the risk analysis.

- Overtopping rates for the entire HPS
- Basin frequency of inundation

- Sub-basin frequency of inundation

These maps show inundation for selected return periods, specifically the 50-, 100-, and 500-year inundations. The risk analysis produced elevation-exceedance curves for all elevations, and the elevations used in the maps were selected from those curves. The maps depict the "best estimate" elevation values and an upper bound value as determined by the uncertainty analysis. Since the risk model determines inundation potential at the sub-basin level, some local areas within a subbasin may have additional drainage conditions that cannot be modeled with the risk model. These areas may show lower levels of inundation, especially near sub-basin boundaries, if a more accurate HEC-RAS type analysis was conducted. Example inundation maps are provided at the end of this report and the complete set of maps is included in Appendix 13.

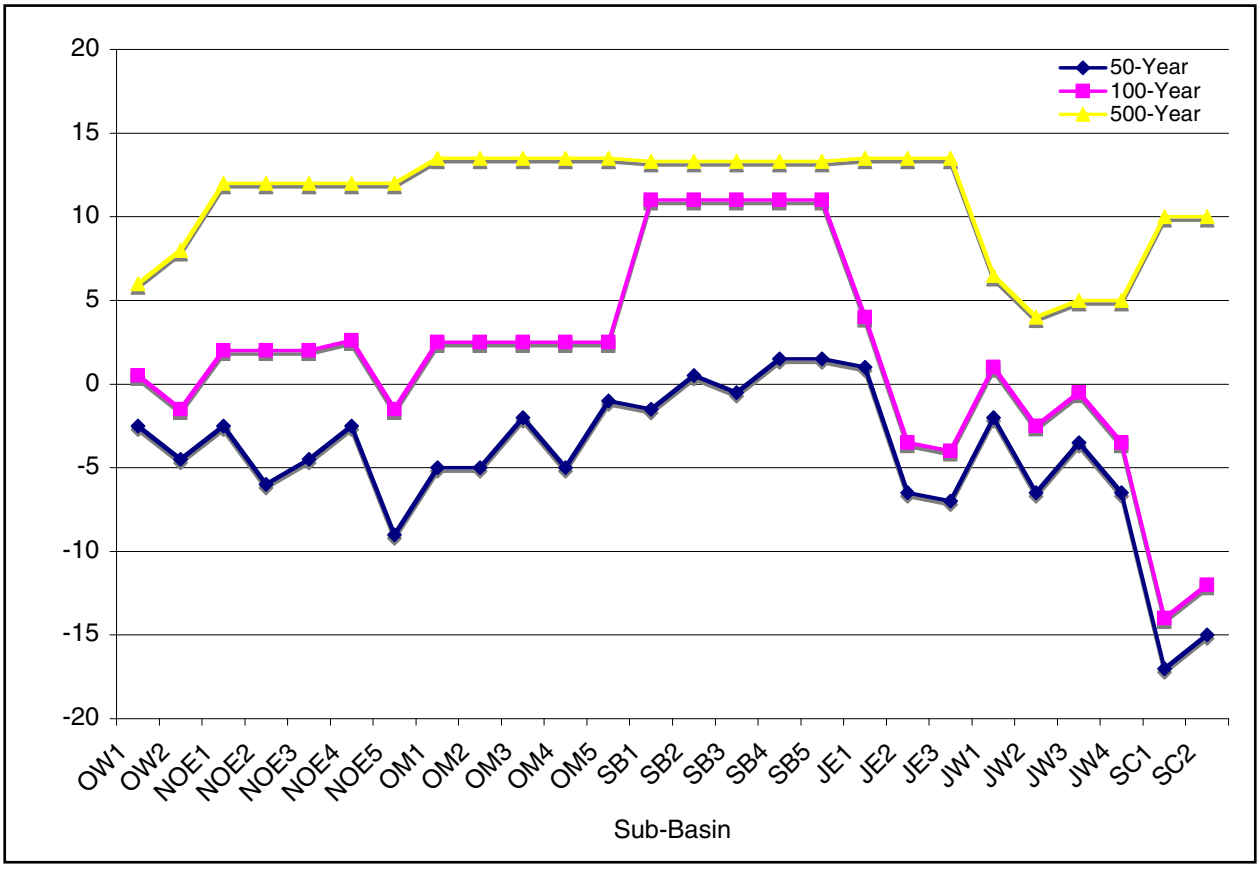

Figure 24. Pre-Katrina HPS mean.

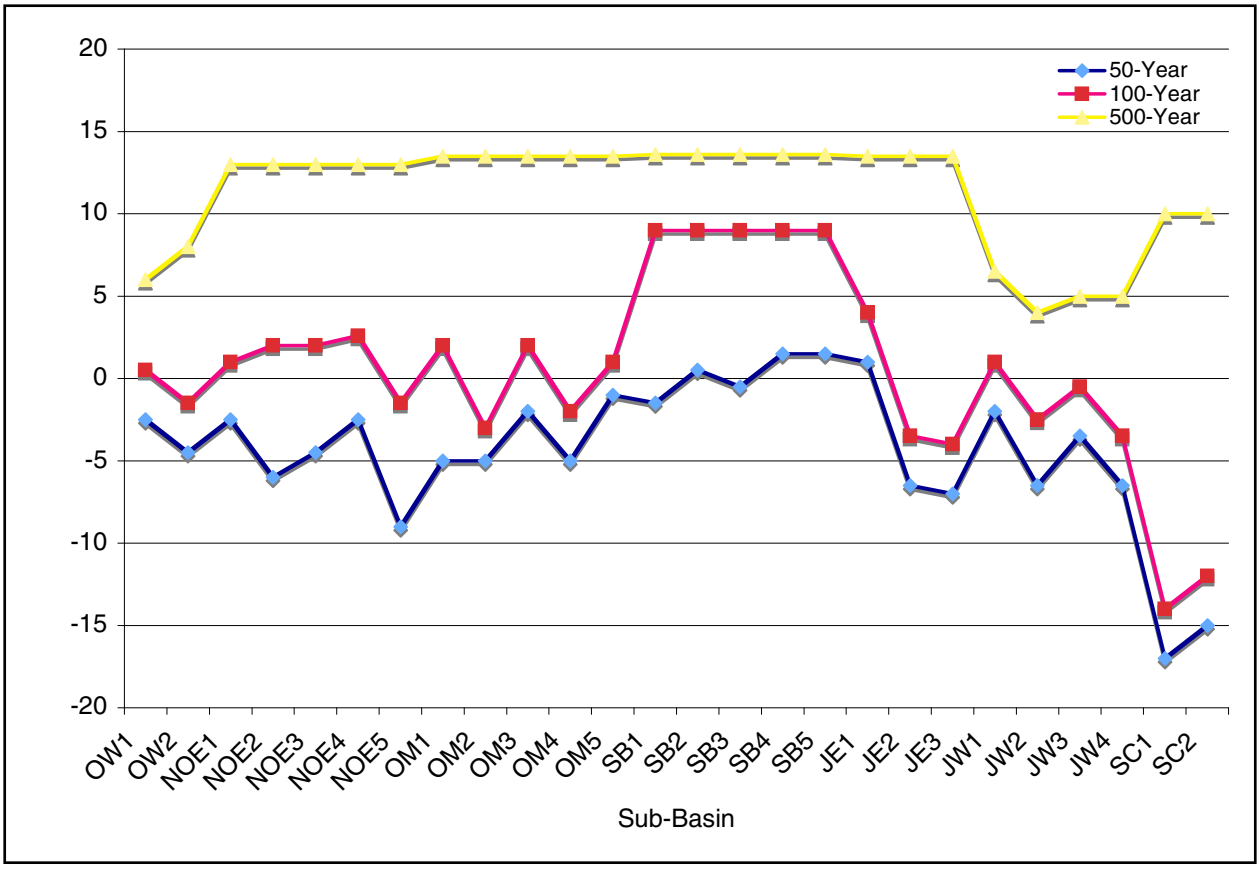

Figure 25. Current HPS mean

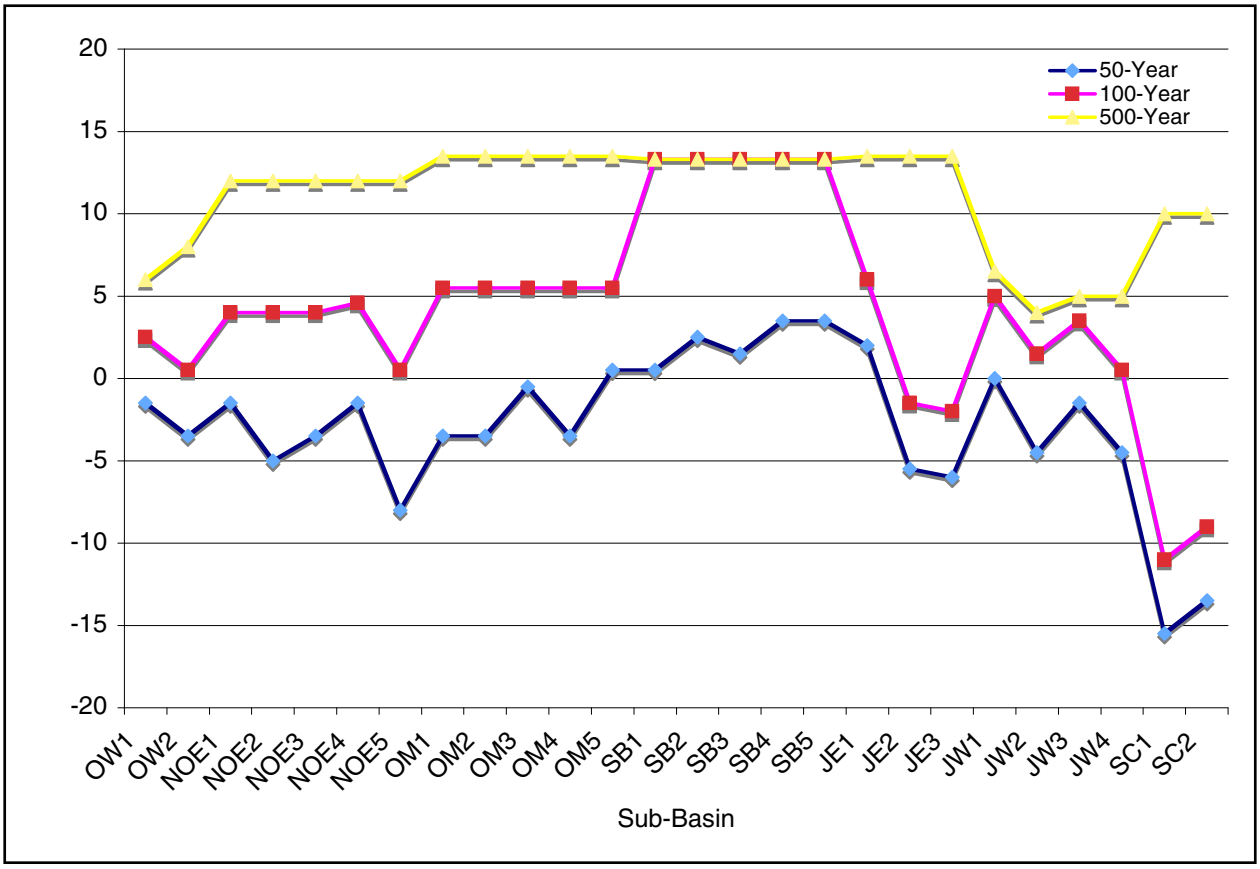

Figure 26. Pre-Katrina HPS with upper uncertainty

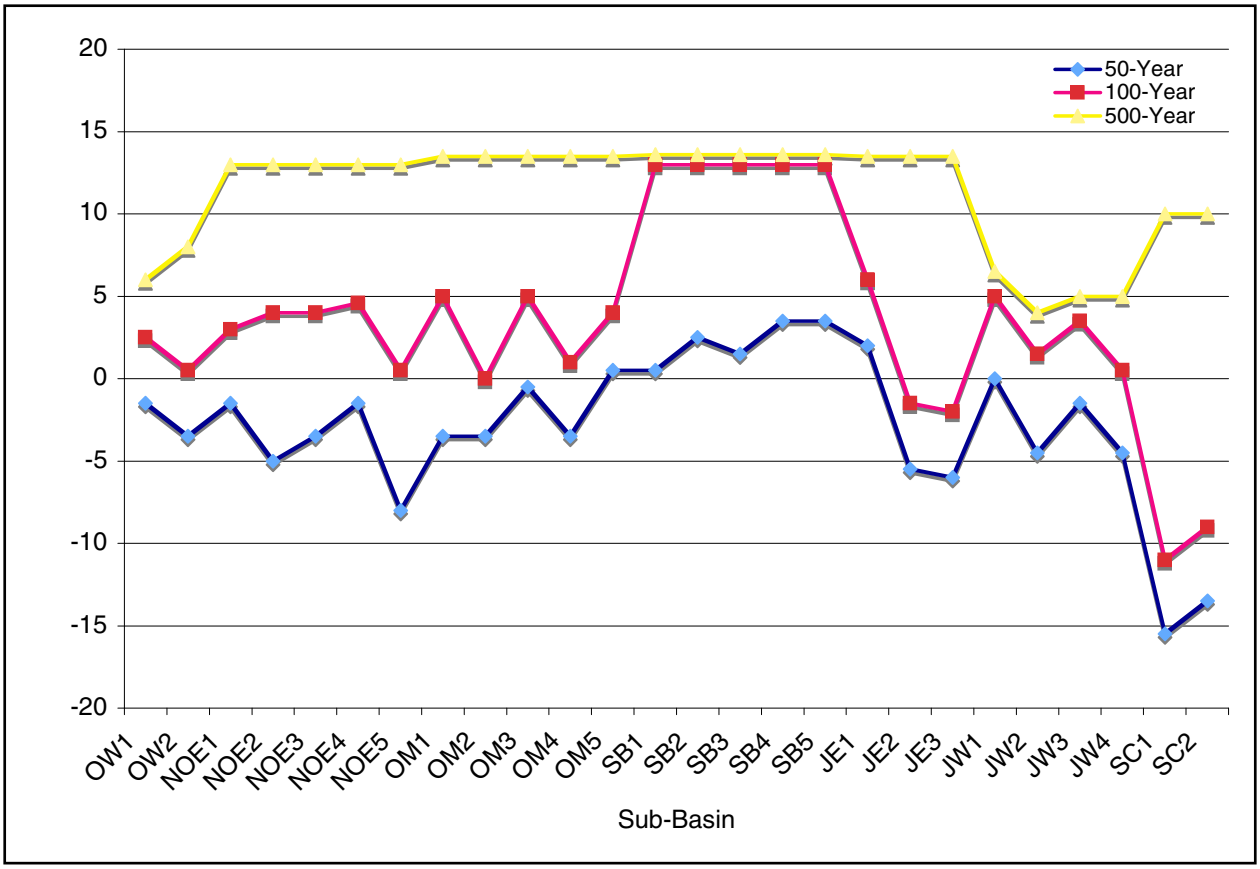

Figure 27. Current HPS with upper uncertainty.

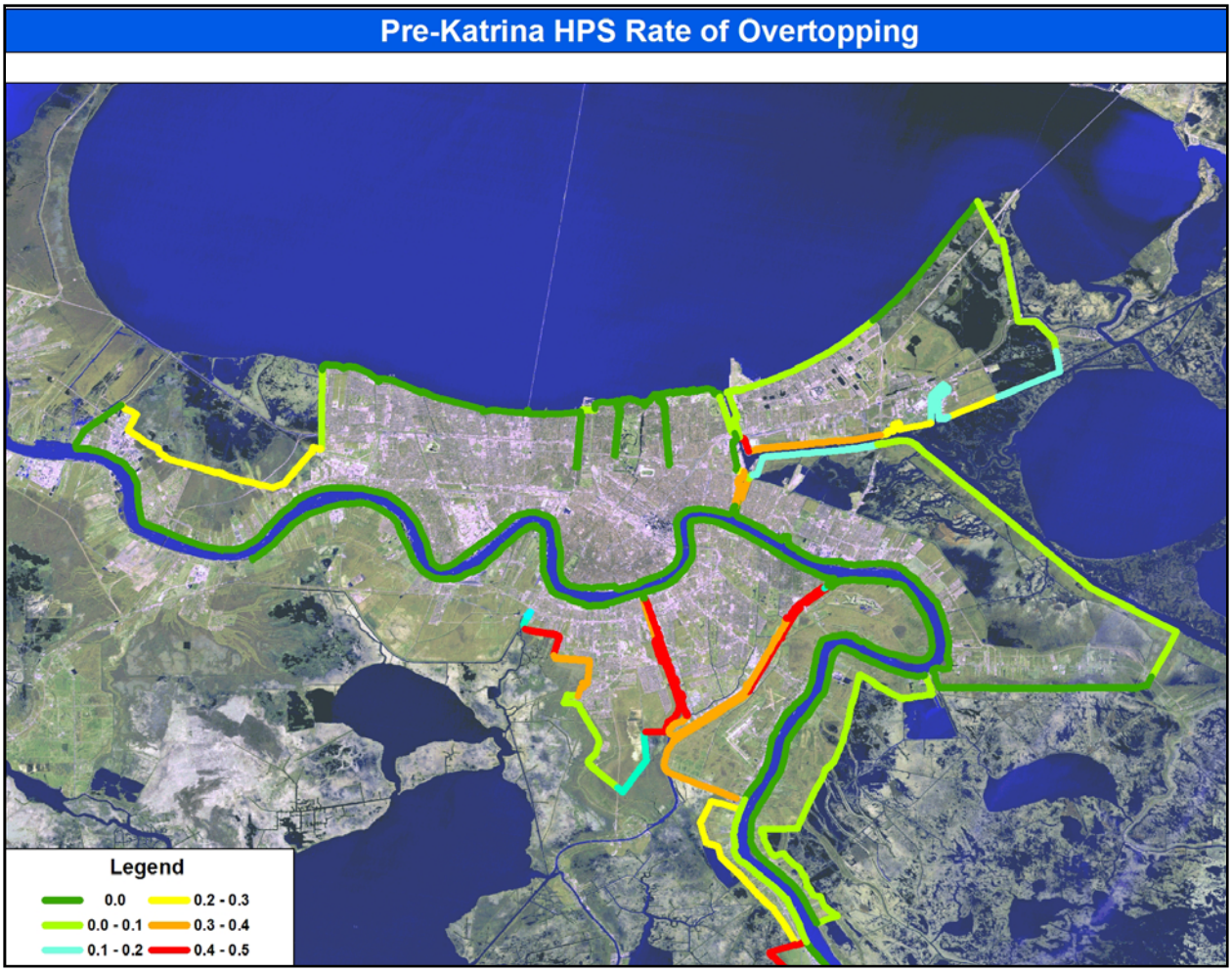

Figure 28. Pre-Katrina rate of overtopping for 152 storm set – Northern

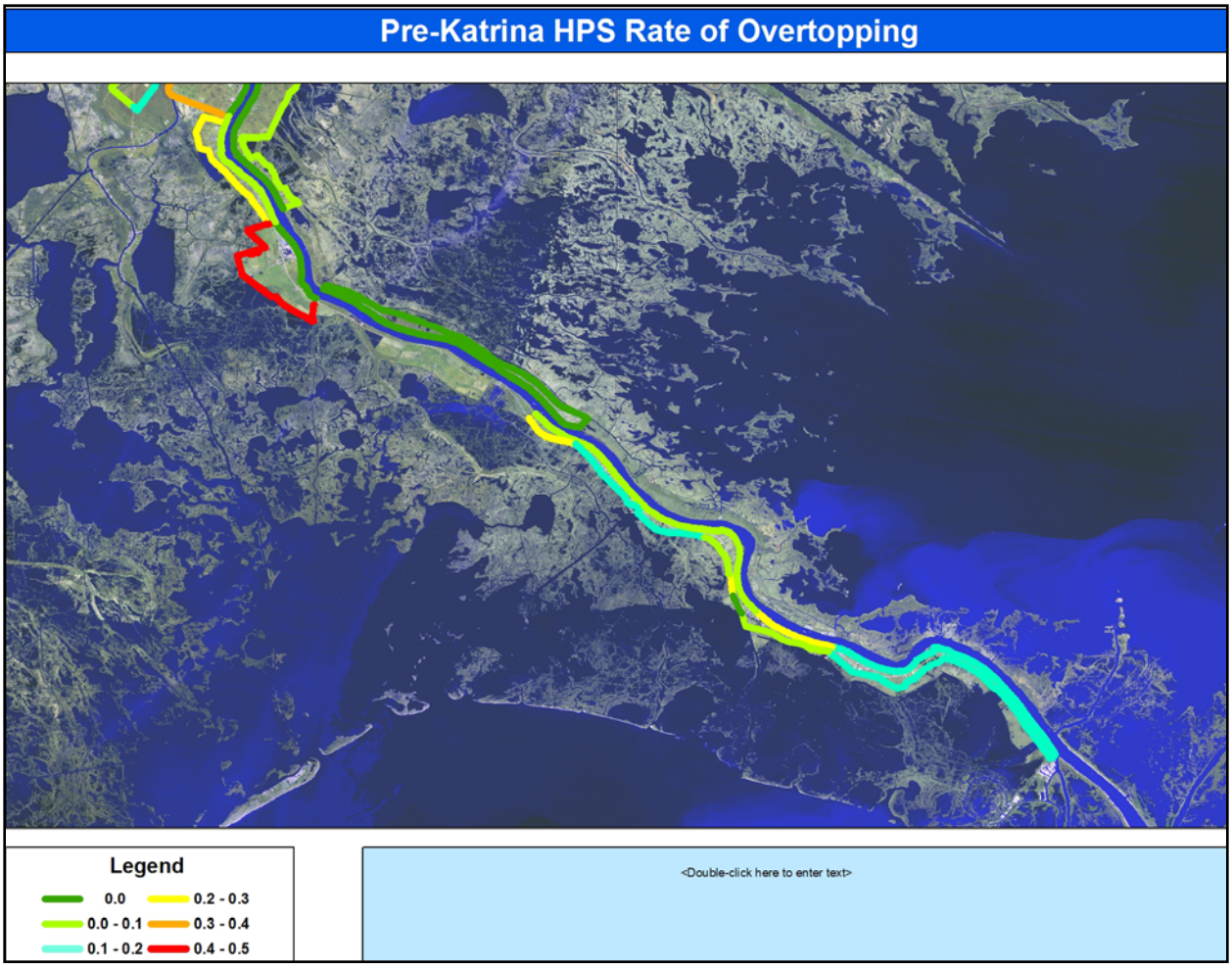

Figure 29. Pre-Katrina rate of Overtopping for 152 Storm Set – Southern

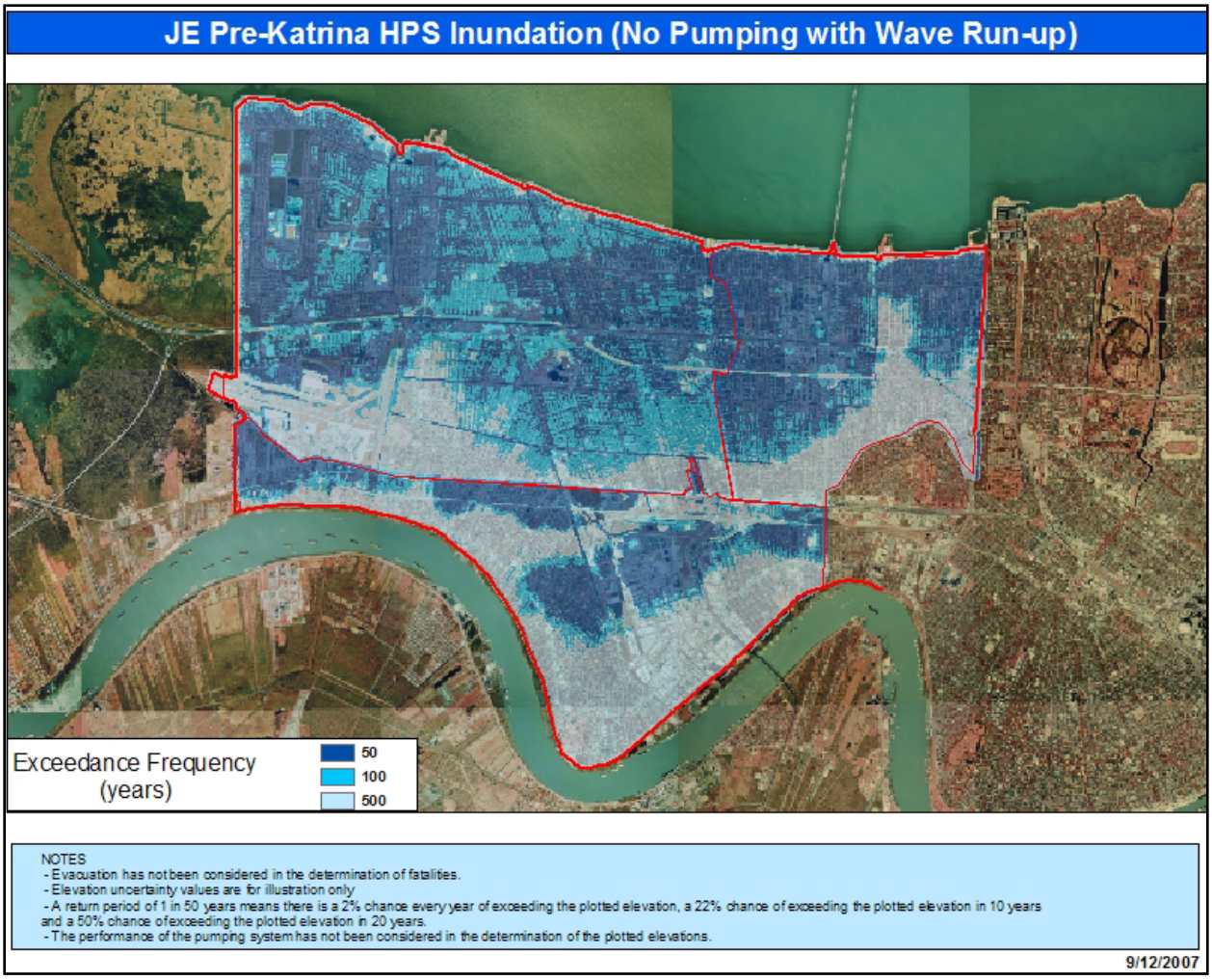

Figure 30. Jefferson Parish East - Pre-Katrina inundation no pumping

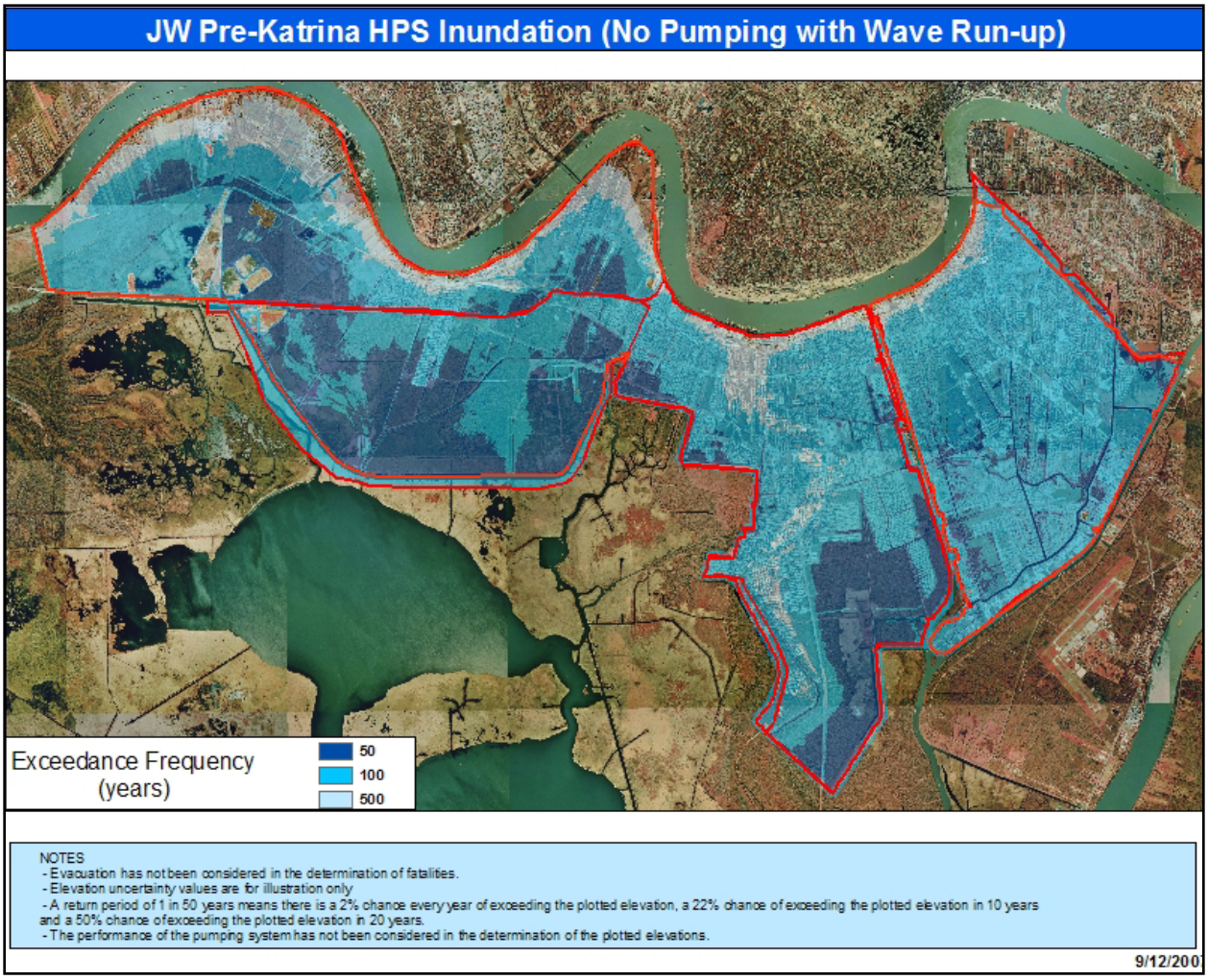

Figure 31. Jefferson Parish West - Pre-Katrina inundation no pumping

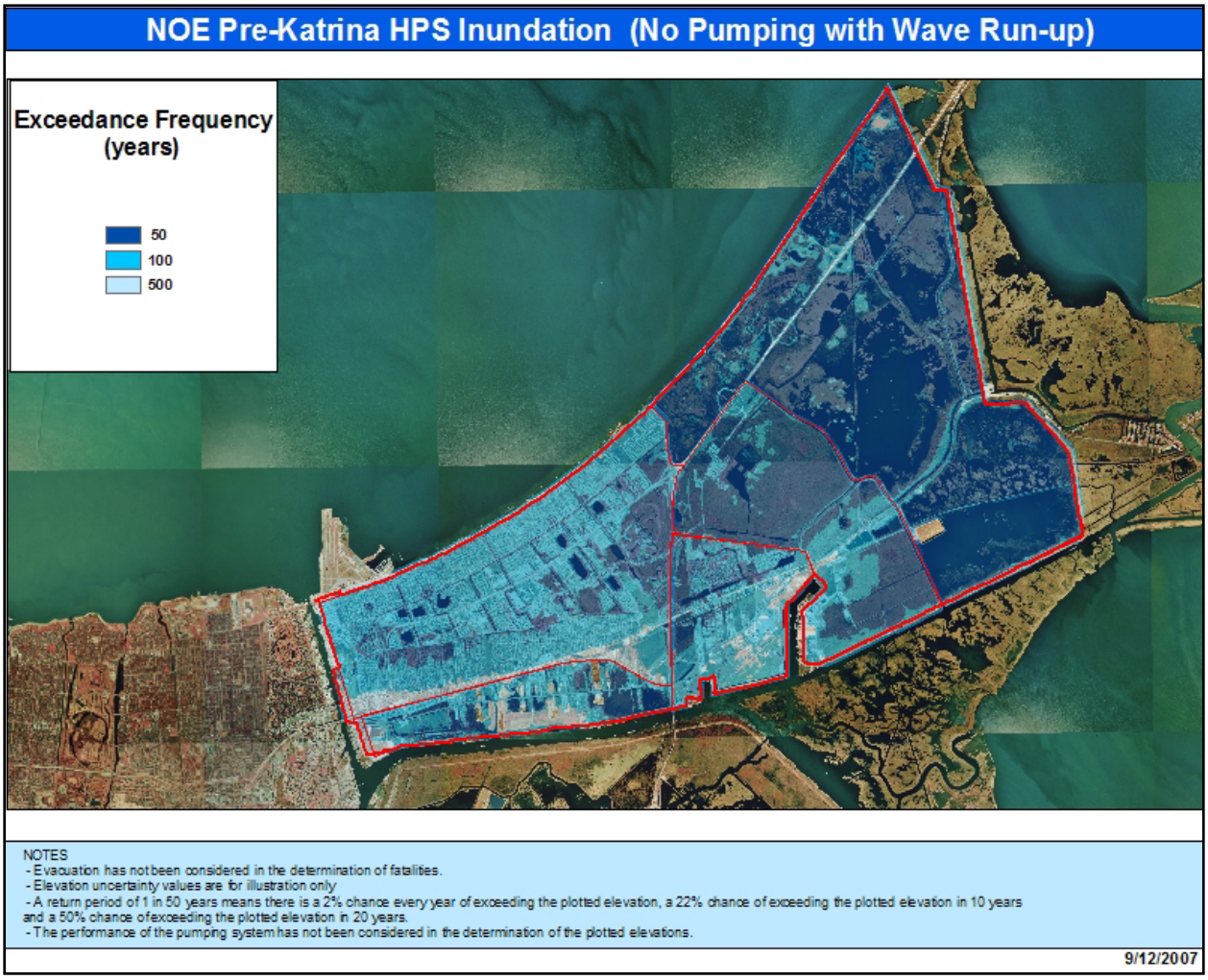

Figure 32. New Orleans East Parish- Pre-Katrina inundation no pumping

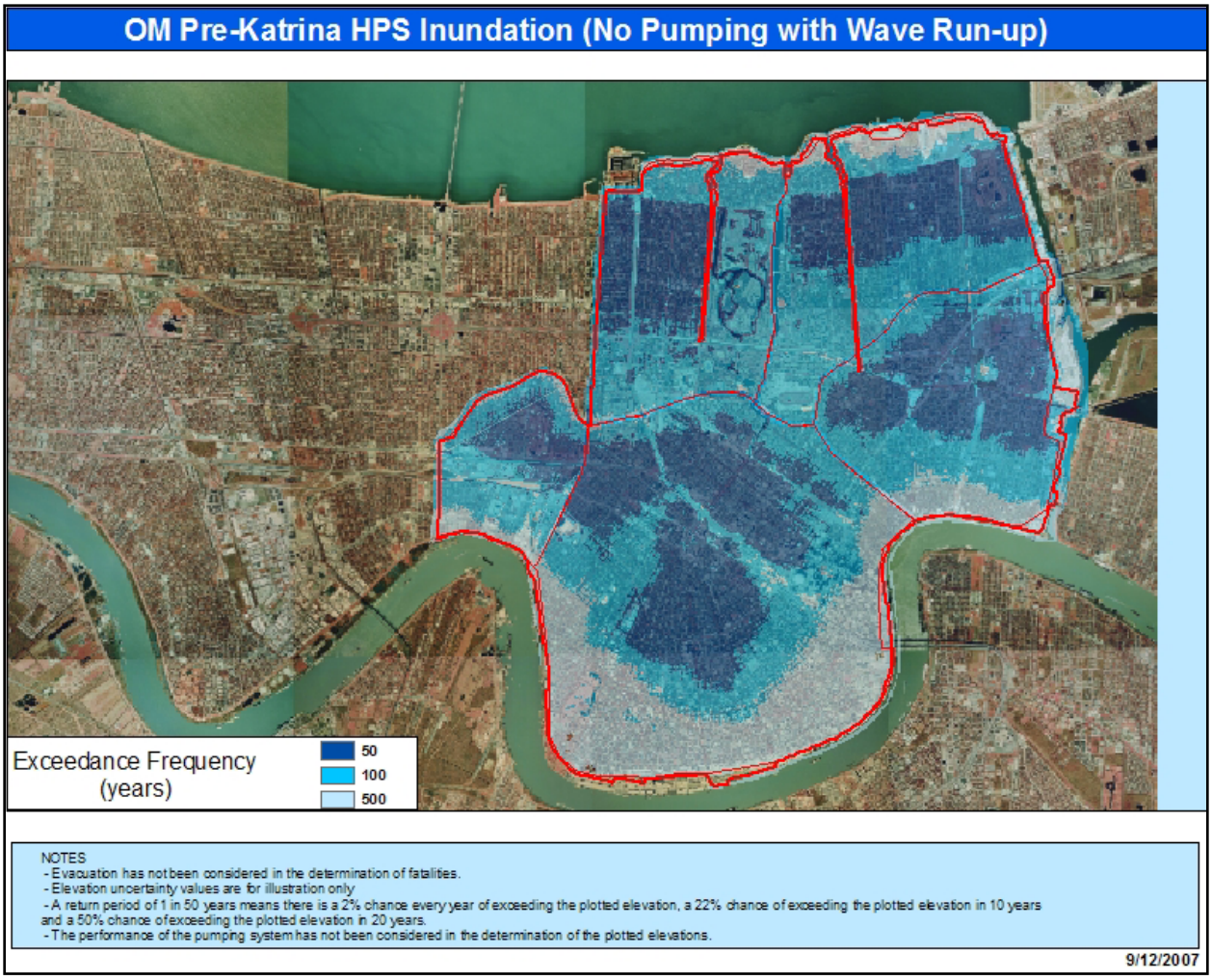

Figure 33. Orleans Parish East - Pre-Katrina inundation no pumping

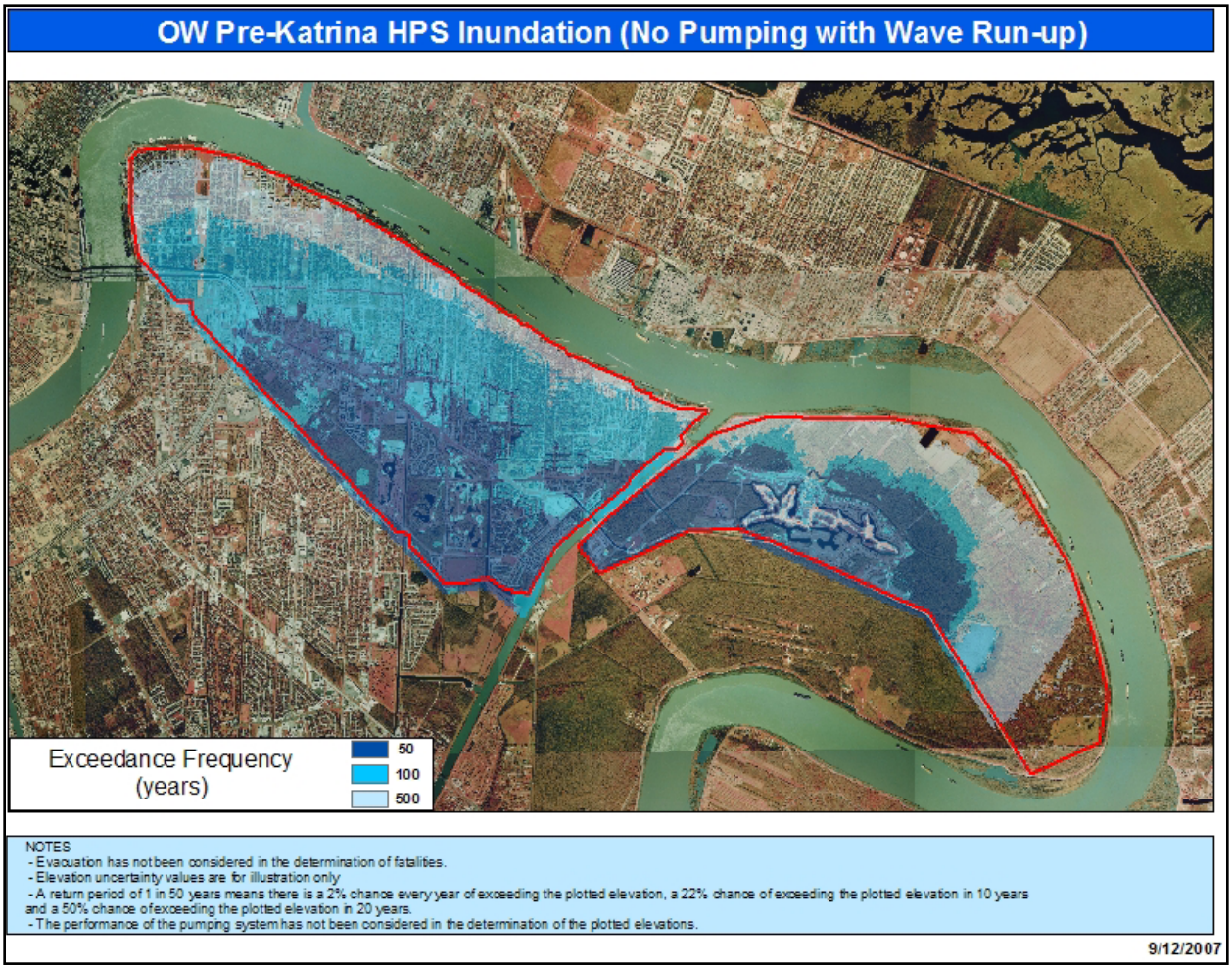

Figure 34. Orleans Parish West Bank - Pre-Katrina inundation no pumping

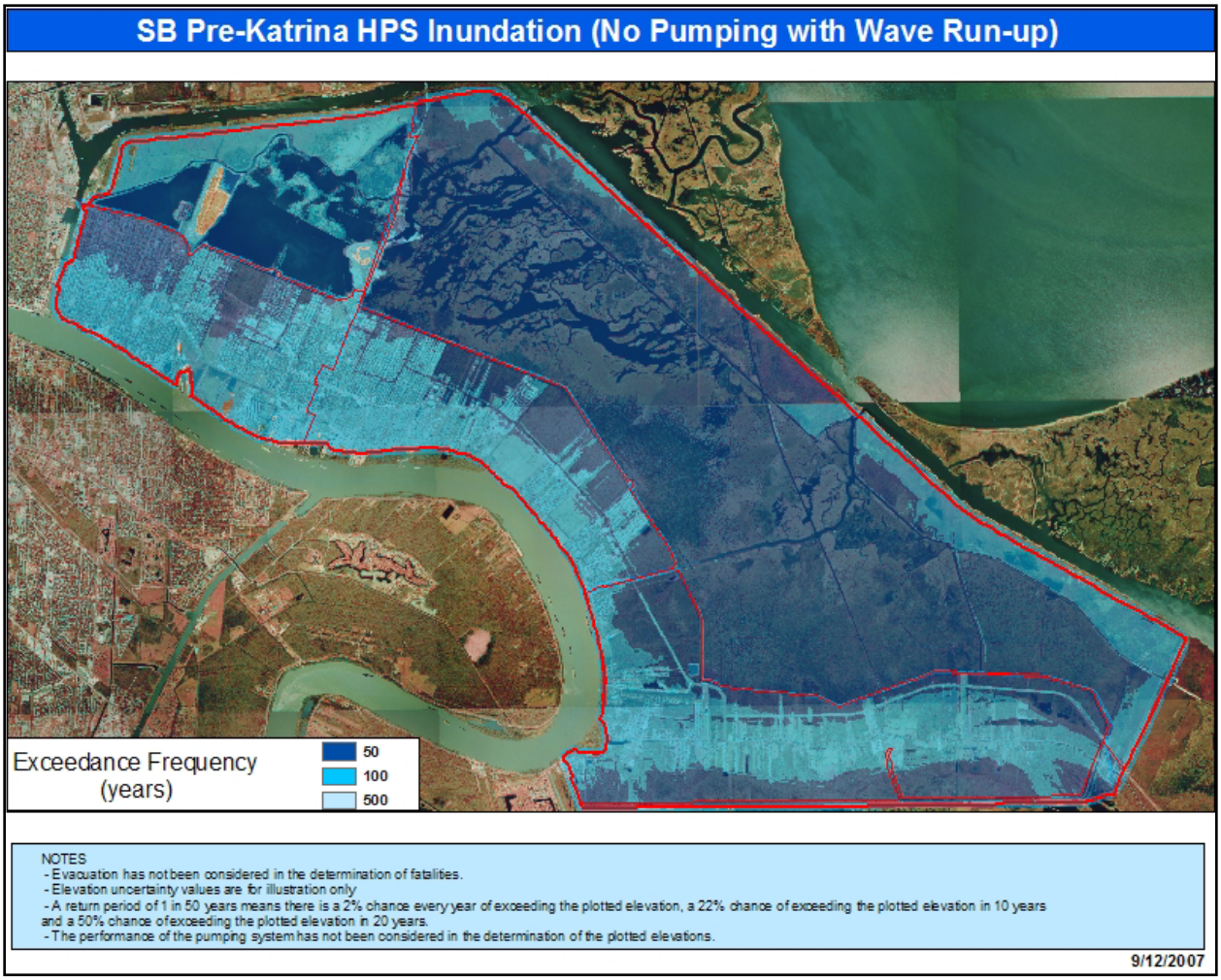

Figure 35. St Bernard Parish - Pre-Katrina inundation no pumping

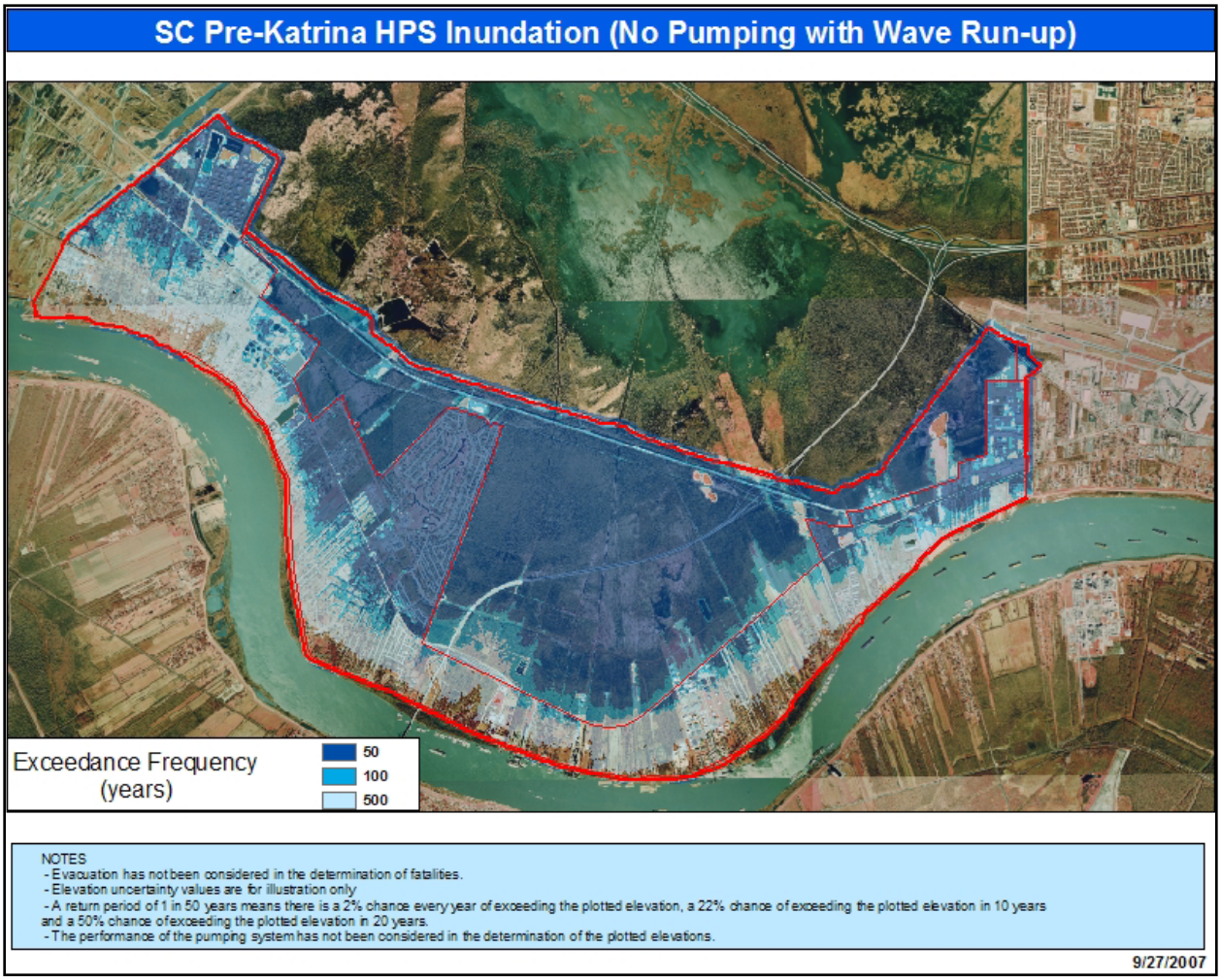

Figure 36. St Charles Parish - Pre-Katrina inundation no pumping

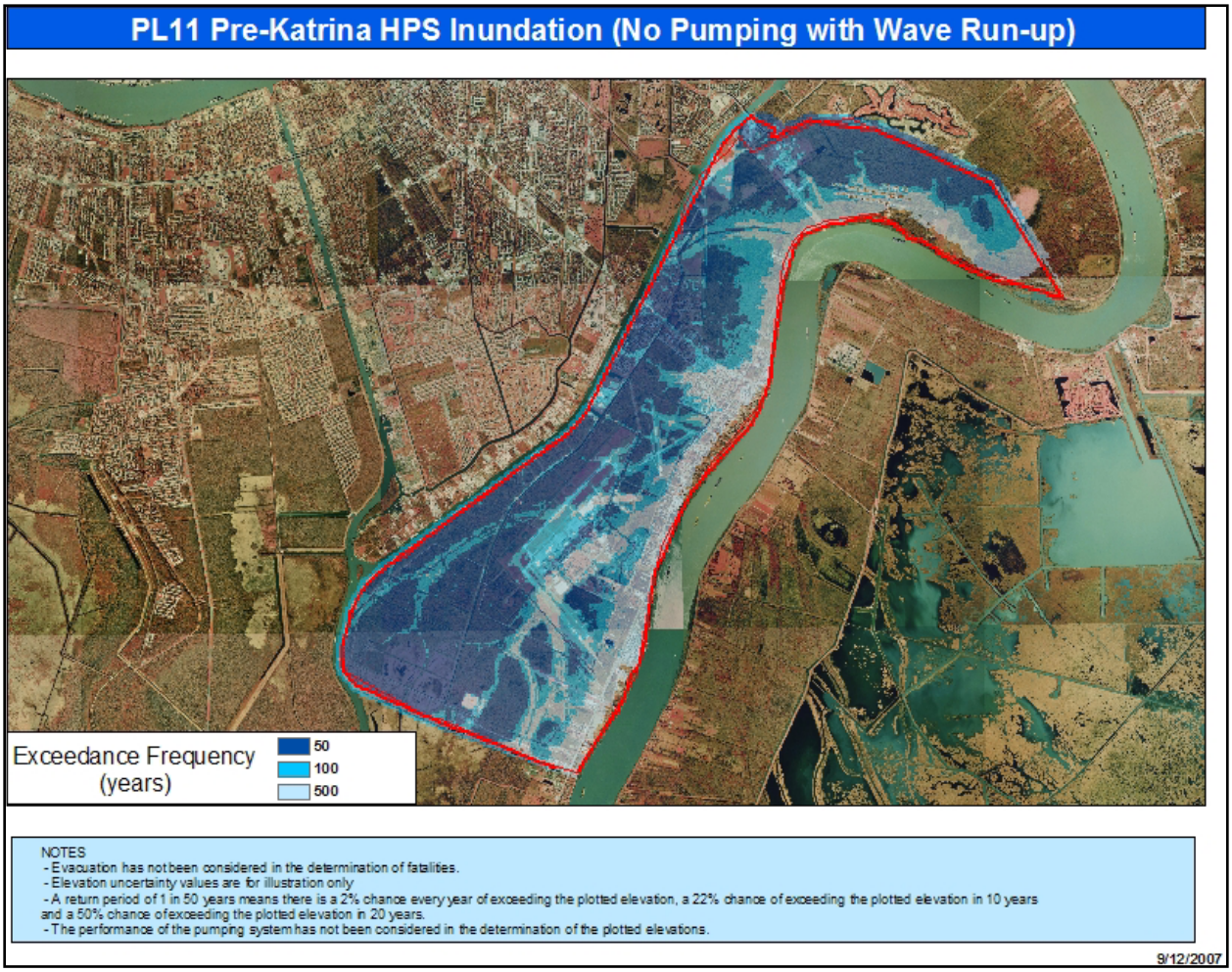

Figure 37. Plaquimines Parish – Pre-Katrina inundation no pumping

Current HPS

Rate of HPS Overtopping – The rates of reach overtopping for the Current HPS due to peak surges and waves from the 152 storm set are depicted in Figures 38 and 39. The values shown were determined by counting the number of times that the reach elevation was exceeded by the peak surge in the storm set and then dividing the sum by 152.

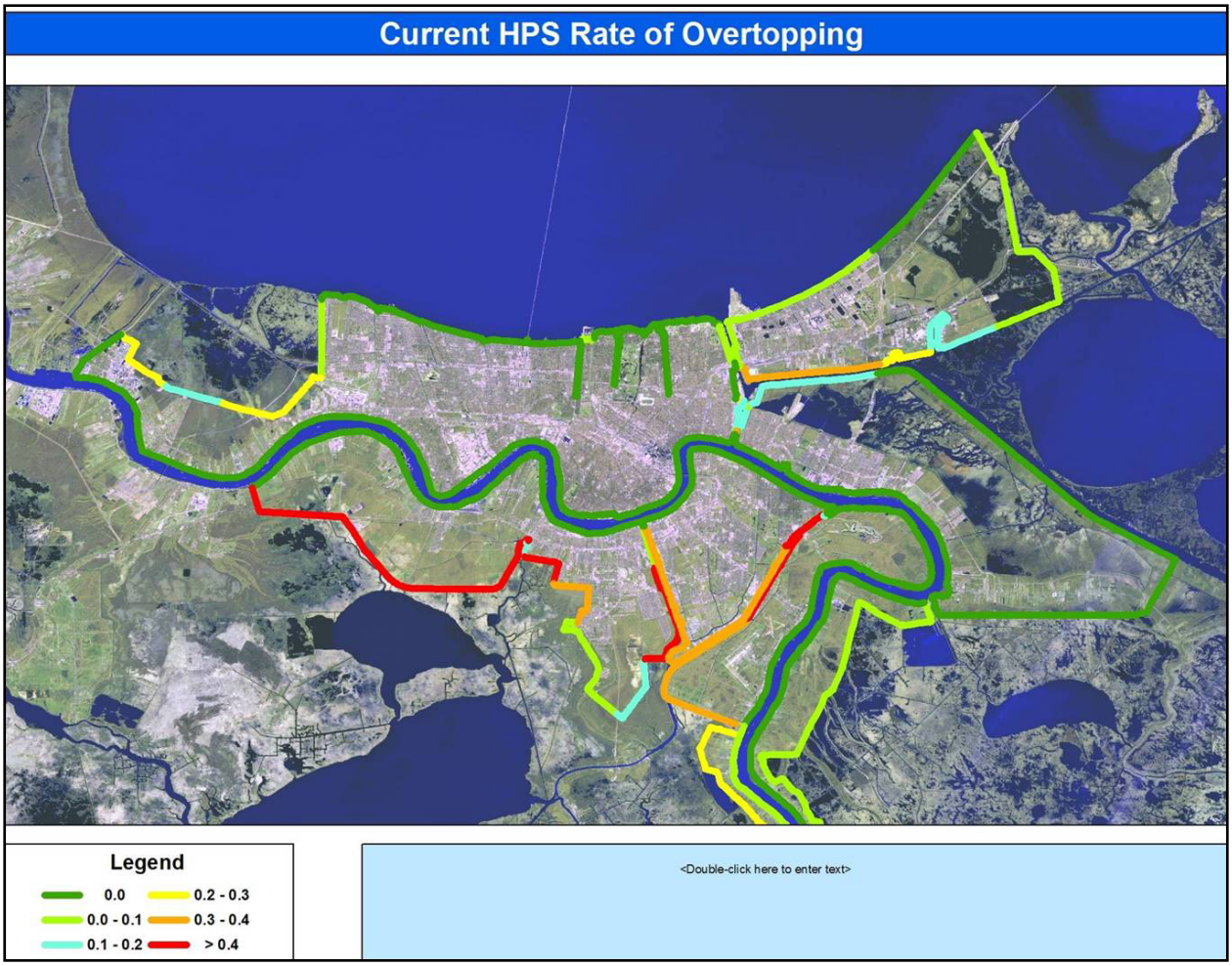

Figure 38. Current HPS Rate of Overtopping for 152 Storm Set – Northern

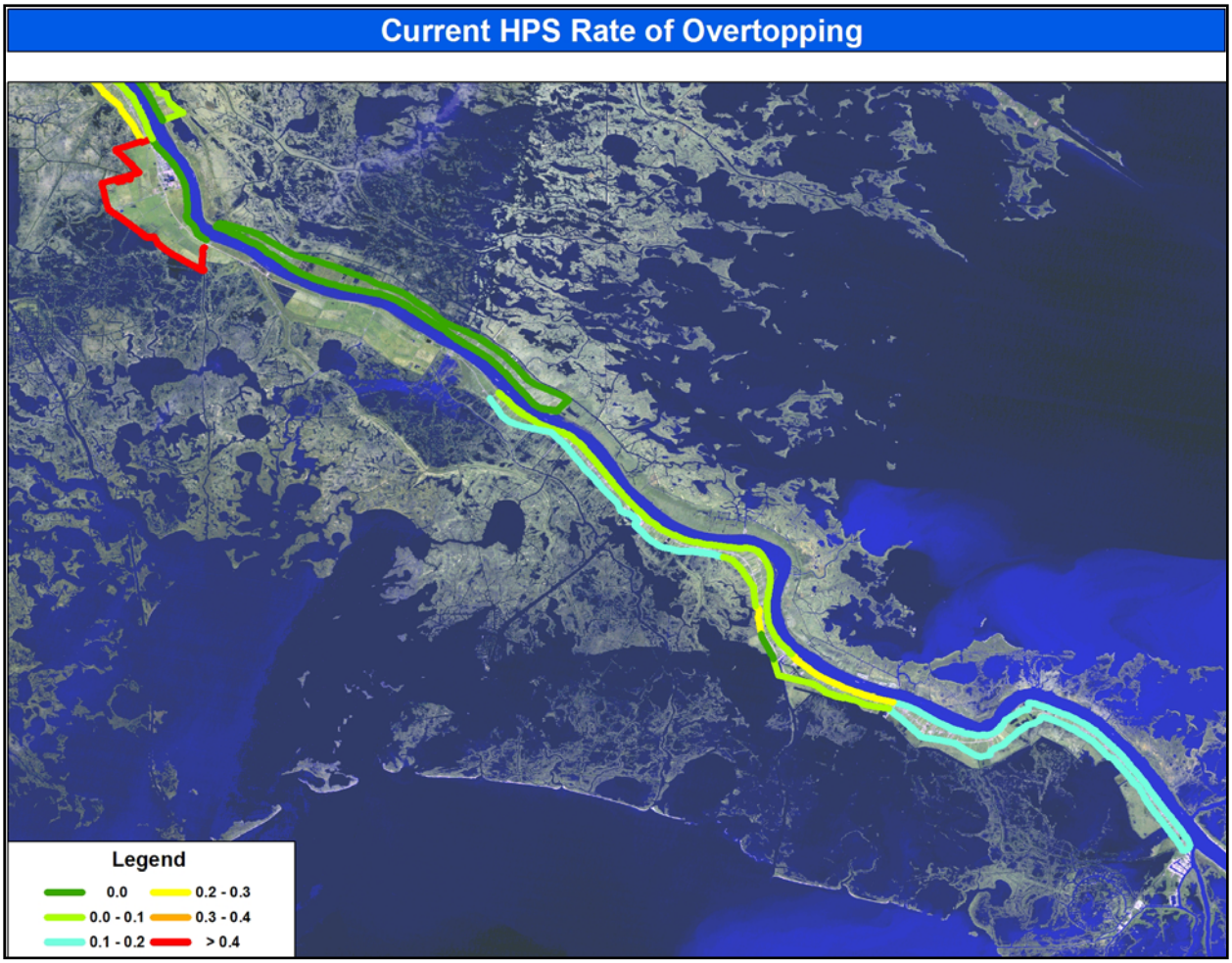

Figure 39. Current HPS Rate of Overtopping for 152 Storm Set - Southern

Inundation Mapping – Maps have been prepared to depict the following results as determined in the risk analysis.

- Overtopping rates for the entire HPS
- Basin frequency of inundation
- Sub-basin frequency of inundation

These maps show inundation for selected return periods, specifically the 1/50, 1/100 and 1/500 year inundation. The risk analysis produced elevation-exceedance curves for all elevations and the elevations used in the maps were selected from those curves. The maps depict the "best estimate" elevation values and an upper bound value as determined by the uncertainty analysis. Example inundation maps are provided at the end of this report and the complete set of maps is included in Appendix 13.

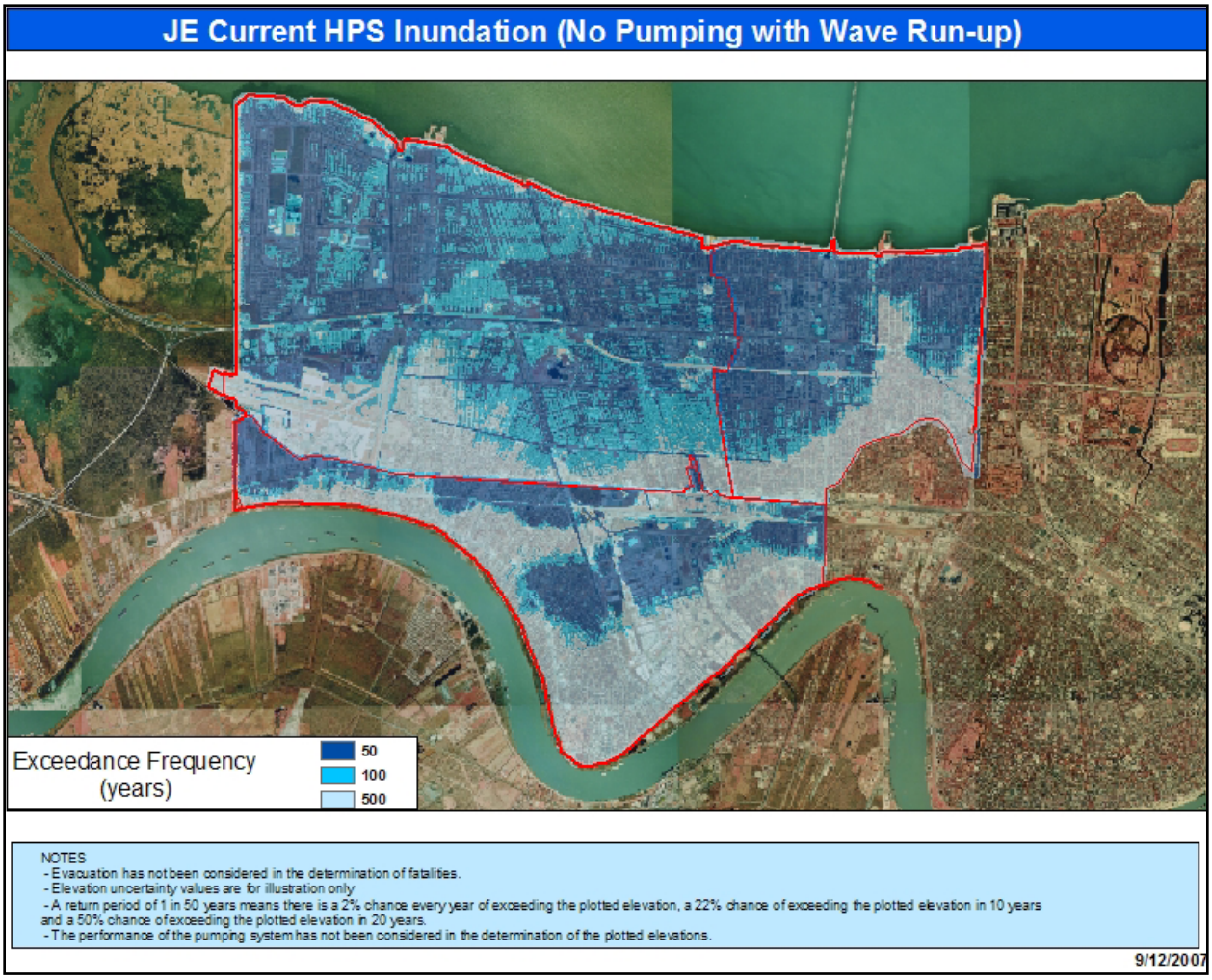

Figure 40. Jefferson Parish East - Current inundation no pumping

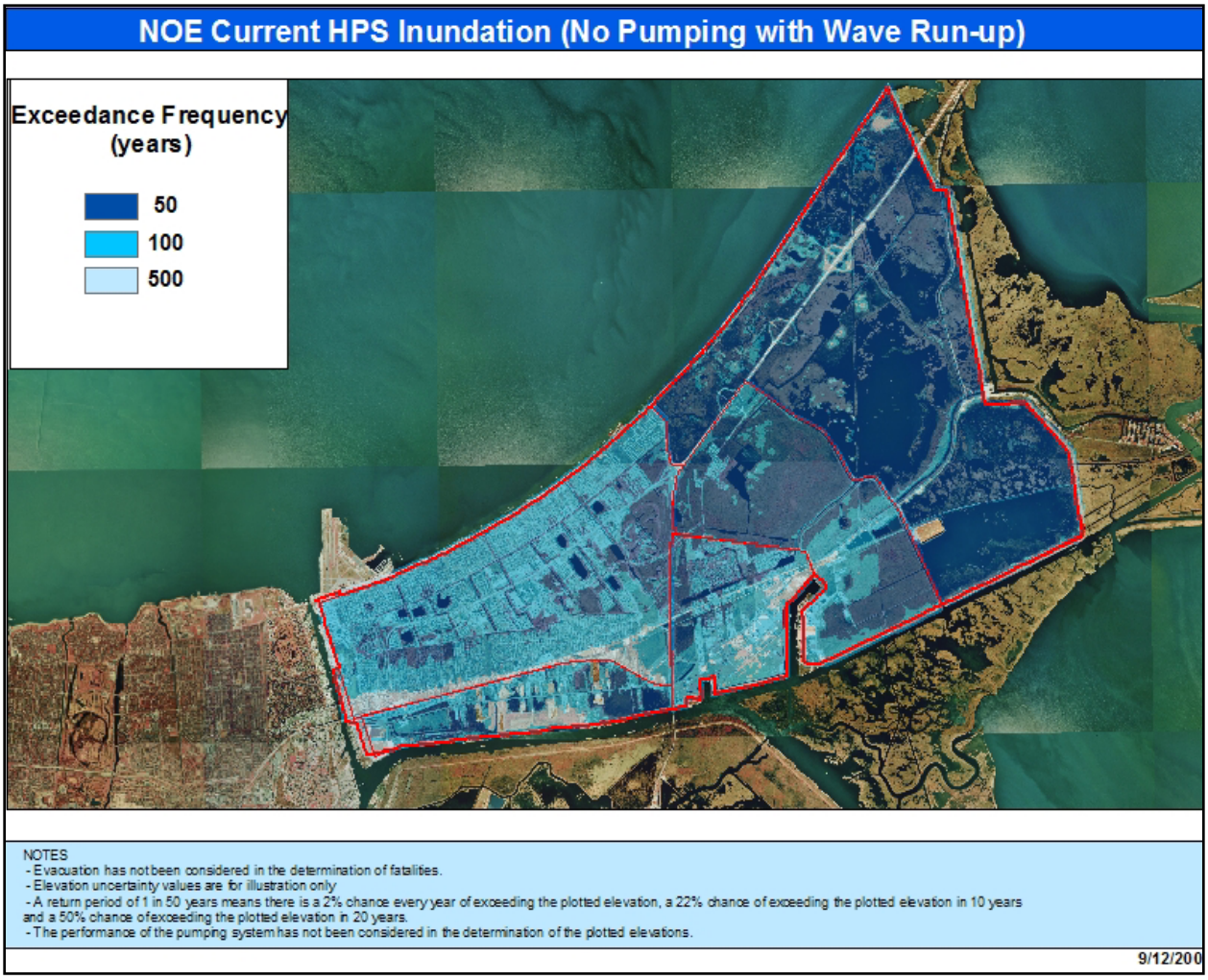

Figure 41. New Orleans East Parish - Current inundation no pumping

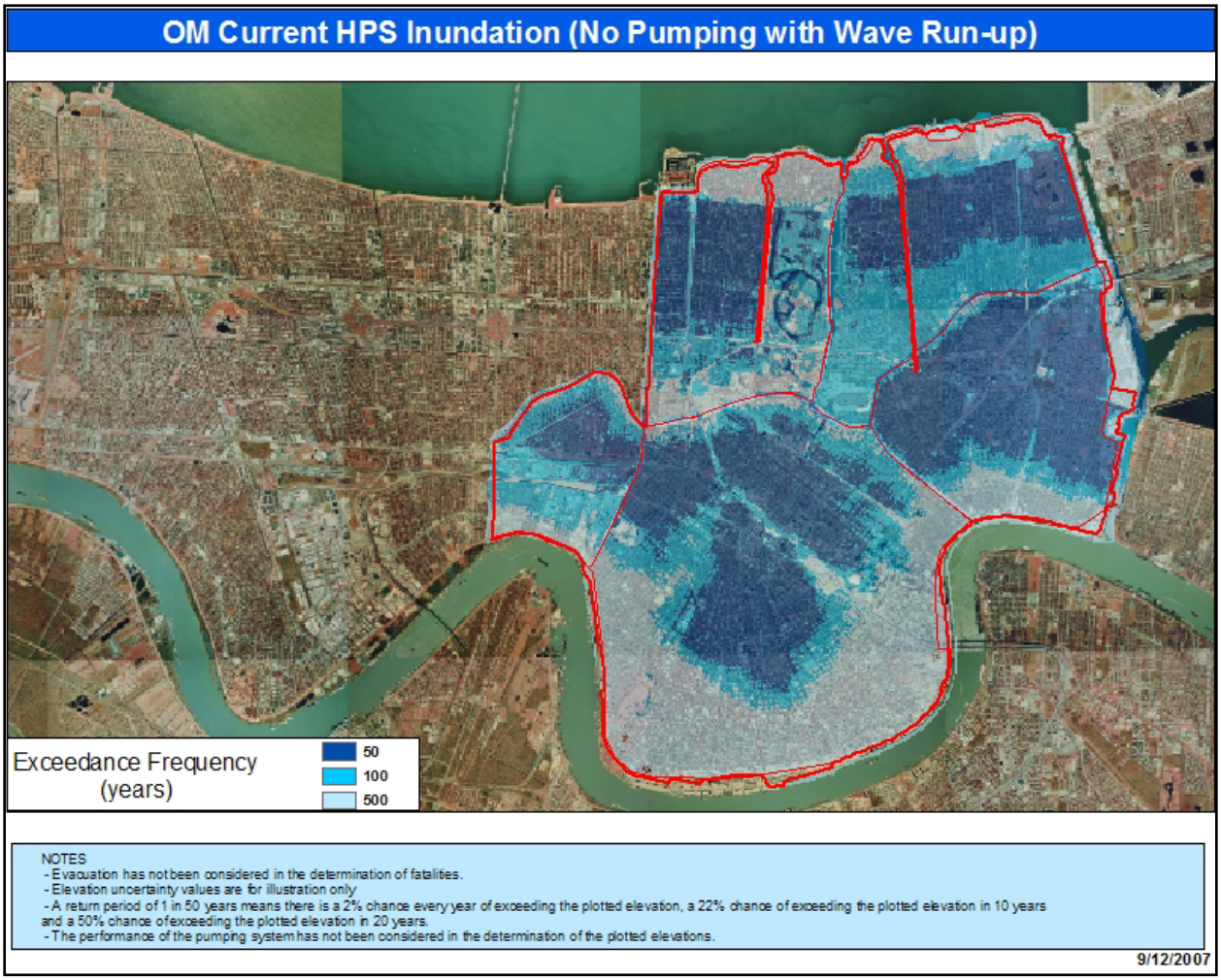

Figure 42. Orleans Parish East - Current inundation no pumping

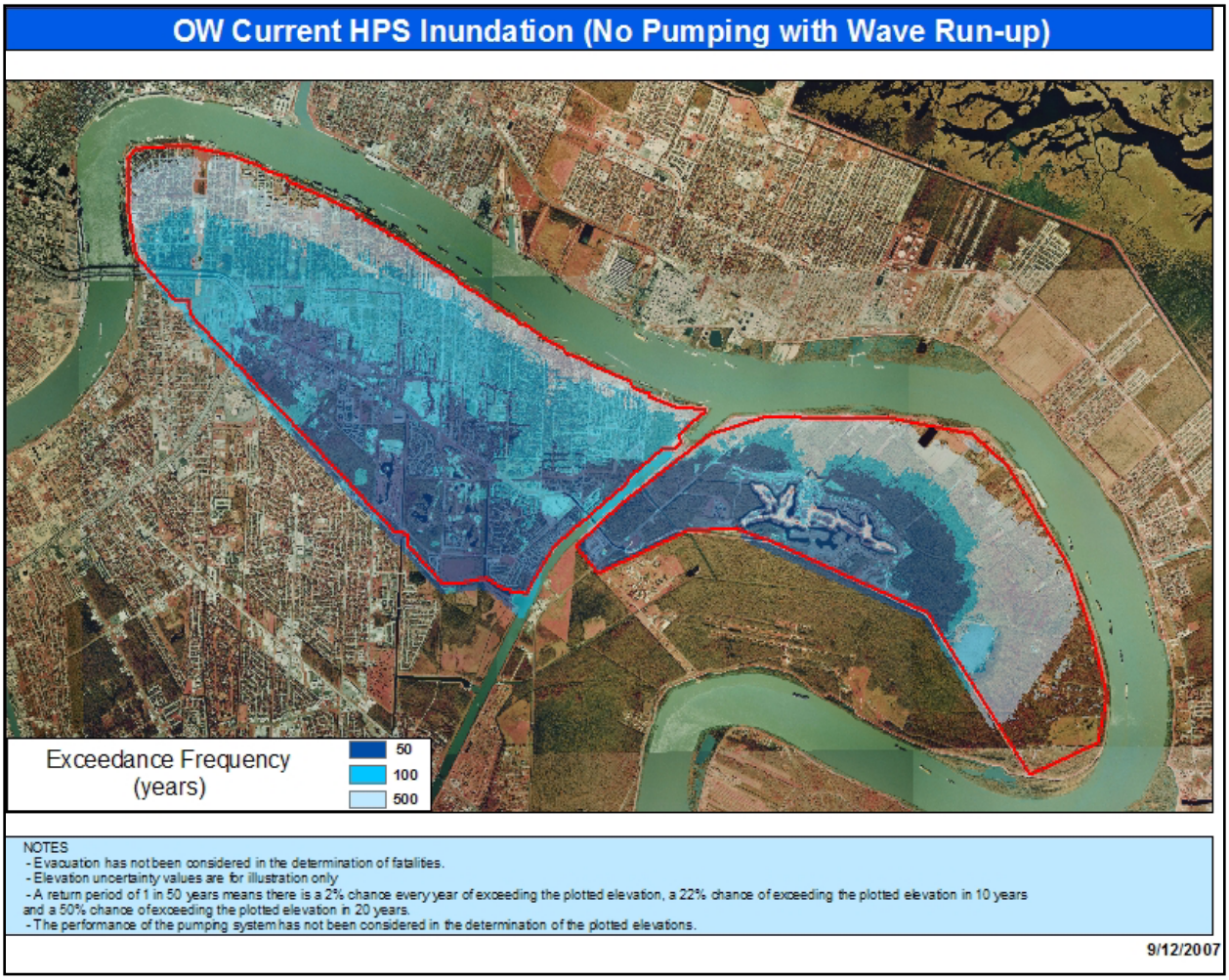

Figure 43. Orleans Parish West Bank - Current inundation no pumping

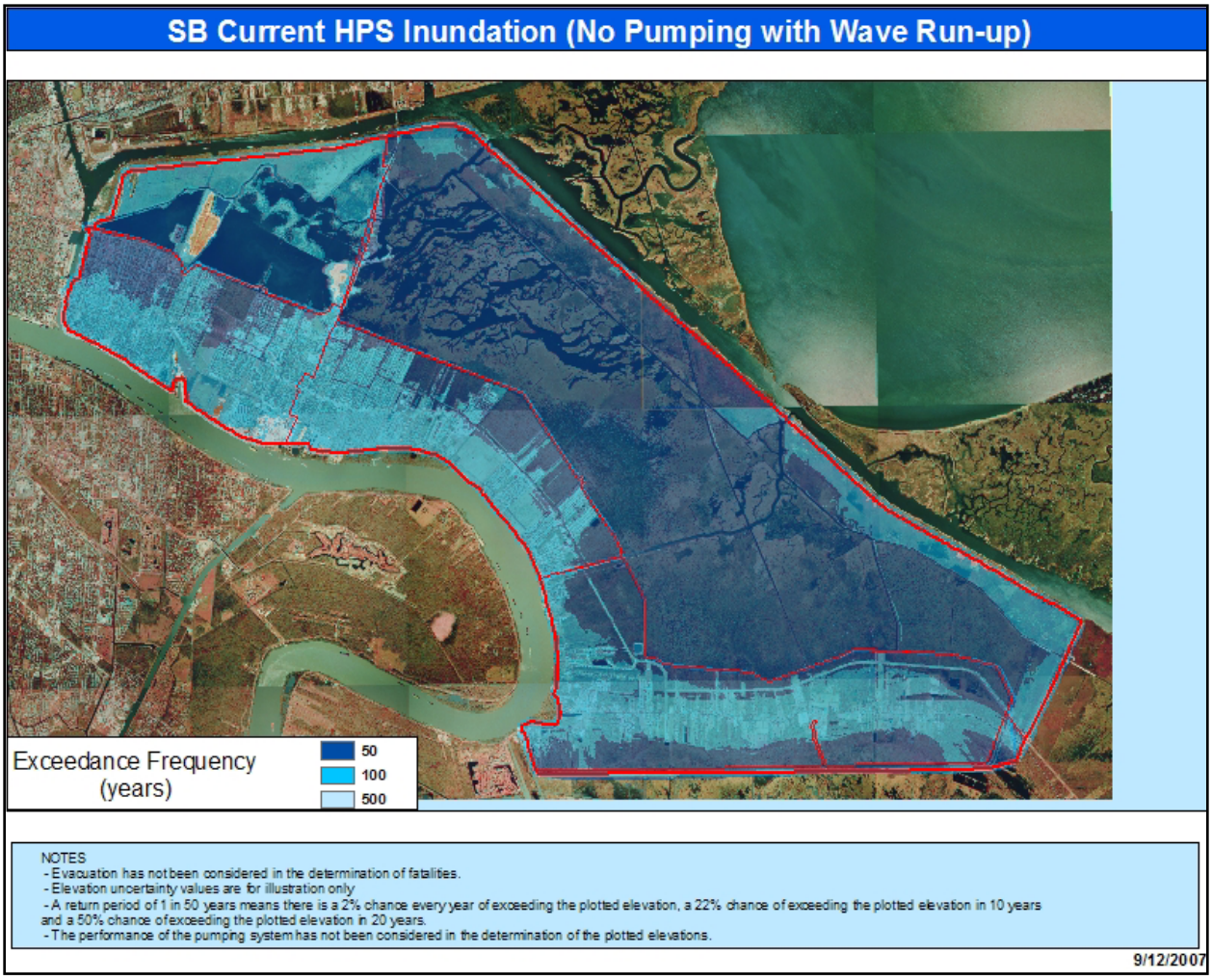

Figure 44. St. Bernard Parish - Current inundation no pumping

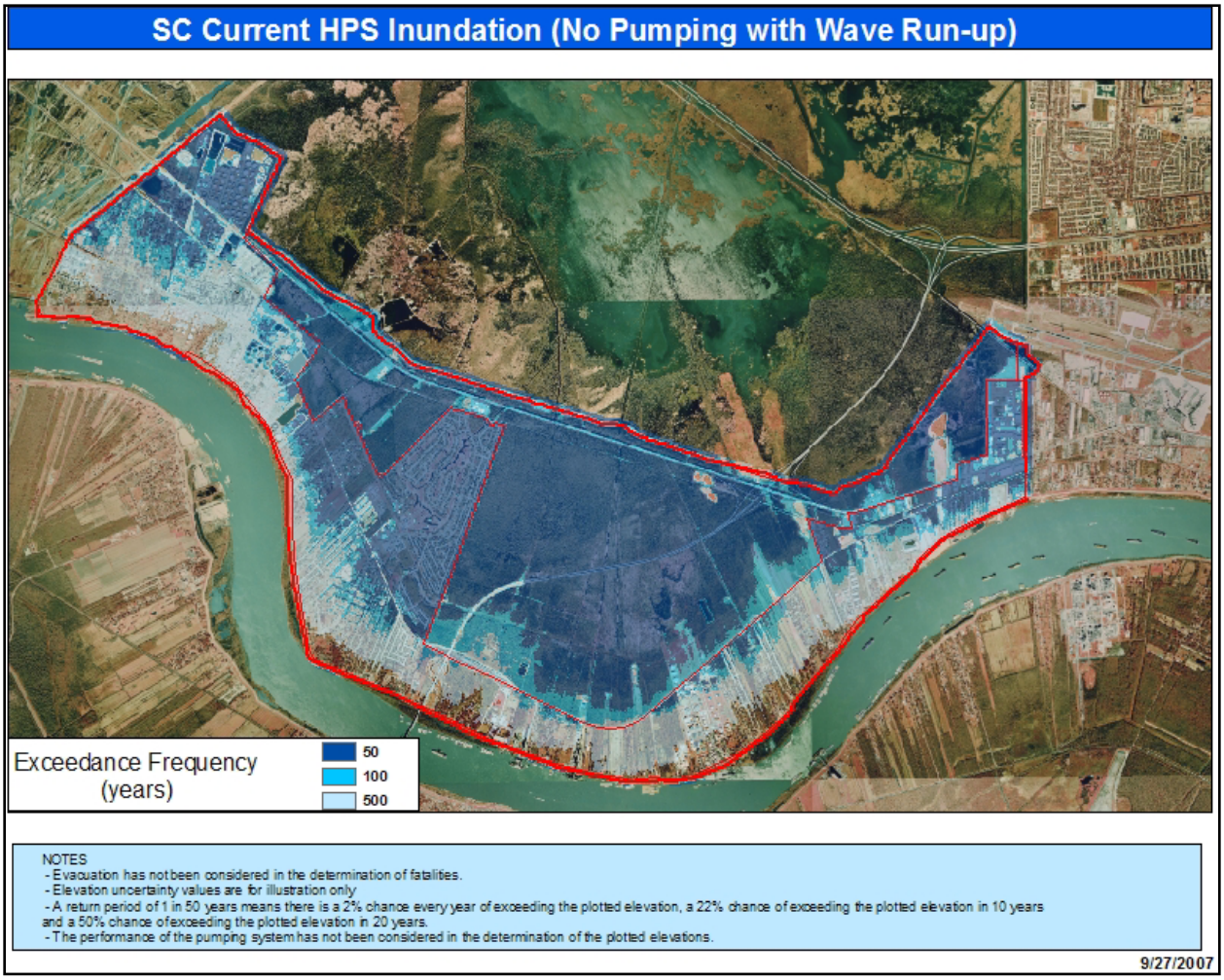

Figure 45. St Charles Parish - Current inundation no pumping

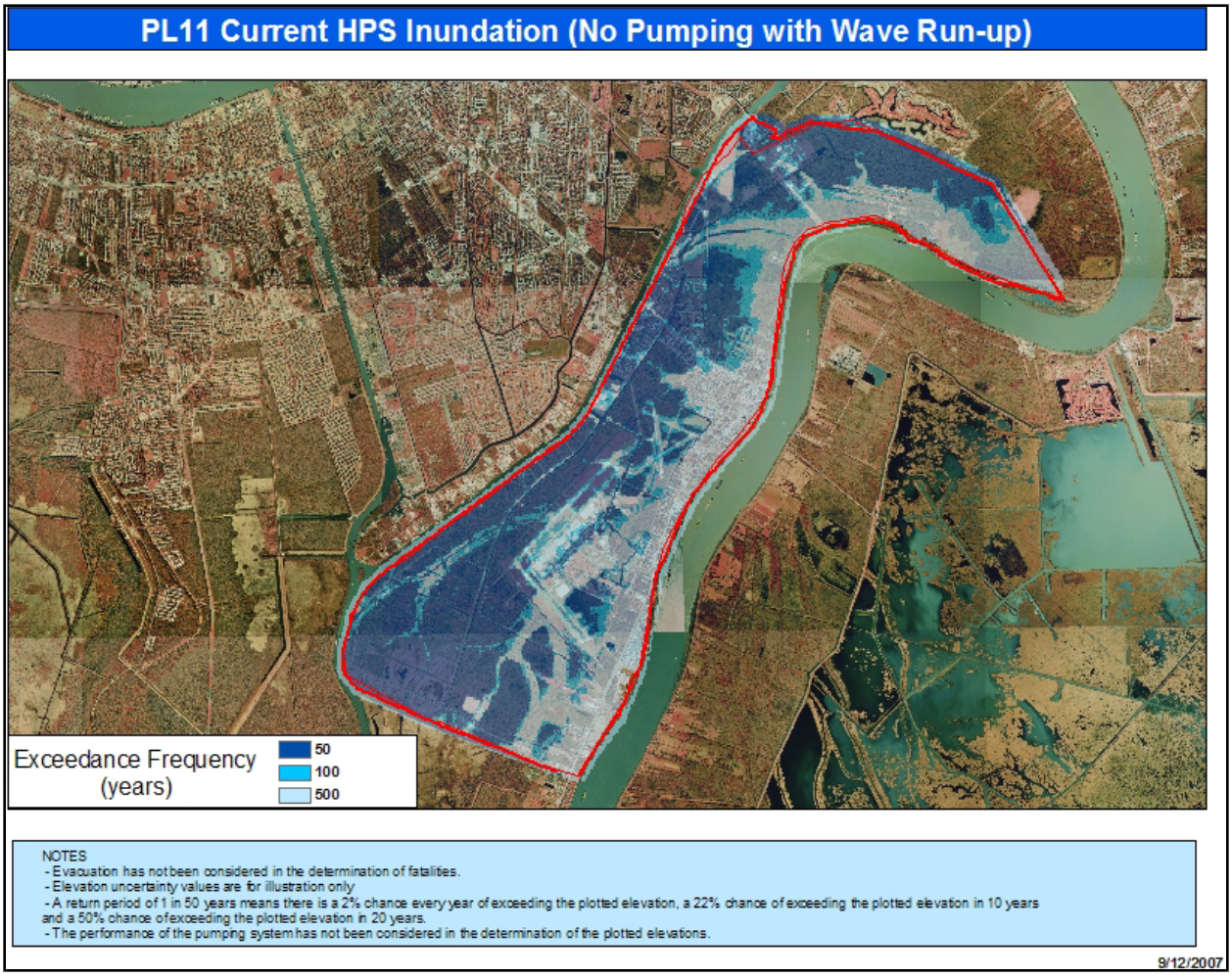

Figure 46. Plaquimines Parish – Current inundation no pumping

References

ADCIRC. 2006. Finite element hydrodynamic model for coastal oceans, inlets, rivers and floodplains. *http://www.nd.edu/~adcirc/index.htm*.

Ang, A.H-S., and W. H. Tang. 2007. *Probability concepts in engineering,* New York: John Wiley and Sons.

ASCE. 1996. *Minimum design loads for buildings and other structures*. ASCE 7-95. New York.

Ayyub, B. M. 2003. *Risk analysis in engineering and economics.* FL: Chapman & Hall/CRC Press.

Baecher, G. B., and J. T. Christian. 2003. *Statistics and reliability in geotechnical engineering.* London and NY: John Wiley and Sons.

Batts, M. E., M. R. Cordes, L. R. Russell, J. R. Shaver, and E. Simiu. 1980. *Hurricane wind speeds in the United States.* Rep. No. BSS-124. Washington, DC: Nat. Bureau of Standards, U.S. Department of Commerce.

Bedford, T., and R. Cooke. 2001. *Probabilistic risk analysis.* Cambridge: Cambridge University Press.

Bister, M., and K. A. Emanuel. 2002. Low frequency variability of tropical cyclone potential intensity. 1: Interannual to interdecadal variability. *J. Geoph. Res.* 107: 4801.

Borgman, L. E., M. Miller, L. Butler, and R. Reinhard. 1992. "Empirical simulation of future hurricane storm histories as a tool in engineering and economic analysis," *Proceedings* Fifth International Conference on Civil Engineering in the Ocean, ASCE, November, College Station, Texas.

Broccoli, A. J., and S. Manabe. 1990. Can existing climate models be used to study anthropogenic changes in tropical cyclone climate? *Geophys. Res. Lett.* 17: 1917-1920.

Cardone, V. J., W. J. Pierson, and E. G. Ward. 1976. Hindcasting the directional spectra of hurricane generated waves. *J. Petrol. Technol.* 28: 385-394.

Chan, J. C. L., and S. L. Liu. 2004. Global warming and Western North Pacific typhoon activity from an observational perspective. *J. Climate* 17: 4590-4602.

Chen, S., M. Lonfat, J. A. Knaff, and F. D. Marks, Jr. 2006. Effects of vertical wind shear and storm motion on tropical cyclone rainfall asymmetries deduced from TRMM. Submitted to *Monthly Weather Review*.

Chouinard, L. E., C. Liu, and C. K. Cooper. 1997. Model for severity of hurricanes in Gulf of Mexico. *J. Waterway, Port, Coastal and Ocean Engineering* 123(3): 120-129.

Chow, S. 1971. A study of the wind field in the planetary boundary layer of a moving tropical cyclone. MS thesis, New York University.

Collins, J. I., and M. J. Viehmann. 1971. A simplified model for hurricane wind fields. Paper 1346, Offshore Technology Conference, Houston, TX.

Dally, W. R., R. G. Dean, and R. A. Dalrymple. 1985. Wave height variation across beaches of arbitrary profile. *Journal of Geophysical Research* 90(6): 11,917-11,927.

Daugherty, R., J. Franzini, and E. Finnemore. 1985. Fluid mechanics with engineering applications. New York: McGraw-Hill Book Co.

DeGroot, D. J., and G. B. Baecher. 1993. Estimating autocovariance of in-situ soil properties. *Journal of the Geotechnical Engineering Division, ASCE, v.119*(GT1): 1247-1265.

Dixon, T. H., F. Amelung, and A. Ferretti. 2006. Subsidence and flooding in New Orleans. *Nature* 441: 587-588.

Dokka, R. K. 2006. Modern-day tectonic subsidence in coastal Louisiana. *Geology* 34(4): 281–284.

Eijgenraam, C. J. J. 2006. *Optimal safety standards for dike-ring areas*. CPB Netherlands Bureau for Economic Policy Analysis: CPB Discussion Paper 62.

Elsner, J. B. 2005. Hurricane science review: The next 5 years? Dept. of Geography, Florida State University. *http://garnet.fsu.edu/~jelsner/www*.

Elsner, J. B., and B. Kocher. 2000. Global tropical cyclone activity: A link to the North Atlantic oscillation. *Geophys. Res. Lett.* 27: 129-132.

Emanuel, K. A. 1987. The dependence of hurricane intensity on climate. *Nature* 326: 483-485.

Emanuel, K. A. 2000. A statistical analysis of tropical cyclone intensity. *Mon. Wea. Rev.* 128: 1139-1152.

Emanuel, K. A. 2005a. Increasing destructiveness of tropical cyclones over the past 30 years. *Nature* 436: 686-688.

Emanuel, K. A. 2005b. Anthropogenic effects on tropical cyclone activity. Dept. of Earth and Planetary Sciences, MIT. *http://wind.mit.edu/~emanuel/anthro2.htm*.

Federal Emergency Management Agency (FEMA). 2006. Mitigation Assessment Team Report: Hurricane Katrina in the Gulf Coast - Building performance observations, recommendations, and technical guidance (July 2006). *http://www.fema.gov/library/viewRecord.do?id=1857*

Free, M., M. Bister, and K. A. Emanuel. 2004. Potential intensity of tropical cyclones: Comparison of results from radiosonde and reanalysis data. *J. Climate* 17: 1722-1727.

Georgiou, P. N., A. G. Davenport, and B. J. Vickery. 1983. Design wind speed in regions dominated by tropical cyclones. *J. Wind Engrg. And Industrial Aerodynamics* 13(1): 139-152.

Goldenberg, S. B., C. W. Landsea, A. M. Mestas-Nunez, and W. M. Gray. 2001. The recent increase in Atlantic hurricane activity: Causes and implications. *Science* 293: 474-479.

Grossi, P., and H. Kunreuther. 2005. Catastrophe modeling: A new approach to managing risk. New York: Springer-Verlag.

Haarsma, R. J., J. F. B. Mitchell, and C. A. Senior. 1992. Tropical disturbances in a GCM. *Climate Dyn.* 8: 247-257.

Hallegatte, S. 2006. A cost-benefit analysis of the New Orleans Flood Protection System. AEI-Brookings Joint Center: Regulatory Analysis 06-02.

Hartford, D. N. D., and G. B. Baecher. 2004. *Risk and uncertainty in dam safety.* London: Thos. Telford Ltd.

Henderson-Sellers, A., H. Zhang, G. Berz, K. A. Emanuel, W. Gray, C. Landsea, G. Holland, J. Lighthill, S-L. Shieh, P. Webster, and K. McGuffie. 1998. Tropical cyclones and global climate change: A post-IPCC assessment. *Bull. Amer. Meteor. Soc.* 79: 9-38.

Ho, F. P., J. C. Su, J. L. Hanevich. R. J. Smith, and F. P. Richards. 1987. Hurricane climatology for the Atlantic and Gulf Coasts of the United States. *NOAA Technical Report NWS 38.* Washington, DC: U.S. Department of Commerce.

Ho, F. P., and V. A. Myers. 1975. *Joint probability method of tide frequency analysis applied to Apalachicola Bay and St. George Sound, Florida.* NOAA Tech. Rep. NWS 18, 43 p.

Ho, F. P., J. C. Su, K. L. Hanevich, R. J. Smith, and F. P. Richards. 1987. Hurricane climatology for the Atlantic and Gulf Coasts of the United States. NOAA Tech. Rep. NWS 38, completed under agreement EMW-84-E-1589 for FEMA, 194 p.

Holland, G. J. 1980. An analytic model of the wind and pressure profiles in hurricanes. *Monthly Weather Review* 108: 1212-1218.

Houghton, J. T., Y. Ding, D. J. Griggs, M. Noguer, P. J. van der Linden, and D. Xiaosu, eds. 2001. Climate Change 2001: The Scientific Basis: Contributions of Working Group I to the Third Assessment Report of the Intergovernmental Panel on Climate Change, Cambridge University Press.

Jarvinen, B. R., C. J. Neumann, and M. A. S. Davis. 1984. A tropical cyclone data tape for the North Atlantic Basin 1886-1893: Contents, limitations and uses. *NOAA Tech. Memo. NWS-NHC-22.* Washington, DC: U.S. Department of Commerce.

Kimball, S. K. 2006. A modeling study of hurricane landfalls in a dry environment. *Mon. Wea. Rev*. 134: 1901-1918.

Myers, V. A. 1954. Characteristics of United States hurricanes pertinent to levee design for Lake Okeechobee, Florida. Hydromet. Rep. No. 32. Washington, DC: U.S. Weather Bureau.

Knutson, T. R., and R. E. Tuleya. 2004. Impact of CO_2-induced warming on simulated hurricane intensity and precipitation: Sensitivity to the choice of climate model and convective parameterization. *J. Climate* 17: 3477-3495.

Landsea, C. W., R. A. Pielke, Jr., A. M. Mestas-Nunez, and J. A. Knaff. 1999. Atlantic Basin Hurricanes: Indices of climatic changes. *Climatic Change* 42: 89-129.

Lighthill, J., G. J. Holland, W. M. Gray, C. Landsea, K. A. Emanuel, G. Craig, J. Evans, Y. Kurihara, and C. P. Guard. 1994. Global climate change and tropical cyclones. *Bull. Amer. Meteor. Soc.* 75: 2147-2157.

Lonfat, M., F. D. Marks, Jr., and S. S. Chen. 2004. Precipitation distribution in tropical cyclones using the tropical rainfall measuring mission (TRMM) microwave imager: A global perspective. *Mon. Wea. Rev.* 132: 1645-1660.

Luettich, R. A., J. J. Westerink, and N. W. Scheffner. 1992. *ADCIRC: An advanced three-dimensional circulation model for shelves, coasts and estuaries; Report 1: Theory and methodology of ADCIRC-2DDI and ADCIRC-3DL.* Technical Report DRP-92-6. Vicksburg, MS: Coastal Engineering Research Center, U.S. Army Engineer Waterways Experiment Station.

Melchers, R. 1999. *Structural reliability analysis and prediction.* New York: John Wiley and Sons.

Michaels, P. J., P. C. Knappenberger, and C. W. Landsea. 2005. Comments on "Impact of CO_2-induced warming on simulated hurricane intensity and precipitation: Sensitivity to the choice of climate model and convective parameterization." *J. Climate,* in press.

Modarres, M., M. Kaminskiy, and V. Krivstov. 1999. Reliability engineering and risk analysis: A practical guide. New York: Marcel Decker Inc.

Morgan, M. G., and M. Henrion. 1990. *Uncertainty: A guide to dealing with uncertainty in quantitate risk and policy analysis.* Cambridge: Cambridge University Press.

Muir-Wood, R., and W. Bateman. 2005. Uncertainties and constraints on breaching and their implications for flood loss estimation. *Philosophical Transactions of the Royal Society A: Mathematical, Physical, and Engineering Sciences* 363(1831): 1423-1430.

Myers, V. A. 1975. Storm tide frequencies on the South Carolina coast. NOAA Tech. Rep. NWS-16.

National Flood Insurance Program (NFIP). 2006. Flood insurance manual: May 2005 (Revised October 2006). *http://www.fema.gov/business/nfip/manual200610.shtm*

Neumann, C. J. 1991. *The National Hurricane Center Risk Analysis Program (HURISK)*. NOAA Tech. Memo. NWS-NHC-38. Washington, DC: U.S. Department of Commerce.

Pielke, R. A., Jr., C. W. Landsea, M. Mayfield, J. Laver, and R. Pasch. 2005. Hurricanes and global warming. *Bull. Amer. Meteor. Soc.* November, 2005: 1571-1575.

Powell, M., G. Soukup, S. Cocke, S. Gulati, N. Morisseau-Leroy, S. Hamid, N. Dorst, and L. Axe. 2005. State of Florida hurricane loss projection model: Atmospheric science component. *J. Wind Engineering and Industrial Aerodynamics* 93: 651-674.

Resio, D. T., and E. A. Orelup. 2006. Potential effects of climatic variability in hurricane characteristics on extreme waves and surges in the Gulf of Mexico, submitted to *J. Climate*.

Russell, L. R. 1971. Probability distribution for hurricane effects. *J. Wtrwy., Harb. and Coast. Engrg. Div., ASCE,* 97(1): 139-154.

Scheffner, N. W., L. E. Borgman, and D. J. Mark. 1996. Empirical simulation technique based storm surge frequency analyses. *J. Wtrwy., Port, Coast., and Oc. Engrg.* 122(2): 93-101.

Schwerdt, R. W., F. P. Ho, and R. R. Watkins. 1979. *Meteorological criteria for standard project hurricane and probable maximum hurricane windfields, Gulf and East Coasts of the United States.* Tech. Rep. NOAA-TR-NWS-23. National Oceanic and Atmospheric Administration.

Simpson, J., R. F. Adler, and G. R. North. 1988. A proposed Tropical Rainfall Measuring Mission (TRMM) satellite. Bulletin of the American Meteorological Society 69:278-295.

Thompson, E. F., and V. J. Cardone. 1996. Practical modeling of hurricane surface wind fields. *ASCE J. Waterway, Port, Coastal, and Ocean Engineering* 122(4): 195-205.

U.S. Army Corps of Engineers. 1984. *Shore protection manual.* Washington, DC: U.S. Government Printing Office.

U.S. Navy (USN). 1983. *Hurricane havens handbook for the North Atlantic Ocean*. Naval Research Laboratory: NAVENVPREDRSCHFAC TR 82-03 (modified August 2005). *http://www.nrlmry.navy.mil/port_studies/tr8203nc/0start.htm*

U.S. Senate. 2006. Hurricane Katrina: A nation still unprepared. Report to the Committee on Homeland Security and Government Affairs, U.S. Senate, Washington, DC.

USACE. 1972. New Orleans East Lakefront Levee Paris Road to South Point, Lake Pontchartrain. Barrier Plan, DM 2 Supplement 5B, New Orleans District, June.

USACE. 2000. Unwatering plan of the Greater Metropolitan Area of New Orleans, LA. USACE New Orleans District.

USACE. 2006. Interagency Performance Evaluation Task Force Draft Report on "Performance Evaluation of the New Orleans and Southeast Louisiana Hurricane Protection System," Draft Volume VIII – Engineering and Operational Risk and Reliability Analysis, USACE, Washington, DC. (1 June 2006). *https://IPET.wes.army.mil*

Van Gelder, M. 2000. Statistical methods for risk-based design of civil structures. PhD diss., Delft University of Technology, Report No. 00-1, The Netherlands.

Van Manen, S. E., and M. Brinkhuis. 2005. Quantitative flood risk assessment for polders. *Reliability Engineering & System Safety* 90: 229-237.

Vanmarcke, E. H. 1977. Reliability of earth slopes. *Journal of the Geotechnical Engineering Division, ASCE, v. 103* (GT11): 1247-1265.

Vickery, P. J., and L. A. Twisdale. 1995a. Prediction of hurricane wind speeds in the United States. *J. of Structural Engineering* 121(11): 1691-1699.

Vickery, P. J., and L. A. Twisdale. 1995b. Wind-field and filling models for hurricane wind-speed predictions. *J. of Structural Engineering* 121(11): 1700-1709.

Vickery, P. J., P. F. Skerlj, and L. A. Twisdale. 2000. Simulation of hurricane risk in the U.S. using empirical track model. *J. of Structural Engineering* 126(10): 1222-1237.

Voortman, H. 2003. Risk-based design of large scale flood defence systems. PhD diss., Delft University of Technology, Report No. 02-3, The Netherlands.

Webster, P. J., G. J. Holland, J. A. Curry, and H.-R. Chang. 2005. Changes in tropical cyclone number, duration, and intensity in a warming environment. *Science* 309: 1844-1846.

White House. 2006. The federal response to Hurricane Katrina: Lessons learned. *http://www.whitehouse.gov/reports/katrina-lessons-learned/*

Willoughby, H. E., and M. E. Rahn. 2004. Parametric representation of the primary hurricane vortex. Part I: Observations and evaluation of the Holland (1980) model. *Monthly Weather Review* 132: 3033-3048.